ics Lib.

VOLUME 37 SECOND SERIES NUMBER 6

MAR 30 1931

THE PHYSICAL REVIEW

A JOURNAL OF EXPERIMENTAL AND THEORETICAL PHYSICS

CONDUCTED BY

THE AMERICAN PHYSICAL SOCIETY

BOARD OF EDITORS

Managing Editor, JOHN T. TATE, University of Minnesota, Minneapolis

Assistant Editor, J. W. BUCHTA, University of Minnesota, Minneapolis

E. U. CONDON, C. J. DAVISSON, F. K. RICHTMYER, K. F. HERZFELD, A. W. HULL, F. W. LOOMIS, A. J. DEMPSTER, DAVID M. DENNISON, J. C. SLATER

MARCH 15, 1931

Theory of Hyperfine Structure Separations — S. GOUDSMIT 663

Van der Waals Forces in Gases — JOHN C. SLATER AND JOHN G. KIRKWOOD 682

Scattering of Unpolarized X-Rays — G. E. M. JAUNCEY AND G. G. HARVEY 698

Appearance of Extra Lines in X-Ray Diffraction Patterns of Mixtures and Absence of Some Lines Peculiar to the Components of the Mixtures — ROY W. DRIER 712

Dependence of X-Ray Absorption Spectra upon Chemical and Physical State — J. D. HANAWALT 715

Infrared Absorption Bands in Hydrogen Sulphide — HAROLD H. NIELSEN AND ERNEST F. BARKER 727

Note on the Interpretation of Certain $^2\Delta, ^2\Pi$ Bands of SiH — ROBERT S. MULLIKEN 733

Collisions of the Second Kind and their Effect on the Field in the Positive Column of a Glow Discharge in Mixtures of the Rare Gases — L. B. HEADRICK AND O. S. DUFFENDACK 736

Relative Intensities of the Magnetic and Electrostatic Illumination Components in the Electrodeless Discharge — CHARLES T. KNIPP 756

Supersonic Interferometers — ELIAS KLEIN AND W. D. HERSHBERGER 760

Letters to the Editor — 775

Relations Between Hall Effect and Resistance, F. W. Warburton and J. W. Todd—775; Note on the Structure of Groups in Crystals, *W. H. Zachariasen*—775; Interpretation of the Spectra of Rare Earth Crystals, *Frank H. Spedding*—777; High Velocity Vapor Jets at Cathodes of Vacuum Arcs, *Joseph Slepian and R. C. Mason*—779; Knowledge of Past and Future in Quantum Mechanics, *Albert Einstein, Richard C. Tolman and Boris Podolsky*—780; Deviations from Kerr's law at high field strengths in polar liquids, *J. W. Beams*—781.

Book Reviews — 783

PUBLISHED BY THE AMERICAN PHYSICAL SOCIETY

EDITORIAL OFFICES: MINNEAPOLIS, MINN.

THE AMERICAN PHYSICAL SOCIETY

OFFICERS OF THE SOCIETY

President:	W. F. G. SWANN	Bartol Research Foundation, Philadelphia, Pa.
Vice-President:	PAUL D. FOOTE	The Gulf Companies, Pittsburgh, Pa.
Secretary:	W. L. SEVERINGHAUS	Columbia University, New York City
Treasurer:	G. B. PEGRAM	Columbia University, New York City
Editor:	JOHN T. TATE	University of Minnesota, Minneapolis, Minn.
Local Secretary for the Pacific Coast:	L. B. LOEB	University of California, Berkeley, Calif.

THE PHYSICAL REVIEW

Published by the American Physical Society. Executive office: University of Minnesota, Minneapolis, Minn. Two volumes annually, twelve issues per volume.

First series. From July 1, 1893, to January 1, 1913, the REVIEW was conducted by Edward L. Nicholas, Ernest Merritt and Frederick Bedell, with the financial support of Cornell University. The first four volumes were issued annually; subsequent volumes, semi-annually; thirty-five volumes in all.

Second series. On January 1, 1913, the REVIEW was transferred to the American Physical Society as announced on the first page of the new series which was then begun. Since then it has been conducted by a Board of Editors elected by the Society. Semi-annual volumes begin in January and July. Since July 1, 1929, the REVIEW has been issued twice a month.

Contributors are referred to page 2 of the advertisements for further information.

Annual subscription, throughout the Postal Union, $12.00 in advance.

General index, 1893-1920, $4.00, in advance.

Back Volumes, $9.00 per volume; Back Numbers, $1.50 per copy for issues prior to July 1, 1929 (Vols. 1-33), $.75 per copy for issues subsequent thereto. Postage is free if remittance accompanies order; otherwise postage is extra. No bound volumes can be supplied. The REVIEW offers to purchase a limited number of First Series, Vol. 1, No. 1 (at $2.00 each); Second Series, Vol. 7, No. 1, January 1916; Vol. 7, No. 2, February 1916; Vol. 7, No. 4, April 1916; and Vol. 7, No. 5, May 1916 (at $2.00 each).

Advertisements. Rates will be supplied by the Editor on request. Copy for each number must be received at Minneapolis two weeks prior to the dates of issue; old copy is used until new copy is received. Send electrotypes direct to the printers, George Banta Publishing Co., Menasha, Wis.

Discount of ten per cent is allowed to members of the American Physical Society on purchase of back numbers.

Changes of Address and Complaints of failure to receive the REVIEW, in the case of members of the Physical Society, should be addressed to the Treasurer; in the case of other subscribers, to the Editor. New copies can be sent free in response to complaint of non-delivery only if notice of non-delivery is received within three months of date of issue.

Editorial Correspondence should be addressed to the PHYSICAL REVIEW, University of Minnesota, Minneapolis, Minn.

Entered at the postoffice at Menasha, Wis., as second class matter.
Acceptance for mailing at special rate of postage provided for in section 1103, Act of October 3, 1917, authorized September 6, 1926.

Second Series *March 15, 1931* *Vol. 37, No. 6*

THE
PHYSICAL REVIEW

THEORY OF HYPERFINE STRUCTURE SEPARATIONS*

By S. Goudsmit
Department of Physics, University of Michigan

(Received February 4, 1931)

Abstract

Expressions are derived for the hyperfine structure separations of the levels of complicated electron configurations in different types of coupling. The few available experimental data are in distinct disagreement with the theoretical calculations. This undoubtedly means that our present knowledge of the interaction with nuclear spin is incomplete. The expressions in this article are derived by the well-known method of the invariance of energy sums.

1. Description of Method

FORMULAE for the interaction energy of a nuclear magnetic moment with a single electron outside of closed electron groups have been given by Fermi,[1] Casimir,[2] Hargreaves,[3] and Breit.[4] If more than one electron is present besides complete groups the formulae are only known for a special case. They have been derived when only *s*-electrons interact appreciably with the nuclear magnetism and the interaction of other electrons may be neglected.[5] This paper is a first attempt to treat the general case of the interaction of several electrons with the nuclear magnetic moment.

The method followed in this paper is very analogous to the one used to derive expressions for multiplet separations.[6] It therefore is the well-known method of the energy sums, which originally goes back to work of Pauli[7] and which found its representation in modern quantum mechanics in an important article by Slater.[8] We will follow closely Slater's procedure, as it shows especially clearly the restrictions of the validity of the results to be obtained.

* The problem studied in this paper was started in the spring of 1927 at Copenhagen in cooperation with L. Pauling, with whom I later corresponded occasionally about the questions involved and to whom I owe many valuable suggestions.

[1] E. Fermi, Zeits. f. Physik **60,** 320 (1930).

[2] H. Casimir, quoted in Pauling and Goudsmit, Structure of Line Spectra, page 225. Also Phys. Rev. in preparation.

[3] Hargreaves, Proc. Roy. Soc. **A127,** 141 (1930).

[4] G. Breit, Phys. Rev. **37,** 51 (1931).

[5] S. Goudsmit and R. F. Bacher, Phys. Rev. **34,** 1501 (1929).

[6] S. Goudsmit, Phys. Rev. **31,** 946 (1928).

[7] W. Pauli, Zeits. f. Physik **16,** 155 (1923).

[8] J. C. Slater, Phys. Rev. **34,** 1293 (1929).

The application of the method of sums goes as follows. One thinks the interaction between the electrons to be removed, in order that each electron can be treated as independent of the others. For certain purposes one may also imagine the interaction between the spin of each electron and its own orbit to be absent. One can think this done by the introduction of a fictitious very strong magnetic field, which should break all couplings between the electrons or their quantum vectors. One now calculates under these circumstances the perturbation energy in which one is interested for each electron separately.[9]

Each state of the complete atom is now characterized by a large set of quantum numbers, each of which can be said to refer to a particular electron.[10] For this state one finds the total perturbation energy by simply adding together the perturbations of the individual electrons. If one next considers the *sum* of the perturbation energies for *all* states having the same total projection of angular momentum M (in units $h/2\pi$) on the direction of the fictitious field, this sum will remain unaltered after one introduces again the proper interactions, which were at the start thought to be absent (or, which is the same, after one reduces the applied strong fictitious magnetic field to a weak one).

This last sentence contains the fundamental principle of the sum rules, as it can be derived from quantum mechanics. It holds only for first order perturbations and moreover as it stands it does not give much information, because the sums are to be taken over *all* states of the atom. In order to get further results out of this sum rule one must make, according to Slater, certain approximations. It is assumed then that the above stated sum rule will hold if one takes the sum only over the states belonging to one electron configuration.[11] This may become quite incorrect when the levels arising from the configuration considered intermix with those of other configurations. This, for instance, is one of the reasons why the relations derived by Slater are not fulfilled very well in the actual spectroscopic data.[12] For special perturbations one can sometimes even go one step further with approximations. Slater, in his above quoted paper, purposely neglects the spin-orbit interaction of each electron. This causes the spins to be independent of the orbital angular momenta. Instead of considering the sum of the perturbation energies for a fixed value of the total projection M, he may consider the sum for the states which

[9] In the above quoted paper of Pauli this was the interaction energy with an external magnetic field, giving rise to the g-sum rule. In the paper on multiplet separations by the present author the spin-orbit interaction was considered, resulting in the Γ-sum rule. Slater treated the interaction between the electrons and it is clearly seen from his paper that his results are obtained by first calculating this interaction for each pair as if it did not disturb the approximate independence of the different electrons. The sum rules finally gave the generally valid relations between multiplet distances.

[10] In the case of a nuclear moment $Ih/2\pi$ the nuclear quantum numbers I and m_I must be added also to this set.

[11] One calls a configuration the assembly of states for which each electron has the quantum numbers n and l fixed. Two states for which one of the electrons has a different n or l are said to belong to different configurations.

[12] Compare on this point a recent paper by E. U. Condon, Phys. Rev. **36**, 1121 (1930).

have a fixed value of both M_S and M_L, the total projection of all spins and all orbits respectively. Each of these sums, which are a part of the total sum for a fixed M, will be invariant. This approximation holds only when the spin-orbit interaction is indeed negligibly small compared to the interaction between different electrons, the case in which Slater is interested. This means that one expects to obtain extreme Russell-Saunders coupling.[13]

In order to make use of the method described here it is obviously necessary to know the effect of the perturbation on one single electron considered as independent of the others.[14] This will be considered in the following section.

In most cases the hyperfine structure is smaller than any other one of the interactions present in the atom. It is possible to apply a magnetic field which will just decouple the nuclear spin from the rest of the atom, giving each an independent projection on the field direction, M_I and M_J. From the theory of the Zeeman effect of hyperfine structure[15] one knows that the interaction between the nucleus and the electron core under those circumstances is given by

$$W = A(J) \cdot M_I M_J. \tag{1}$$

The constant A in front is exactly the one which will govern the magnitude of the hyperfine multiplet of that particular level after one removes the magnetic field. That is, the levels of the hyperfine multiplet are given by

$$W_J = A(J) IJ \cos(I, J) = \tfrac{1}{2} A(J) \{F(F+1) - I(I+1) - J(J+1)\} \tag{2}$$

Here F denotes as usual the resultant of I and J.

As we are finally interested in the magnitude of just that factor A, we may all the time think that there is such a field present which causes M_I and the total projection of the core to be independent. This simplifies our calculation very much. We do not need to calculate the sums for all states with the same total $M_F = M_I + M_J$. According to Slater the sum rules will also be valid for the smaller group of states which have a fixed value for both M_I and M_J. We take therefore in the following procedure a particular value of M_I in our mind and extend the sums over levels with a fixed value of M_J.

It has to be kept in mind that the independence of M_I and M_J can only be used in case their interaction is indeed very much smaller than any of the other interactions which are to be taken into account. One can not use it, for instance, in the case of ionized Lithium. Here the hyperfine structure happens to be of the same order of magnitude as the multiplet splitting.[16]

2. Interaction between a Single Electron and a Nuclear Magnetic Moment

The interaction of a magnetic nucleus and an electron in an s-state has been treated in detail before. The energy happens to be simply proportional

[13] If one needs information about the interaction between electrons in a case of (j, j) coupling one has to alter the procedure followed by Slater somewhat.

[14] In Slater's special case one needs it for each electron *pair*.

[15] E. Back and S. Goudsmit, Zeits. f. Physik **47,** 174 (1928), see also Pauling and Goudsmit reference 2, p. 215.

[16] S. Goudsmit and D. R. Inglis, Phys. Rev. **37,** 283 (1931).

to the Landé cosine between the spin s of the electron and the nuclear moment I. It is therefore possible to treat the cases where an s-electron is a part of a configuration, completely with the vector model. We will now consider the case of a non-s electron.

We think the spin-orbit interaction to be removed (or apply a fictitious strong magnetic field). In the classical theory the interaction energy consists of two parts. The nuclear magnetic moment is acted upon by a magnetic field caused by the orbital motion of the electron and also by a field produced by the electron spin. According to perturbation theory one must write down the instantaneous values for the interaction energy and must average this over the unperturbed motion. The expression for this interaction energy is:[17]

$$W_l + W_s = a[Il\cos(I,l) - Is\cos(I,s) + 3Is\cos(I,r)\cos(r,s)]. \quad (3)$$

The factor a in front of this expression governs the absolute magnitude of the interaction energy. We are not interested in it for our problem. For a hydrogenic orbit its value is given by

$$a = \left(\frac{eh}{4\pi m_0 c}\right)^2 g(I)\left(\frac{1}{r^3}\right) = \frac{Rhc\alpha^2 Z^3}{n^3 l(l+\frac{1}{2})(l+1)} g(I). \quad (4)$$

The symbols used in Eqs. (3) and (4) have the usual meaning, r denotes the radius vector combining the nucleus with the electron, $g(I)$ stands for the Landé g value of the nucleus and as the nuclear magnetism is believed to arise from protons, one expects $g(I)$ to be only of the order 1/1840.

We start out with the case where we neglect all interactions between the quantum vectors; these will each have independent projections on the direction of the fictitious field H. These projections we denote by M_I, m_l and m_s, the nuclear, the orbital and the spin moment respectively. The vectors I, l and s will have independent Larmor precessions about the field direction and we can therefore expand the cosines of Eq. (3) and obtain:

$$W_l + W_s = a[M_I m_l - M_I m_s\{1 - 3\overline{\cos^2(H,r)}\}]. \quad (5)$$

Our problem thus reduces to finding the average of $\cos^2(H,r)$. In the classical picture with a plane orbit the vector r would be at any time perpendicular to the angular momentum vector l. This, however, is no longer true in quantum mechanics. The relative probability that r makes an angle θ with the field direction is given by the square of the tesseral harmonic $P_l^{m_l}(\cos\theta)$. Thus the required average becomes

$$\begin{aligned}\overline{\cos^2(H,r)} &= \int_0^\pi \cos^2\theta [P_l^{m_l}]^2 \sin\theta d\theta \Big/ \int_0^\pi [P_l^{m_l}]^2 \sin\theta d\theta \\ &= \frac{2(l^2 - m_l^2) + 2l - 1}{(2l-1)(2l+3)}.\end{aligned} \quad (6)$$

[17] L. Pauling and S. Goudsmit, reference 2, p. 205.

Substituting this in Eq. (5) gives finally

$$W = W_l + W_s = aM_I\left\{m_l - m_s\frac{6m_l^2 - 2l(l+1)}{(2l-1)(2l+3)}\right\}. \tag{7}$$

One verifies easily that for large values of l Eq. (6) approaches the classical result: $\frac{1}{2}\sin^2(l, H) = (l^2 - m_l^2)/2l^2$.

Expression (7) will be the fundamental formula for all further applications. It is, however, not valid for s-electrons.

3. The Sum Rule Applied to one Electron

The application of the sum rule and Eq. (7) to the case of a single electron provides a very simple derivation of the results obtained by Fermi, Casimir, Hargreaves and Breit. It also gives an illustration of the method before we apply it to the many electron case. A single electron gives rise to a doublet state, one level with $j_1 = l + \frac{1}{2}$, the other with $j_2 = l - \frac{1}{2}$. In a weak magnetic field, which just decouples the nuclear spin, the interaction with the nuclear magnetism is (compare Eq. (1)):

$$W_{j_1} = a' M_I m_{j_1} \quad \text{and} \quad W_{j_2} = a'' M_I m_{j_2}. \tag{8}$$

In a very strong magnetic field this interaction is (Eq. (7)):

$$W = aM_I\left\{m_l - m_s\frac{6m_l^2 - 2l(l+1)}{(2l-1)(2l+3)}\right\}. \tag{9}$$

The sum rule says that, keeping M_I fixed, the sums of the energies for all levels with a given value of $m_j = m_s + m_l$ must come out the same, whether we use Eq. (8) or (9). We choose first $m_j = l + \frac{1}{2}$. This occurs only once; in (8) for j_1 and in (9) when $m_l = l$ and $m_s = +\frac{1}{2}$. The sum rule states

$$a' M_I \cdot (l + \tfrac{1}{2}) = aM_I\left\{l - \frac{1}{2}\,\frac{6l^2 - 2l(l+1)}{(2l-1)(2l+3)}\right\}. \tag{10}$$

One obtains at once

$$a' = a\frac{l(l+1)}{(l+\frac{1}{2})(l+1\frac{1}{2})} = a\frac{l(l+1)}{j_1(j_1+1)}. \tag{11}$$

Next we choose $m_j = l - \frac{1}{2}$. This occurs twice, namely in (8) both for j_1 and j_2, and in (9) for $m_l = l$, $m_s = -\frac{1}{2}$ and $m_l = l-1$, $m_s = +\frac{1}{2}$. Applying the sum rule gives

$$a' M_I \cdot (l - \tfrac{1}{2}) + a'' M_I \cdot (l - \tfrac{1}{2}) \tag{12}$$

$$= aM_I\left\{l + \frac{1}{2}\,\frac{6l^2 - 2l(l+1)}{(2l-1)(2l+3)}\right\} + aM_I\left\{(l-1) - \frac{1}{2}\,\frac{6(l-1)^2 - 2l(l+1)}{(2l-1)(2l+3)}\right\}$$

As we know a' already we can solve for a'' and find

$$a'' = a\frac{l(l+1)}{(l-\frac{1}{2})(l+\frac{1}{2})} = a\frac{l(l+1)}{j_2(j_2+1)}. \tag{13}$$

These expressions for a' and a'' are indeed identical with the results obtained by other authors. Substituting them in Eq. (2) gives the hyperfine structure in the absence of a field. The result shows that for the two levels of a doublet the interval constant of the hyperfine structure is inversely proportional to $j(j+1)$. The absolute magnitude can only be given when the constant a can be calculated. This would require an exact knowledge of the eigenfunctions of the state under consideration. For penetrating orbits one can make the same kind of an approximation as was applied by Landé to the calculations of doublet separations. One obtains for such cases, instead of Eq. (4), the approximate expression

$$a = \frac{Rhc\alpha^2 Z_i Z_0^2}{n_e^3 l(l+\frac{1}{2})(l+1)}\, g(I). \tag{14}$$

In this expression Z_i and Z_o stand for the effective nuclear charge in the inner and outer part of the orbit respectively, n_e represents the "effective" quantum number or Rydberg denominator.

4. The Sum Rule Applied to Configurations

We will give as an illustrative example the case of three equivalent p-electrons. The first column of Table I gives the values of m_s and m_l for the individual electrons, chosen in agreement of course with the Pauli exclusion principle. The quantum numbers l and n are supposed to be the same for all three electrons and are therefore omitted from the table. We need only to consider the states which give rise to positive values of the total projection M_J, given in the second column, negative values of M_J do not give any additional information. The last column gives the interaction with the nuclear magnetism obtained by applying Eq. (9) to each electron individually and adding the result for the three together. As they are equivalent electrons they have the same constant a.

Table I. *Interaction for p^3 in strong field.*

m_{s_1}	m_{l_1}	m_{s_2}	m_{l_2}	m_{s_3}	m_{l_3}	M_J	Eq. (7)	
$\frac{1}{2}$	1	$\frac{1}{2}$	0	$-\frac{1}{2}$	1	$2\frac{1}{2}$	$2\frac{2}{5}\ aM_I$	
$\frac{1}{2}$	1	$\frac{1}{2}$	0	$\frac{1}{2}$	-1	$1\frac{1}{2}$	$0\ aM_I$	
$\frac{1}{2}$	1	$\frac{1}{2}$	0	$-\frac{1}{2}$	0		$\frac{1}{5}\ aM_I$	sum
$\frac{1}{2}$	1	$\frac{1}{2}$	-1	$-\frac{1}{2}$	1		$\frac{1}{5}\ aM_I$	$3\frac{1}{5}\ aM_I$
$\frac{1}{2}$	1	$-\frac{1}{2}$	0	$-\frac{1}{2}$	1		$1\frac{3}{5}\ aM_I$	
$\frac{1}{2}$	1	$\frac{1}{2}$	0	$-\frac{1}{2}$	-1	$\frac{1}{2}$	$\frac{2}{5}\ aM_I$	
$\frac{1}{2}$	1	$\frac{1}{2}$	-1	$-\frac{1}{2}$	0		$-\frac{1}{5}\ aM_I$	
$\frac{1}{2}$	0	$\frac{1}{2}$	-1	$-\frac{1}{2}$	1		$\frac{2}{5}\ aM_I$	sum
$\frac{1}{2}$	0	$-\frac{1}{2}$	1	$-\frac{1}{2}$	0		$1\frac{1}{5}\ aM_I$	$2\frac{2}{5}\ aM_I$
$\frac{1}{2}$	1	$-\frac{1}{2}$	1	$-\frac{1}{2}$	-1		$1\frac{1}{5}\ aM_I$	

The states in the table are ordered according to their values of M_J. The configuration gives rise to five levels, one with $J=2\frac{1}{2}$, three with $J=1\frac{1}{2}$ and one with $J=\frac{1}{2}$. We want to know the constants A for each of these levels and shall denote them by $A(2\frac{1}{2})$, $A(1\frac{1}{2})$, $A'(1\frac{1}{2})$, $A''(1\frac{1}{2})$ and $A(\frac{1}{2})$ respectively.

The sum rule applied to the projection $M_J = 2\frac{1}{2}$, which occurs only once, gives

$$A(2\tfrac{1}{2}) \cdot M_I \cdot 2\tfrac{1}{2} = 2\tfrac{2}{3} a M_I . \tag{15}$$

The projection $M_J = 1\frac{1}{2}$ occurs four times, namely $J = 2\frac{1}{2}$ as well as all three levels with $J = 1\frac{1}{2}$ can give this projection on the field direction. It also occurs four times in Table I. The sum rule gives

$$\{A(2\tfrac{1}{2}) + A(1\tfrac{1}{2}) + A'(1\tfrac{1}{2}) + A''(1\tfrac{1}{2})\} M_I \cdot 1\tfrac{1}{2} = 3\tfrac{1}{3} a M_I . \tag{16}$$

Finally $M_J = \frac{1}{2}$ occurs five times, giving

$$\{A(2\tfrac{1}{2}) + A(1\tfrac{1}{2}) + A'(1\tfrac{1}{2}) + A''(1\tfrac{1}{2}) + A(\tfrac{1}{2})\} M_I \cdot \tfrac{1}{2} = 2\tfrac{2}{3} a M_I . \tag{17}$$

Solving these equations one obtains finally

$$\left.\begin{aligned} A(2\tfrac{1}{2}) &= {}^{24}/_{25} a \\ A(1\tfrac{1}{2}) + A'(1\tfrac{1}{2}) + A''(1\tfrac{1}{2}) &= 1^{13}/_{75} a \\ A(\tfrac{1}{2}) &= 2\tfrac{2}{3} a \end{aligned}\right\} \tag{18}$$

Exactly as in the case of the well-known g-sum rule we are only able to obtain the sum of the A's for the levels with the same value of J. That we find the individual values for the levels with $J = 2\frac{1}{2}$ and $J = \frac{1}{2}$ is because there is only one level with each of these J values.

The values of the individual A's will in general depend upon the type of coupling between the quantum vectors of the electrons, just as in the case of g-values. The method to obtain their values for extreme couplings will be described in following sections of this paper.

It is not at all difficult to make a table like Table I for any other example. When the electrons are not equivalent each has a different constant a which one has to carry along into the final result. We want to mention once more that most of the formulae used here are only valid for the interaction of a non-s electron with the nuclear magnetism. For an s electron one has to replace Eq. (7) by the simple expression

$$W = b M_I m_s . \tag{19}$$

Here follow the results for a number of configurations

TABLE II. *Hyperfine structure sums.**

p and p^5	$J = 1\frac{1}{2}$	$A = {}^{8}/_{15} a$	ps and $p^5 s$	$J = 2$	$A = \frac{2}{3} a + \frac{1}{4} b$
	$\frac{1}{2}$	$A = 2\frac{2}{3} a$		1	$\Sigma A = 2a + \frac{1}{4} b$
p^2 and p^4	$J = 2$	$\Sigma A = 1\frac{1}{3} a$	$p^2 s$ and $p^4 s$	$J = 2\frac{1}{2}$	$\Sigma A = 1^{7}/_{25} a + \frac{2}{3} b$
	1	$A = 0a$		$1\frac{1}{2}$	$\Sigma A = 1^{23}/_{25} a - {}^{1}/_{15} b$
p^3	$J = 2\frac{1}{2}$	$A = {}^{24}/_{25} a$		$\frac{1}{2}$	$\Sigma A = 0a + 1\frac{1}{3} b$
	$1\frac{1}{2}$	$\Sigma A = 1^{13}/_{75} a$	$p^3 s$	$J = 3$	$A = \frac{1}{3} a + \frac{1}{3} b$
	$\frac{1}{2}$	$\Sigma A = 2\frac{2}{3} a$		2	$\Sigma A = 2a + {}^{7}/_{12} b$
				1	$\Sigma A = 2\frac{1}{3} a - \frac{1}{4} b$

* The constant a refers to the p- and b to the s-electron.

5. Hyperfine Structure for Extreme (j, j) Coupling

The above described method gives only the sums of the factors which govern the hyperfine structure separations. Their individual values for each level are only determined completely in extreme couplings. The simplest case is that of extreme (j, j) coupling which we shall now discuss with the example of the p^3 configuration. We mean by extreme (j, j) coupling that the spin vector s of each electron is strongly coupled to its own orbital vector l and that therefore one can ascribe to each one of the electrons of the configuration its own resultant vector j. The spin-orbit coupling has to be considerably stronger than the interaction energy between the different electrons. It is then possible to think of an applied magnetic field which is strong enough to decouple the different electrons so as to make them independent of each other, but not yet strong enough to decouple the s and l for each of the electrons.

Under these ideal circumstances the quantum state of each electron will be characterized by the quantum numbers j and m_j, its resultant moment and the projection on the field, rather than by m_s and m_l. We now have to make again a table similar to Table I but now with the different designation for each electron. We also need to know what the interaction with the nucleus will be for each electron, when its state is characterized by j and m_j, that is when its spin and orbit are coupled. But this is just the problem solved in Section 3. Eq. (8) is the one we must use now, especially after we introduce for a' and a'' the results of Eqs. (11) and (13).

Table III. *Configuration p^3 in (j, j) coupling.*

j_1	m_{j_1}	j_2	m_{j_2}	j_3	m_{j_3}	M_J	Eq. (8)	
$1\frac{1}{2}$	$1\frac{1}{2}$	$1\frac{1}{2}$	$\frac{1}{2}$	$1\frac{1}{2}$	$-\frac{1}{2}$	$1\frac{1}{2}$	$1\frac{1}{2}a'M_I$	
	$1\frac{1}{2}$		$\frac{1}{2}$		$-1\frac{1}{2}$	$\frac{1}{2}$	$\frac{1}{2}a'M_I$	
$1\frac{1}{2}$	$1\frac{1}{2}$	$1\frac{1}{2}$	$\frac{1}{2}$	$\frac{1}{2}$	$\frac{1}{2}$	$2\frac{1}{2}$.	$(2a'+\frac{1}{2}a'')M_I$	
	$1\frac{1}{2}$		$\frac{1}{2}$		$-\frac{1}{2}$	$1\frac{1}{2}$	$(2a'-\frac{1}{2}a'')M_I$	sum
	$1\frac{1}{2}$		$-\frac{1}{2}$		$\frac{1}{2}$		$(a'+\frac{1}{2}a'')M_I$	$3a'M_I$
	$1\frac{1}{2}$		$-1\frac{1}{2}$		$\frac{1}{2}$	$\frac{1}{2}$	$\frac{1}{2}a''M_I$	sum
	$1\frac{1}{2}$		$-\frac{1}{2}$		$-\frac{1}{2}$		$(a'-\frac{1}{2}a'')M_I$	$(a'+\frac{1}{2}a'')M_I$
	$\frac{1}{2}$		$-\frac{1}{2}$		$\frac{1}{2}$		$\frac{1}{2}a''M_I$	
$1\frac{1}{2}$	$1\frac{1}{2}$	$\frac{1}{2}$	$\frac{1}{2}$	$\frac{1}{2}$	$-\frac{1}{2}$	$1\frac{1}{2}$	$1\frac{1}{2}a'M_I$	
	$\frac{1}{2}$		$\frac{1}{2}$		$-\frac{1}{2}$	$\frac{1}{2}$	$\frac{1}{2}a'M_I$	

Table III represents the equivalent of Table I for the extreme (j, j) coupling. The example chosen is again the configuration p^3. For reasons to be discussed later the values for a' and a'' have not been substituted.

In the ideal extreme case the electrons are quite independent of each other. Following Slater we therefore need not take the sums over all levels with a fixed value of the total M_J. The sum-rule will hold already for the levels which are designated by a special set of values of j and m_j for each of the electrons. If we choose a set of values for these quantum numbers it

happens that we find only one state in our table which possesses just this set. Thus we do not need to consider any sums at all and the third column of the table gives at once the correct value of the interaction with the nuclear spin for this extreme case.

We are, however, not yet finished. When we now gradually remove the field which decoupled the electrons, the quantum numbers m_j for the individual electrons will lose their significance and be converted together into the total M_J. In the extreme (j, j) coupling the values of j for each electron will keep their meaning. This means that for this last transition the sum rules will hold within each group of levels characterized by fixed values of the individual j, but no longer for the individual m_j. Table III has been arranged accordingly.

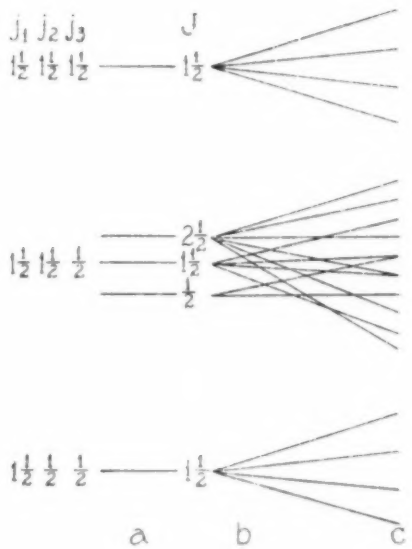

Fig. 1. Schematical representation of Paschen-Back effect for p^3 in extreme (j,j) coupling. (a) without field, quantum numbers: j_1, j_2, j_3, J. (b) weak field, quantum numbers: j_1, j_2, j_3, J, M_J. (c) strong field, quantum numbers: $j_1, j_2, j_3, m_{j1}, m_{j2}, m_{j3}$.

Figure 1 may help to understand the situation described above. At the left is shown the p^3 configuration in extreme (j, j) coupling. The highest level arises when all three electrons have maximum energy, that is when they all have $j=1\frac{1}{2}$. The next lower group occurs when one of the electrons has $j=\frac{1}{2}$. The lowest level has two electrons with $j=\frac{1}{2}$ and one with $j=1\frac{1}{2}$.[18] The hyperfine structure is not included in the figure. Going to the right in Fig. 1 the effect of an applied magnetic field is represented. In a weak field each level splits into its Zeeman components. With increasing field strength each level group will undergo a Paschen-Back transition and the result is rep-

[18] There exists here no lower state with all three electrons having $j=\frac{1}{2}$, because our example consists of equivalent electrons for which the Pauli principle allows only two with $j=\frac{1}{2}$. This also will be clear from considering Table III where all states are gathered which do agree with the Pauli principle. Compare Pauling and Goudsmit, l.c., page 257.

resented at the right of Fig. 1. Notice that the field does not yet break the coupling of each spin with its orbit, the three level groups are still distinctly separated. A further increase in the field would also break up this last coupling, all couplings would be broken and one would have the case represented in Table I. One sees that the right side of Fig. 1 is to be correlated with Table III. The sum rule as applied in Table III means simply that we may assume the sum rule for fixed M_J to hold within each level group separately in this extreme coupling. This gives us a means to go from the strong field to the intermediate field and to obtain our final information.

In this intermediate field, which we suppose just to decouple the nuclear spin from the rest of the atom, the interaction with the nucleus for each level will be given again by Eq. (1):

$$W = AM_IM_J.$$

Our problem is to find the value of A for each one of the many levels.

Applying the sum rule to the states which have $j_1=j_2=j_3=1\frac{1}{2}$, that is the upper level, we find at once

$$A(1\tfrac{1}{2}) = a'.$$

This result is found by choosing M_J either $1\frac{1}{2}$ or $\frac{1}{2}$.

For the middle group of levels, $j_1=j_2=1\frac{1}{2}$, $j_3=\frac{1}{2}$, one finds the following sums

$$\begin{aligned} M_J &= 2\tfrac{1}{2}: && A(2\tfrac{1}{2})M_I\cdot 2\tfrac{1}{2} = (2a' + \tfrac{1}{2}a'')M_I, \\ M_J &= 1\tfrac{1}{2}: && \{A(2\tfrac{1}{2}) + A'(1\tfrac{1}{2})\}M_I\cdot 1\tfrac{1}{2} = 3a'M_I, \\ M_J &= \tfrac{1}{2}: && \{A(2\tfrac{1}{2}) + A'(1\tfrac{1}{2}) + A(\tfrac{1}{2})\}M_I\cdot \tfrac{1}{2} = (a' + \tfrac{1}{2}a'')M_I. \end{aligned}$$

From this one obtains

$$A(2\tfrac{1}{2}) = \tfrac{4}{5}a' + \tfrac{1}{5}a''; \; A'(1\tfrac{1}{2}) = 1\tfrac{1}{5}a' - \tfrac{1}{5}a''; \; A(\tfrac{1}{2}) = a''.$$

Finally the lowest level gives

$$A''(1\tfrac{1}{2}) = a'.$$

After one substitutes the values of a' and a'' from Eqs. (11) and (13) the results become

$$A(1\tfrac{1}{2}) = {}^{8}/_{15}a; \; A(2\tfrac{1}{2}) = {}^{24}/_{25}a; \; A'(1\tfrac{1}{2}) = {}^{8}/_{75}a; \; A(\tfrac{1}{2}) = 2\tfrac{2}{3}a; \; A''(1\tfrac{1}{2}) = {}^{8}/_{15}a.$$

As is to be expected the sums agree with those given in Section 4 and Table II.

6. Use of the Vector Model for Extreme (j, j) Coupling

When the spin and orbit of an electron are coupled the interaction with the nuclear magnetism is given by the Eq. (2)

$$W = a'Ij\cos(I, j) \quad \text{or} \quad a''Ij\cos(I, j). \tag{20}$$

The choice of a' or a'' depends on whether one considers the state with $j=l+\frac{1}{2}$ or the one with $j=l-\frac{1}{2}$. This simple expression brings it about that one often can use the vector model with advantage in extreme (j, j) coupling.

For several electrons the total interaction with the nucleus is

$$W = \sum a_k I j_k \overline{\cos(I, j_k)}. \tag{21}$$

The sum has to be extended over all electrons, which we shall distinguish by the index k. As all j_k form together the resultant J one can average over their precession about this resultant and obtains

$$W = \sum a_k I j_k \cos(I, J) \overline{\cos(J, I j_k)}. \tag{22}$$

We may write this

$$W = AIJ \cos(I, J) \tag{23}$$

in which expression we finally want to know the value of

$$A = \sum a_k \frac{j_k}{J} \overline{\cos(J, j_k)}. \tag{24}$$

The problem is thus to evaluate the average cosines of each of the individual j_k with the resultant J. This can be done easily when only two j_k form the resultant J, but with more electrons it is in general impossible, unless we use again the method of sums instead of the vector model. For a restricted but interesting number of cases we can find relations between these cosines and the g values of the levels. The magnetic moment gJ of a state is given by the sum of the magnetic moments $g_k j_k$ of each electron resolved along the resultant J, thus

$$gJ = \sum g_k j_k \overline{\cos(J, j_k)} \quad \text{or} \quad g = \sum g_k \frac{j_k}{J} \overline{\cos(J, j_k)}. \tag{25}$$

This defines the g value for this level. Futhermore, as J is the resultant of all j_k we have

$$J = \sum j_k \overline{\cos(J, j_k)} \quad \text{or} \quad 1 = \sum \frac{j_k}{J} \overline{\cos(J, j_k)}. \tag{26}$$

If we now restrict ourselves to the case of equivalent electrons the sums in expressions 24, 25 and 26 fall apart into two sums, one over the electrons with $j' = l + \frac{1}{2}$ and one over those with $j'' = l - \frac{1}{2}$. We shall again denote these two kinds by a prime and a double prime. The formulae become

$$A = a' \sum \frac{j_k'}{J} \overline{\cos(J, j_k')} + a'' \sum \frac{j_k''}{J} \overline{\cos(J, j_k'')} \tag{24a}$$

$$g = g' \sum \frac{j_k'}{J} \overline{\cos(J, j_k')} + g'' \sum \frac{j_k''}{J} \overline{\cos(J, j_k'')} \tag{25a}$$

$$1 = \sum \frac{j_k'}{J} \overline{\cos(J, j_k')} + \sum \frac{j_k''}{J} \overline{\cos(J, j_k'')}. \tag{26a}$$

For equivalent electrons a', a'', g' and g'' can be placed before the summation, as they have the same value for each of the electrons inside any one sum.

We next can eliminate the two unknown sums between the three expressions and obtain finally

$$A = a' \frac{g - g''}{g' - g''} + a'' \frac{g - g'}{g'' - g'} . \tag{27}$$

The values of g' and g'' are the known g values for a single electron, the values of g to be used are those for the extreme (j, j) coupling of the configuration which we consider.[19] For our standard example of the p^3 configuration the results are again:

	$g' = 1\frac{1}{3}$	$g'' = \frac{2}{3}$	
$J = 2\frac{1}{2}$	$g = 1\frac{1}{5}$	$A = \frac{4}{5}a' + \frac{1}{5}a''$	
$J = \frac{1}{2}$	$g = \frac{2}{3}$	$A = a''$	
$J = 1\frac{1}{2}$	$g = 1\frac{1}{3}$	$A = a'$	upper level.
$1\frac{1}{2}$	$g = 1^7/_{15}$	$A' = 1\frac{1}{5}a' - \frac{1}{5}a''$	middle level.
$1\frac{1}{2}$	$g = 1\frac{1}{3}$	$A'' = a'$	lower level.

The addition of a single s electron to a level of which A is known can always be done with the vector model, provided the coupling is of the extreme (j, j) type. We denote with A^+ and J^+ the values for the state to which we add the s electron. The s electron itself is characterized by b and s, the resulting level finally by A and J. One obtains with the vector model

$$A = A^+ \frac{J^+}{J} \cos(J, J^+) + b \frac{s}{J} \cos(J, s) . \tag{28}$$

Substituting the Landé cosines this becomes

$$\begin{aligned} A = {} & A^+ \frac{J(J+1) + J^+(J^+ + 1) - s(s+1)}{2J(J+1)} \\ & + b \frac{J(J+1) + s(s+1) - J^+(J^+ + 1)}{2J(J+1)} . \end{aligned} \tag{29}$$

One can simplify this formula if one considers that $s = \frac{1}{2}$ and that therefore J can only be $(J^+ + \frac{1}{2})$ or $(J^+ - \frac{1}{2})$. One can also again express A in terms of the g-values.

Table IV gives the results for a few configurations in extreme (j, j) coupling.

[19] For equivalent electrons the g values for extreme (j, j) coupling can be obtained in general only with the help of the method of sums. This Section does therefore in reality not avoid the use of the sum rule, but it gives a connection between the hyperfine structure constants and the g values. The latter are considered to be better known and more easily derivable.

TABLE IV. *Hyperfine structure for (j, j) coupling.**

	j_k	J^+	J	g	A
p^2	$1\frac{1}{2}$ $1\frac{1}{2}$		2	$1\frac{1}{2}$	a'
	$1\frac{1}{2}$ $\frac{1}{2}$		2	$1\frac{1}{6}$	$\frac{3}{4}a'+\frac{1}{4}a''$
			1	$1\frac{1}{2}$	$1\frac{1}{4}a'-\frac{1}{4}a''$
p^3	$1\frac{1}{2}$ $1\frac{1}{2}$ $1\frac{1}{2}$		$1\frac{1}{2}$	$1\frac{1}{3}$	a'
	$1\frac{1}{2}$ $1\frac{1}{2}$ $\frac{1}{2}$		$2\frac{1}{2}$	$1\frac{1}{5}$	$\frac{4}{5}a'+\frac{1}{5}a''$
			$1\frac{1}{2}$	$1^7/_{15}$	$1\frac{1}{5}a'-\frac{1}{5}a''$
			$\frac{1}{2}$	$\frac{2}{3}$	a''
	$1\frac{1}{2}$ $\frac{1}{2}$ $\frac{1}{2}$		$1\frac{1}{2}$	$1\frac{1}{3}$	a'
ps	$1\frac{1}{2}$	$1\frac{1}{2}$	2	$1\frac{1}{2}$	$\frac{3}{4}a'+\frac{1}{4}b$
			1	$1\frac{1}{6}$	$1\frac{1}{4}a'-\frac{1}{4}b$
	$\frac{1}{2}$	$\frac{1}{2}$	1	$1\frac{1}{3}$	$\frac{1}{2}a''+\frac{1}{2}b$
p^2s	$1\frac{1}{2}$ $1\frac{1}{2}$	2	$2\frac{1}{2}$	$1^7/_{15}$	$\frac{4}{5}a'+\frac{1}{5}b$
			$1\frac{1}{2}$	$1\frac{1}{3}$	$1\frac{1}{5}a'-\frac{1}{5}b$
		0	$\frac{1}{2}$	2	b
	$1\frac{1}{2}$ $\frac{1}{2}$	2	$2\frac{1}{2}$	$1\frac{1}{3}$	$\frac{3}{5}a'+\frac{1}{5}a''+\frac{1}{5}b$
			$1\frac{1}{2}$	1	$^9/_{10}a'+^3/_{10}a''-\frac{1}{8}b$
		1	$1\frac{1}{2}$	$1\frac{2}{3}$	$\frac{5}{6}a'-\frac{1}{6}a''+\frac{1}{2}b$
			$\frac{1}{2}$	$1\frac{1}{3}$	$\frac{5}{6}a'-\frac{1}{6}a''-\frac{1}{2}b$
	$\frac{1}{2}$ $\frac{1}{2}$	0	$\frac{1}{2}$	2	b

* The values of j_k are given for the p electrons only, the s electron has $j_k=\frac{1}{2}$. Levels with $J=0$ are omitted. The results for the configurations p^5, p^4, p^3s, p^4s, are similar to the following ones in the same order p, p^2, ps, p^2s.

7. HYPERFINE STRUCTURE FOR EXTREME RUSSELL-SAUNDERS COUPLING

When the interaction between the different electrons of a configuration is very large compared to the interaction between the spins of the electrons and their orbital motion, one speaks of Russell-Saunders coupling. The spin vectors form together a resultant spin moment S, the orbital moments l form a resultant L and the total angular momentum vector J is the resultant of these two. To this one the nuclear spin I is again added to form the resultant F. This type of coupling yields the ordinary multiplet structure.

In the case of Russell-Saunders coupling one can imagine an applied magnetic field which is strong enough to overcome the coupling between the spins and orbits; that is, between the resultant S and the resultant L, but not yet strong enough to decouple the different electrons from each other. This situation is represented at the right of Fig. 2. The left of Fig. 2 gives the levels without magnetic field, whereas the middle shows them in an intermediate field. The strong field has caused a complete Paschen-Back effect for each of the multiplets, but the splitting up which it causes is supposed to be still small compared to the distances between the different multiplets. In this strong field each state will be characterized by the projections M_S and M_L of S and L on the field direction. As these two are supposed to have a negligible interaction under these circumstances, they will be independent and will restrict our sum rules. According to Slater's procedure the sums will now be invariant over states which have the same value of the pair of quantum numbers M_S, M_L. Table V shows the states of the example p^3 arranged in this order. This configuration yields a ^4S, a ^2D and ^2P state. When we increase the field more

and more until it breaks the electron coupling, the total projection M_S of the resultant spin will remain invariant and can finally be interpreted as the sum

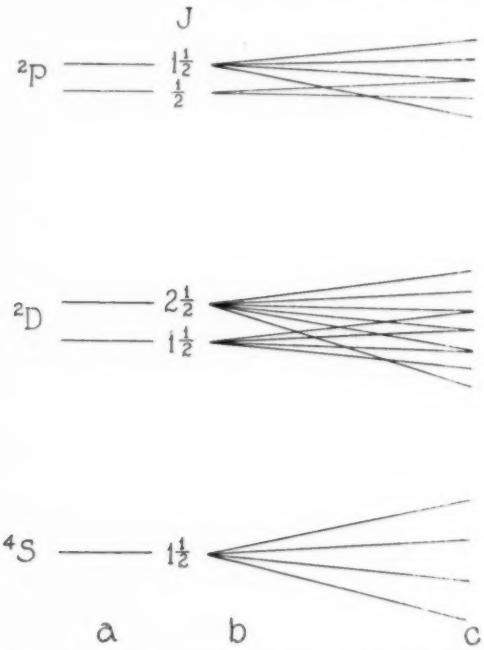

Fig. 2. Schematical representation of Paschen-Back effect for p^3 in extreme Russell-Saunders coupling. (a) without field, quantum numbers: L, S, J. (b) weak field, quantum numbers L, S, J, M_J. (c) strong field, quantum numbers· L, S, M_L, M_S.

of the m_s of the electrons. In the same way M_L will be converted into the sum of m_l of the individual electrons. It is in this way that a certain pair M_S, M_L can be correlated to each of the states in Table V, simply

$$M_S = \sum m_s, \quad M_L = \sum m_l. \tag{30}$$

TABLE V. *Configuration p^3 in Russell-Saunders coupling.*

m_{s_1}	m_{s_2}	m_{s_3}	m_{l_1}	m_{l_2}	m_{l_3}	M_S	M_L	M_J	Eq. (7)
½	½	−½	1	0	1	½	2	2½	$2\frac{2}{5}\ aM_I$
½	½	½	1	0	−1	1½	0	1½	$0\ aM_I$
½	½	−½	1	0	0	½	1	1½	$\frac{4}{5}\ aM_I$
			1	−1	1				$\frac{4}{5}\ aM_I$
½	−½	−½	1	0	−1	−½	2	1½	$1\frac{3}{5}\ aM_I$
½	½	−½	1	0	−1	½	0	½	$\frac{2}{5}\ aM_I$
			1	−1	0				$-\frac{1}{5}\ aM_I$
			0	−1	1				$\frac{2}{5}\ aM_I$
½	−½	−½	0	1	0	−½	1	½	$1\frac{1}{5}\ aM_I$
			1	1	−1				$1\frac{1}{5}\ aM_I$

With this table we hope to get information about the interaction with the nucleus for each multiplet if placed in a strong magnetic field. If we knew

this we could again apply the sum rule to each multiplet separately and obtain the interaction in a weak field or without field. Table V does not help us much in this respect, however. The different states are labeled with M_S and M_L only and we do not know the values of S and L to which they belong. For instance the pair $M_S=\frac{1}{2}$ and $M_L=0$ occurs three times. We do not know which one of these three belongs to the ^4S, the ^2D or the ^3P, which can each give this pair in a strong field. The answer to this question is that neither of the three belongs to any one of the multiplets. In the language of Slater's paper we should say that the energies entered in the last column of Table V have been calculated with eigenfunctions which do not take into account the interaction between the electrons. The correct eigenfunctions which can be associated with each multiplet are certain linear combinations of the ones which give the perturbation energies used here. The straightforward way to get further results is to use these linear combinations, which can be found in the literature,[20] and to use the quantum mechanics method for first order energy perturbations. In the following section we will describe a method, however, which does not involve the knowledge of the correct linear combinations of unperturbed eigenfunctions but uses certain general properties of multiplets.[21]

8. Hyperfine Structure of a Multiplet

The properties of a multiplet are in many respects a generalization of the properties of a doublet arising from a single electron. Darwin[22] was very successful in explaining every detail of the magnetic properties of a multiplet by treating it as if it were a single electron with an orbital moment L and a spin moment S. It is obvious that not all characteristics of a multiplet state can be obtained in this way; for instance, one would find with Darwin's method that the transition $L\rightarrow L$ is forbidden, whereas in the correct theory it is not. As we are interested here in the magnetic interaction with the nucleus, it is possible that we may use again Darwin's simplification.

For the magnetic interaction with the nucleus we assume a generalization of Eq. (7):

$$W_L + W_S = \lambda M_I M_L - \sigma M_I M_S \frac{6M_L^2 - 2L(L+1)}{(2L-1)(2L+3)}. \tag{31}$$

Before using this expression two important remarks have to be made. This formula does not apply to the interaction between the nucleus and an unbalanced s-electron in the configuration. The interaction with an s-electron is of the simple cosine form and gives therefore

$$W_S = \beta M_I M_S. \tag{32}$$

[20] J. A. Gaunt, Phil. Trans. **A228,** 184 (1929); J. H. Bartlett, Jr., Phys. Rev. **34,** 1247 (1929).

[21] Table V, as it is now, does not give us much more information than we obtained with the general sum rule data of Table I. The only additional information one gets is by considering the state with $M_S=1\frac{1}{2}$, $M_L=0$. This pair can only arise from the ^4S; the table gives an interaction energy zero, thus the ^4S will have $A=0$ in extreme Russell-Saunders coupling. So the sum of the energies belongs to the $^2D_{1\frac{1}{2}}$ and the $^2P_{1\frac{1}{2}}$, but further separation is not possible with this method.

[22] C. G. Darwin. Proc. Roy. Soc. **A115,** 1 (1927).

If the configuration to which the multiplet belongs contains such an s-electron one must add a term like Eq. (32) to Eq. (31). The second remark concerns the factors λ and σ. For the case of one single electron these were both equal to a. For a more complicated configuration one should not expect the coefficient for the orbital part to be the same as for the spin part. As we shall see later on it is possible to obtain a relation between λ and σ in certain simple cases.

In order to find the values of $A(J)$ for each level of the multiplet we must again consider the sums of the results of Eq. (31) for a fixed choice of $M_J = M_S + M_L$. One takes first $M_J = S+L$, which occurs only once, next $M_J = S+L-1$, occurring twice, and so on. The procedure is exactly the same as that followed in Section 3, but of course much longer, depending upon the values of S and L. It is possible to do it for general values of S and L and one obtains finally the general formula

$$A(J) = \lambda(2 - g) - \sigma\frac{6\Gamma(2 - g) - 2(g - 1)L(L + 1)}{(2L - 1)(2L + 3)} + \beta(g - 1). \qquad (33)$$

The last term occurs only when there is an unbalanced s-electron. In this formula g is the ordinary Landé g value, and Γ stands as usual for[23]

$$\Gamma = SL\cos(S, L) = \{J(J + 1) - L(L + 1) - S(S + 1)\}/2. \qquad (34)$$

The derivation of this formula is elementary but too cumbersome and long to be given here, but I am willing to give personal information about it to anyone who really might need it.

In the preceding sections of this paper we have always taken together the interaction W_S with the spin and W_l with the orbital moment. It is quite simple, however, to go back to Eq. (7) and keep these two separate. If we then know these interactions for only one level of a multiplet, we can determine λ and σ and find A for all other levels of the same multiplet. The sum rule of Table I or Table V will, in practically all cases, furnish us with sufficient information to do this. We shall show this again with the p^3 example.

For p^3 the sum rule gives that for $^2D_{2\frac{1}{2}}$ $A = {}^{24}/_{25}a$. If we go back to Eq. (7) via Table I we find that this is divided as follows between the interactions with spins and orbits:

$$\text{with spins: } {}^{4}/_{25}a, \quad \text{with orbits: } \tfrac{4}{5}a,$$

Furthermore, we know that for $^2D_{2\frac{1}{2}}$: $\Gamma = +1$, $g = 1\frac{1}{5}$ and we find from Eq. (33) (omitting the last term):

$$\tfrac{4}{5}a = \lambda\tfrac{4}{5}, \quad {}^{4}/_{25}a = -\sigma\frac{4\frac{4}{5} - 2\frac{2}{5}}{21}$$

from which

$$\lambda = a, \quad \sigma = -1\tfrac{2}{5}a.$$

[23] Γ is the deplacement of the level from the center of gravity of the multiplet.

With these values we find for the A of $^2D_{1\frac{1}{2}}$, for which $\Gamma = -1\frac{1}{2}$, $g = \frac{4}{5}$,

$$A(^2D_{1\frac{1}{2}}) = \lambda 1\tfrac{1}{5} - \sigma\frac{-10\frac{4}{5} + 2\frac{2}{5}}{21} = {}^{16}/_{25}a.$$

It is possible to find relations between λ and σ for the different multiplets of a configuration, or for the multiplets which arise after the addition of an s-electron. Lack of material to test such formulae make it useless to go into more detail, also with respect to the remarks made in the following section.

For intermediate coupling one can apply to a great extent the same method as used in a previous paper.[24]

9. Serious Discrepancies

The hyperfine structure is in many spectra caused by a deeply penetrating s electron, the influence of other electrons being negligibly small. For such cases the theory is simple, hyperfine structure separations can be expressed in terms of Landé cosines and the experimental data have been shown to agree with the theory.[25] For non-s electrons no such check has been obtained until now.

The following enumeration of data shows that there are large discrepancies between the theory and the observations for non-s electrons. Though the experimental results are very scarce and often uncertain, the reality of these discrepancies in the example of bismuth is beyond all doubt. The present material is quite insufficient, however, to give quantitative information about the deviations.

A part of the deviations will be due to higher order corrections. The method used in this paper assumes that it is sufficient to consider only first order perturbations for the interaction between the electrons and the spin orbit interactions. This means that our results are obtained by using only zeroth order eigenfunctions in the correct stabilized linear combinations. For heavy elements one must also consider the first order terms of the spin-orbit perturbation in the eigenfunctions. This will cause the hyperfine structure formulae to contain correction terms which are of exactly the same nature as those derived by Fermi[26] for the anomalies in the alkali doublet intensities. An estimate of the order of magnitude of these corrections shows that they are probably not large enough to account for the deviations.

Bismuth I[27] $(I = 4\frac{1}{2})$

$$6s^2 6p^3\ ^2D_{2\frac{1}{2}}: \quad \tfrac{4}{5}a' + \tfrac{1}{5}a'' = 0.081 \pm 0.002$$

$$^2P_{1\frac{1}{2}}: \quad a'' = 0.375$$

$$(^2D_{1\frac{1}{2}}: \ 1\tfrac{1}{5}a' - \tfrac{1}{5}a'' = -0.040 \pm 0.002).$$

[24] S. Goudsmit, Phys. Rev. **35,** 1325 (1930).

[25] S. Goudsmit and R. F. Bacher, Phys. Rev. **34,** 1501 (1929).

[26] E. Fermi, Zeits. f. Physik **59,** 680 (1930). This remark about the second order terms I owe to Dr. H. Casimir, with whom I discussed the discrepancies during his stay here last summer. Phys. Rev. in preparation.

[27] P. Zeeman, E. Back and S. Goudsmit, Zeits. f. Physik **66,** 1 (1930).

The coupling is not of the extreme (j, j) type. This does not, however, affect the validity of the formulae given for the first two levels, as they are the only ones with $J=2\frac{1}{2}$ and $\frac{1}{2}$ in this configuration. The two first equations give

$$6p\,J = \tfrac{1}{2}\colon\ a'' = 0.375$$
$$1\tfrac{1}{2}\colon\ a' = 0.007 \pm 0.003.$$

The second order corrections for this case are uncertain, a study of the levels of Bi III makes one believe that they should decrease a'' and increase a' by not more than about 5 percent. One sees that a' is much too small for the theory predicts that $a' = \frac{1}{5}a''$. Though the formula given for $^2D_{1\frac{1}{2}}$ is not strictly valid here, the negative value of its separation factor corroborates our conclusion that a' is much too small.

Bismuth II[28]

$$6s^2\,6p_1 7s \quad 2_1{}^0\colon \tfrac{1}{2}a'' + \tfrac{1}{2}b = 0.391 \pm 0.001$$
$$6p_{1\frac{1}{2}}7s \quad 9_2{}^0\colon \tfrac{3}{4}a' + \tfrac{1}{4}b = 0.109 \pm 0.007.$$

One expects the values for a'' and a' of the $6p$ electron in Bi II to be about the same as in Bi I. The above equations are indeed in agreement with this and give both for b about 0.38. If one assumed, however, that a' were really $\frac{1}{5}a''$ one would obtain an impossible negative value for b and a too large value for a' and a''.

Bi III

$$6s^2\,7p\ ^2P_{\frac{1}{2}}\colon\ a'' = 0.102 \pm 0.003$$
$$^2P_{1\frac{1}{2}}\colon\ a' = 0.021 \pm 0.004.$$

The second order corrections for the $7p$ electron are expected to be somewhat larger than for the $6p$. They tend to increase a'' by perhaps 10% and to decrease a' by about 5%. We have here a case where indeed the theoretical ratio between a' and a'' is close to the observed one, but one has to keep in mind that a' is not known with accuracy.

Manganese[29] $(I=2\frac{1}{2})$. Most of the hyperfine structure in manganese is caused by the $4s$ electron. For a few levels the hyperfine structure is due to the $3d$ and $4p$ electrons, but for these levels the separations are not known with sufficient accuracy to check any formulae.

Indium.[30] The measurements on the principal doublet of the indium spectrum made by McLennan and Allin and by Jackson differ so entirely from each other that they are useless.[31] This example would have been a very significant check of the theory.

[28] New observations on Bi II and III made by R. A. Fisher and the present author, to be published shortly. Classification and notation from J. C. McLennan, A. B. MacLay and M. F. Crawford, Proc. Roy. Soc. A. **129,** 579 (1931).

[29] H. E. White and R. Ritschl, Phys. Rev **35,** 1146 (1930).

[30] J. C. McLennan and E. J. Allin, Proc. Roy. Soc. **A128,** 508 (1930). D. A. Jackson, Proc. Roy. Soc. **A129,** 208 (1930).

[31] The fair agreement which Jackson seems to obtain between his measurements and the theory is caused by an unfortunate error in a paper by Fermi. Fermi (ref. 2) gives formulae for the hyperfine splitting of a $^2P_{1\frac{1}{2}}$ level in case $I \geqq 1\frac{1}{2}$. He mentions in the text how these formulae change for a case where $I<1\frac{1}{2}$ and just this sentence happens to be incorrect. Jackson's results again give a' too small.

Thallium I. ($I=\frac{1}{2}$). Only one of the two lines of the principal doublet of thallium has been studied in detail.[32] The present data on the other line are insufficient to draw any certain conclusions, though they also seem to indicate for this case that a' is too small.

Thallium III.[33]

$$7p\ {}^2P_{\frac{1}{2}}: \quad a'' = 0.375$$
$$ {}^2P_{1\frac{1}{2}}: \quad a' = 0.218.$$

The second order corrections are rather large in this case, namely about 15%. They would increase a'' and decrease a'. For this example a' is much larger than the theoretical value.

Conclusion

Though the experimental data are scarce we come to the conclusion that the present theory of the hyperfine structure separations is incorrect or at least incomplete. The method used in this paper is not the cause, for it has been applied very successfully to many other problems, but the use of the classical Eq. (3),

$$W_l + W_s = a[Il\cos(I,l) - Is\cos(I,s) + 3Is\cos(I,r)\cos(r,s)].$$

The correct quantum mechanical expression for the spin-spin interaction will perhaps contain different terms. The generalizations of the Dirac theory for the two-body problem given by Gaunt[34] and Breit[35] contain indeed extra terms for the spin-spin interaction. From a study of the helium triplet, with which one can test a part of these extra terms, Breit[36] concluded that their presence was in disagreement with the experimental data on the spin-spin interaction of two electrons. Perhaps such terms do have a real significance for the interaction between nuclear and electron spin[37].

This discussion shows the importance of the study of hyperfine structure as a guide for the further development of the quantum theory, especially for the generalization of the Dirac equation. Let us, therefore, hope that experimental physics will soon provide us with at least one doublet state for which the hyperfine structure of both levels can be given with certainty and accuracy.

Appendix

Just before sending off this paper I received a letter from Dr. John Wulff, National Research Fellow at Tübingen, in which he describes important new measurements on the hyperfine structure as well as the Zeeman effect of the principal thallium doublet. The $6p_{\frac{1}{2}}$ level has $a''=0.708$, whereas the $6p_{1\frac{1}{2}}$ level is unresolvably small. The value for a' is probably of the order 0.015, thus about ten times too small.

[32] E. Back and J. Wulff, Zeits. f. Physik **66,** 31 (1930).
[33] J. C. McLennan and E. J. Allin, Proc. Roy. Soc. **A129,** 43 (1930).
[34] J. A. Gaunt, Phil. Trans. **228,** 151 (1929). Proc. Roy. Soc. **A122,** 153 (1929).
[35] G. Breit, Phys. Rev. **34,** 553 (1929).
[36] G. Breit, Phys. Rev. **36,** 383 (1930).
[37] This will be discussed in a paper by D. R. Inglis, to be published soon.

THE VAN DER WAALS FORCES IN GASES

By John C. Slater and John G. Kirkwood
Massachusetts Institute of Technology

(Received February 5, 1931)

Abstract

A calculation of van der Waal's potential of two atoms at large separation has been carried out for hydrogen and helium. The method depends upon a representation of the perturbed wave function of the system as

$$\psi = \psi_0 (1 + vR)$$

where ψ_0 is the unperturbed wave function, v the perturbing potential and R is a function of the radial coordinates of the electrons. The method is equally well adapted to the calculation of polarizabilities. A computation of the mutual energy of two hydrogen atoms confirms the results of Eisenschitz and London. The polarizability of helium is calculated as 0.210×10^{-24} cc which agrees well with the experimental value, 0.205×10^{-24}. The mutual energy of two helium atoms is found to be $-3.18\, E_0 / (R/a_0)^6$. A correlation between the mutual energy of the two molecules, ϵ, and the polarizability, α, is obtained:

$$\epsilon = -1.36\, \nu_0^{1/2}\, a_0^{3/2}\, \alpha^{3/2}\, E_0\, R^6$$

where ν_0 is the number of electrons in the highest quantum state in the molecule, E_0 the energy of the hydrogen atom in the normal state, and R is the separation of the molecules. By means of this formula, the van der Waals cohesive pressure constant is calculated for Xe, A, N_2, H_2, O_2, and CH_4.

I. Introduction

IT HAS been recognized for some time that the van der Waals forces in gases have their origin in a mutual polarization of the molecules. The idea was suggested by Debye,[1] but his calculation of intermolecular energies, based upon an electrostatic molecular model, did not meet with great success. This fact is not surprising in the light of recent work, which has shown that a rapidly pulsating field associated with the internal motion of the electrons in the molecule is the chief factor in determining the mutual energy of two molecules at separations sufficiently large to prevent the exchange of electrons. This fact was suggested, although not explicitly stated, in a calculation of the mutual energy of two hydrogen atoms by Wang.[2] Recently, Eisenschitz and London[3] have presented a general method of calculating the mutual energy of two molecules at large separation. Their method depends upon an expansion of the wave function of the system in terms of a selected set of the unperturbed wave functions of the two molecules. They have confirmed the form of Wang's result for two hydrogen atoms, although they have shown

[1] Debye, Phys. Zeits. **21,** 178 (1920).

[2] S. C. Wang, Phys. Zeits. **28,** 663 (1927).

[3] Eisenschitz and London, Zeits. f. Physik **60,** 491 (1930); London, Zeits. f. Physik **63,** 245 (1930).

it to be numerically in error. Hassé,[4] with a variational method, has calculated the polarizability of helium. The wave function obtained by Waller[5] in a treatment of the quadratic Stark effect in hydrogen, serves as a basis for the calculation. An empirical extension of the method employed in this case permits him to calculate the mutual energy of two atoms at large separation both for hydrogen and helium.

The present method resembles that of Hassé in that use is made of the variation principle. However, his choice of wave function was more or less empirical and the perturbation energy was calculated as a part of the total energy. On the other hand, we have formulated the variation problem for a direct determination of the perturbation energy by itself, and from the original wave equation have obtained a simplified Euler equation for this variation problem, which when it cannot be solved directly, serves as a guide in choosing an approximate function. The method, while lacking the generality of that of London and Eisenschitz, is applicable to most non-polar molecules in the normal state.

II. Polarizability and Interatomic Energy of Hydrogen

We shall begin by considering a system of ν electrons with an unperturbed wave function ψ_0, while the correct wave function under the influence of a perturbing potential v is ψ. The wave equations in the two cases may be written

$$\begin{aligned} \nabla^2\psi_0 + \kappa^2(E_0 - V_0)\psi_0 &= 0 \\ \nabla^2\psi + \kappa^2(E - V)\psi &= 0 \\ \kappa^2 &= 8\pi^2 m/h^2 \\ E &= E_0 + \epsilon \\ V &= V_0 + v. \end{aligned} \tag{1}$$

Here E_0 and V_0 are the initial total and potential energies of the system and ϵ is the energy acquired by virtue of the perturbation. The operator ∇^2 is understood to be referred to the 3ν dimensional configuration of the system of ν electrons. If we let

$$\psi = \psi_0(1 + \phi) \tag{2}$$

we obtain the following equation

$$\nabla^2\phi + 2\sum_{i=1}^{3\nu} \frac{\partial \ln \psi_0}{\partial x_i} \frac{\partial \phi}{\partial x_i} + \kappa^2(\epsilon - v)(1 + \phi) = 0. \tag{3}$$

Since we shall not be interested in perturbation effects of higher order than the second, it is only necessary to retain terms of the first order in v and ϕ. Thus we can replace the factor $(1+\phi)$ by 1, since it is multiplied by a small quantity. Further, in all the cases to which our method is applicable, the mean value of the perturbing potential over the unperturbed wave function

[4] H. R. Hassé, Proc. Camb. Phil. Soc. **26,** 542 (1930).
[5] Waller, Zeits. f. Physik **38,** 635 (1926).

is zero, the first order perturbation in the energy vanishes, and ϵ is small of the second order. For this reason we may replace $\epsilon - v$ by $-v$, obtaining an equation which does not contain an energy parameter at all. When we make these approximations, Eq. (3) becomes

$$\nabla^2\phi + 2\sum_{j=1}^{3v} \frac{\partial \ln \psi_0}{\partial x_j} \frac{\partial \phi}{\partial x_j} - \kappa^2 v = 0. \tag{4}$$

The polarization of the hydrogen atom in its normal state by an homogeneous electric field, F, affords the simplest example of the application of Eq. (4). Here

$$\begin{aligned} \psi_0 &= e^{-r} \\ v &= \sum_{j=1}^{3} g_j x_j \end{aligned} \tag{5}$$

where r is the radial distance of the electron from the nucleus expressed in units of a_0, the Bohr radius of the normal state, and

$$g_j = -eF_{x_j}.$$

The components F_{x_j} of the field, F, are referred to a rectangular system of coordinates with origin in the nucleus of the atom. If we choose as new variables, r and v, and if we let

$$\phi = \frac{vR(r)}{E_0} \tag{6}$$

where E_0 is the absolute value of the energy of the hydrogen atom in the normal state, a separation of variables in Eq. (4) is effected and there results

$$\frac{d^2R}{dr^2} + \left(\frac{4}{r} - 2\right)\frac{dR}{dr} - \frac{2R}{r} - 1 = 0 \tag{7}$$

where r is measured in units of a_0. The solution is

$$R = -\frac{1}{2}\left(1 + \frac{r}{2}\right) + C_1\left(\frac{1}{r} + \frac{1}{r^2} + \frac{1}{2r^3}\right) + C_2\frac{e^{2r}}{r}.$$

In order that the integral

$$\int \psi\bar{\psi}d\tau$$

may exist, it is necessary to set C_1 and C_2 equal to zero. The new wave function takes the form

$$\psi = e^{-r}\left(1 - \frac{v}{2E_0}\left[1 + \frac{r}{2}\right]\right).$$

If the original rectangular coordinate system is chosen with z-axis parallel to the field, $v = -eFz$, and the above wave function becomes identical with that obtained by Waller.[6] The energy is given by

[6] Waller, reference 5.

$$E = E_0 + \epsilon = -\frac{1}{\kappa^2}\frac{\int \bar{\psi} H \psi d\tau}{\int \psi \bar{\psi} d\tau}.$$

When ϕ has the form, $vR(r)$, and ψ_0 is a function of r alone, the integrals occurring in the evaluation of ϵ are of the form

$$\int v^n f(r) d\tau \quad n = 1, 2, 3.$$

If v is a harmonic function which vanishes when r is zero, the term for $n=1$ (and $n=3$) vanishes. That is, the first order perturbation energy is zero. Then the only term which we need consider is the one with $n=2$. This condition is of course fulfilled in the problem which we have just considered, and will be fulfilled in the subsequent problems to be treated. The expression for ϵ now becomes

$$\epsilon = \frac{\int v\phi\psi_0^2 d\tau}{\int \psi_0^2 d\tau} \tag{8}$$

with the neglect of perturbation terms in the normalization of ψ. These will contribute only to terms in ϵ of higher order than the second.

A computation of the polarization energy of the hydrogen atom using the wave function which we have obtained yields

$$\epsilon = -2.25 a_0^3 F^2$$

which corresponds to a polarizability

$$\alpha = 4.5 a_0^3.$$

These, values, of course, agree with those obtained by Waller.

In this simple case, the solution of Eq. (7) offers no difficulty. It is of interest, nevertheless, to see what value of the energy may be obtained, if our information is restricted to the fact that $\phi = vR(r)$. Let us try as a representation of $R(r)$ the expression, λr^r. The energy integral becomes

$$\epsilon = \frac{\int v\phi[1 - \rho[R]]\psi_0^2 d\tau}{\int \psi_0^2 d\tau} \tag{8}$$

where

$$\rho[R] = \frac{d^2R}{dr^2} + \left(\frac{4}{r} - 2\right)\frac{dR}{dr} - \frac{2R}{r} - 1.$$

If we minimize the integral with respect to the parameters λ and ν, we obtain

$$\epsilon = -2.24 a_0^3 F^2$$
$$\lambda = -0.728/E_0; \quad \nu = 0.5.$$

This value agrees with the exact one to somewhat better than 0.50%.

The method may be applied with almost equal simplicity to the interaction of two hydrogen atoms. If the separation, R_0, of the two atoms is sufficiently large to prevent electron interchange, the wave function of the system is

$$\psi_0 = \psi_{01}\psi_{02} = e^{-(r_1+r_2)}$$

where r_1 and r_2 are the respective radial distances of each electron from its own nucleus. When referred to two rectangular coordinate systems with their respective origins in the two nuclei and with z-axes directed along R_0, the dipole term in the perturbing potential is given by

$$\frac{e^2}{R_0^3}[x_1x_2 + y_1y_2 - 2z_1z_2].$$

Terms due to multipoles of higher order will be neglected. If we let

$$\phi = \frac{vR(r_1, r_2)}{E_0}$$

and change the variables in Eq. (4) to v, r_1 and r_2, a separation is again effected and we have

$$\frac{\partial^2 R}{\partial r_1^2} + \frac{\partial^2 R}{\partial r_2^2} + \left(\frac{4}{r_1} - 2\right)\frac{\partial R}{\partial r_1} + \left(\frac{4}{r_2} - 2\right)\frac{\partial R}{\partial r_2} - 2R\left(\frac{1}{r_1} + \frac{1}{r_2}\right) - 1 = 0 \quad (9)$$

The existence of a solution of this equation is assured by the negative value of the coefficient of R.[7] A solution by successive approximation may be obtained in the following manner. Let us write Eq. (9) as

$$R = -\frac{1}{2}\frac{r_1r_2}{r_1 + r_2}\left\{1 - \left[\frac{\partial^2 R}{\partial r_1^2} + \frac{\partial^2 R}{\partial r_2^2} + \left(\frac{4}{r_1} - 2\right)\frac{\partial R}{\partial r_1} + \left(\frac{4}{r_2} - 2\right)\frac{\partial R}{\partial r_2}\right]\right\}.$$

If the differential function is neglected

$$R = -\frac{1}{2}\frac{r_1r_2}{r_1 + r_2}. \quad (10)$$

Substitution of this expression in the differential function will yield a second approximation. Repetition of this process will yield a still closer approximation. If we use merely the first approximation (10), we calculate a value of the energy,

$$\epsilon = -0.14\frac{e^2a_0^5}{R_0^6}.$$

[7] Goursat, Cours d'Analyse Mathematique, vol. III, 249.

This is about 5 percent higher than the value

$$-6.47\frac{e^2a_0^5}{R_0^6}$$

obtained by Eisenschitz and London.[8] The use of higher terms in the expansion of R would permit us to approach the true value as closely as we pleased. Although no difficulty is encountered in the evaluation of the integrals occurring in the energy expression, the tedium of the calculation is reduced by using the variation method. Eq. (10) suggests as a representation of R, the expression

$$\lambda r_1^{\nu} r_2^{\nu}.$$

If the function is inserted in the energy integral and the latter is minimized with respect to the parameters λ and ν one obtains

$$\epsilon = -6.49\frac{e^2a_0^5}{R_0^6}$$

$$\nu = 0.325.$$

This is in excellent agreement with the result of London and Eisenschitz. The fact that their value lies slightly higher instead of slightly lower than the one which has just been obtained is doubtless attributable to an error in estimating the contribution of the continuous spectrum in their expansion of ψ, since the variation method cannot give too low a value of the energy.

The fact that the wave function in the two cases which have been considered may be expressed as

$$\psi_0(1 + vR)$$

where R is a function of the radial distances of the electrons from their nuclei, is indeed logical from a physical point of view. In the absence of degeneracy, one would expect the distortion of the wave function to depend in some simple way upon the perturbing potential. Moreover, for a given value of the perturbing potential it is evident that the distortion will be greater, as the distance of the electron from the nucleus becomes greater, since the restoring force exerted by the nucleus will be smaller. The function R provides for this effect. The separation of the differential Eq. (4) in terms of v and the r's appears to depend upon the linear properties of v in the rectangular coordinates of the electrons, and the spherical symmetry of the unperturbed wave function.

III. Generalization of the Method: Polarizability and Interatomic Energy of Helium

For the helium atom, or in general for an atom with ν electrons each having a spherically symmetrical distribution, the wave function may be approximately represented by

$$\psi_0 = \prod_{i=1}^{\nu}\psi_i(r_i) \tag{11}$$

[8] Eisenschitz and London, reference 3.

where the function ψ_j depends only upon the radial coordinate of the electron j. Such a function may be approximated by an expression

$$r^{n-1}e^{-(Z-s)r/n}$$

where n is an effective quantum number, s a screening constant, Z the total nuclear charge. If we wish to represent the wave function accurately in the region of its maximum, we may choose n and s by minimizing the total energy, as Zener has done. If, however, we are more interested in the value of the function for large values of r, we may choose s to be equal to the total number of electrons except for the one being considered, and use an effective quantum number which is non-integral. Thus for He, in the neighborhood of the maximum, we choose $Z-s=1.6875$ (or, for some purposes, 1.70), $n=1$; while for large r's, we take $Z-s=1$, $n=0.745$.[9] We use these formulas for approximate computation of polarizability and interatomic force.

A better representation of the wave function can be obtained by more complicated methods, as that of Hartree,[10] or the method used by one of the authors on He.[11] These give almost identical results for He, as far as the purposes of this paper go, and for quantitative work we make use of the latter in one calculation of the polarizability and interatomic energy of helium.

We shall first consider the polarization of the molecule by an homogeneous field F. The perturbing potential is

$$v = \sum_{j=1}^{\nu} v_j$$

where

$$v_j = -e\sum_{k=1}^{3} F_{zjk}x_{jk}$$

If we let

$$\phi = \frac{1}{E_0}\sum_{j=1}^{\nu} v_j R(r_j) \tag{12}$$

and make use of the facts that $\partial \ln \psi_0/\partial r_j$ depends only upon r_j, the distance of electron j from the nucleus and that

$$\sum_{k=1}^{3} x_{jk}\frac{\partial v}{\partial x_{jk}} = v_j$$

we find that Eq. (4) splits into ν equations of the form

$$\frac{d^2R}{dr^2} + \left(\frac{4}{r} + 2\frac{d \ln \psi_0}{dr}\right)\frac{dR}{dr} + \frac{d \ln \psi_0}{dr}\frac{R}{r} - 1 = 0. \tag{13}$$

If we use a wave function of the simpler type discussed above this equation becomes

[9] C. Zener, Phys. Rev. **36,** 51 (1930); J. C. Slater, Phys. Rev. **32,** 349 (1928); J. C. Slater, Phys. Rev. **36,** 57 (1930).

[10] D. R. Hartree, Proc. Camb. Phil. Soc. **24,** 89 (1928).

[11] J. C. Slater, Phys. Rev. **32,** 349 (1928).

$$\frac{d^2R}{dr^2} + 2\left(\frac{n+1}{r} - \frac{Z-s}{n}\right)\frac{dR}{dr} + 2\left(\frac{n-1}{r^2} - \frac{Z-s}{nr}\right)R - 1 = 0. \quad (14)$$

The energy given by Eq. (8) is

$$\epsilon = \frac{\int \sum_{j=1}^{\nu} \sum_{k=1}^{\nu} v_j \phi_k \psi_0^2 d\tau}{\int \psi_0^2 d\tau}.$$

Since upon integration all terms involving $v_j\phi_k$ with $j \neq k$ vanish

$$\epsilon = \sum_{j=1}^{\nu} \epsilon_j$$

and

$$\epsilon_j = \frac{\int v_j \phi_j \psi_0^2 d\tau}{\int \psi_0^2 d\tau}.$$

In the computation of ϵ_j it will be convenient to use the variation method rather than to solve Eq. (14) explicitly. The expression becomes

$$\epsilon_j = \frac{\int v_j \phi_j [1 - \rho[R_j]] \psi_0^2 d\tau}{\int \psi_0^2 d\tau}$$

where

$$\rho[R_j] = \frac{d^2R_j}{dr_j^2} + 2\left(\frac{n_j+1}{r_j} - \frac{Z-s_j}{n_j}\right)\frac{dR_j}{dr_j} + 2\left(\frac{n_j-1}{r_j^2} - \frac{Z-s_j}{n_j r_j}\right)R_j - 1.$$

We shall try

$$R = \lambda e^{\beta(z-s)r/n}$$

which is analytically somewhat more convenient than the representation λr^{ν} employed in the case of hydrogen. When the energy integral is minimized with respect to the parameter λ there results

$$\epsilon = \frac{1}{E_0}\frac{J_1^2}{J_2}e^2F^2$$

where

$$J_1 = \frac{\int r^{2n}\cos^2\theta e^{\beta(z-s)r/n}\psi_0^2 d\tau}{\int \psi_0^2 d\tau}$$

$$= \frac{(n+1)(n+\frac{1}{2})}{3}\left(\frac{n}{Z-s}\right)^2 a_0^2 \frac{1}{(1-\beta/2)^{2n+3}}$$

$$J_2 = \frac{\int \left\{ \left(\frac{n}{Z-s} \right)^2 (\beta^2 - 2\beta) r^{2n} + \frac{n}{Z-s} [(n+1)\beta - 1] r^{2n-1} + 2(n-1) r^{2n-2} \right\}}{\int \psi_0^2 d\tau}$$

$$e^{2\beta(z-s)r/n} \cos^2\theta \psi_0^2 d\tau = -a_0 \frac{1 + (2n-5)\beta/3 + (2n^2 - n + 5)\beta^2/6}{(1-\beta)^{2n+3}}.$$

For the energy we have

$$\epsilon_j = -2 \frac{(n_j+1)^2 (n_j + \frac{1}{2})^2 n_j^4}{9(Z-s_j)^4} a_0^3 F^2 (1+\theta_j) \tag{13a}$$

where

$$\theta_j = \frac{(1-\beta)^{2n_j+3}}{(1-\beta/2)^{4n_j+6}[1 + (2n_j - 5)\beta/3 + (2n_j^2 - n_j + 5)\beta^2/6]} - 1$$

Minimizing with respect to β shows that for $n=1$, $\theta_j = 0.124$. In general $0.124 \geqq \theta_j \geqq 0$; $n_j \geqq 1$. For the total polarization energy we may write

$$\epsilon = -2a_0^3 F^2 \sum_{j=1}^{\nu} \frac{n_j^4 (n_j+1)^2 (n_j + \frac{1}{2})^2 (1+\theta_j)}{9(Z-s_j)^4}$$

and for the polarizability

$$\alpha = 4a_0^3 \sum_{j=1}^{\nu} \frac{n_j^4 (n_j+1)^2 (n_j + \frac{1}{2})^2 (1+\theta_j)}{9(Z-s_j)^4}.$$

We shall first compute the polarizability of helium taking n as 1 and $Z-s$ as 1.6875, the values obtained by minimizing the total energy of the atom. We obtain

$$\alpha = 1.11 a_0^3 = 0.164 \times 10^{-24} \text{cc}.$$

If on the other hand we use the limiting values at large distances for n and $Z-s$ we have $n=0.745$; $Z-s=1$, and we obtain

$$\alpha = 1.51 a_0^3 = 0.222 \times 10^{-24} \text{cc}.$$

The value of α corresponding to measurements of the refractive index is 0.205×10^{-24}. As we should have anticipated it lies between the two values which we have calculated. The first wave function which emphasizes the smaller r's at the expense of the larger gives a value of α about 20 percent below the experimental one, while the second wave function which emphasizes the larger r's gives a value about 8 percent higher than the experimental one. The second wave function which is accurate only for large values of r gives a surprisingly good result.

A more exact determination of the polarizability of helium may be obtained with the use of the more accurate wave function mentioned above. After normalization and integration over the configuration space of one electron, the square of the wave function for each electron may be represented by

$$0.7604(1 + 1.440e^{-1.692r})e^{-3r+0.0214r^2};\ r < 3$$

$$0.6048(1 + 1.440e^{-1.692r})e^{-2.688r}r^{-0.510}\left(1 + \frac{0.1414}{r} + \cdots\right);\ r > 3.$$

We shall use as a representation of R the function λr^ν. Minimizing the energy integral with respect to the parameter λ gives

$$\epsilon = \frac{1}{E_0}\frac{J_1^2}{J_2 J_0}e^2a_0^2F^2$$

where

$$J_0 = \int \psi_0^2 d\tau$$

$$J_1 = \int r^{\nu+2}\psi_0^2 d\tau$$

$$J_2 = \int \left\{ \nu(\nu + 2)r^{2\nu} + 2(\nu + 1)\frac{d \ln \psi_0}{dr} r^{2\nu+1} \right\} \psi_0^2 d\tau.$$

Properly, this expression should be computed for different ν's and the minimum chosen. On account of the labor of the integration, however, we have arbitrarily chosen the value $\nu = 0.5$. This was the value found for the simple wave functions used above, and moreover it was found that the result was so insensitive to ν that a variation of ± 0.1 in ν did not affect the final result by more than one percent. The above integrals have been computed graphically for $\nu = 0.5$ and the polarizability of helium was found to be

$$\alpha = 1.43a_0^3 = 0.210 \times 10^{-24}\text{cc}.$$

This yields a value of the dielectric constant at 0° and 1 atm. of 1.0000715 which is slightly lower than the experimental value, 1.000074. It is however, somewhat higher than the square of the measured refractive index extrapolated to infinite wave-length, 1.000070. The agreement among the various values is not unsatisfactory when one remembers that the accuracy in the measured refractive index, and dielectric constant cannot be very great, in view of the experimental difficulties in such measurements.

A calculation of the mutual energy of two atoms may be carried out in a similar manner. The dipole term in the perturbation potential may be written

$$v = \sum_{j=1}^{p}{}' \sum_{k=1}^{p}{}' v_{jk}$$

where the sum is understood to be taken over all possible electron pairs between the two atoms. Each v_{jk} has the form

$$\frac{e^2}{R_0^3}[x_k x_j + y_k y_j - 2z_k z_j].$$

If we let

$$\phi = \frac{1}{E_0} \sum_{j=1}^{\nu}{}' \sum_{k=1}^{\nu}{}' v_{jk} R(r_j, r_k).$$

Eq. (4) separates into ν^2 equations of the form

$$\frac{\partial^2 R}{\partial r_j^2} + \frac{\partial^2 R}{\partial r_k^2} + \left(\frac{4}{r_j} + \frac{2\partial \ln \psi_0}{\partial r_j} \right) \frac{\partial R}{\partial r_j} + \left(\frac{4}{r_k} + \frac{2\partial \ln \psi_0}{\partial r_k} \right) \frac{\partial R}{\partial r_k} + 2R \left(\frac{1}{r_j} \frac{\partial \ln \psi_0}{\partial r_j} + \frac{1}{r_k} \frac{\partial \ln \psi_0}{\partial r_k} \right) - 1 = 0. \tag{17}$$

Moreover the energy may be written

$$\epsilon = \sum_{j=1}^{\nu}{}' \sum_{k=1}^{\nu}{}' \epsilon_{jk}$$

where

$$\epsilon_{jk} = \frac{\int v_{jk} \phi_{jk} (1 - \rho_{jk}) \psi_0^2 d\tau}{\int \psi_0^2 d\tau}.$$

If an exact solution of Eq. (17) is used, ρ_{jk} which is the differential expression on the left hand side of Eq. (17) vanishes. We shall use the two representations

$$R_{jk} = \lambda r_j^{\nu} r_k^{\nu}; \quad R_{jk} = \lambda e^{\beta(r_j + r_k)}$$

which proved effective in the case of hydrogen, according to their analytical convenience in conjunction with the unperturbed wave function which is chosen. The parameters are determined by minimizing the energy integral. The details of the calculation are quite similar to those in the calculation of polarizabilities. With the simple wave function

$$\psi_0 = \prod_{j=1}^{\nu} r_j^{n_j - 1} e^{-\gamma_j r_j / n_j}; \quad \gamma_j = Z - s_j$$

we obtain the following result

$$\epsilon = -\frac{13}{27} \frac{e^2 a_0^5}{R_0^6} \sum_{j=1}^{\nu} \sum_{k=1}^{\nu} \frac{n_j^4 n_k^4 (n_j+1)^2 (n_j+\frac{1}{2})^2 (n_k+1)^2 (n_k+\frac{1}{2})^2}{\gamma_j^2 \gamma_k^2 \{ \gamma_k^2 n_j^2 (n_j+1)(n_j+\frac{1}{2}) + \gamma_j^2 n_k^2 (n_k+1)(n_k+\frac{1}{2}) \}} \tag{18}$$

For convenience in representation certain factors $1+\theta_{jk}$ occurring in each term have all been assigned the value which they assume for 1-quantum electrons. Since

$$0 \leqq \theta_{jk} \leqq 0.07$$

the above formula will approximate the true one to within a few percent in every case. We shall calculate the mutual energy of two helium atoms first taking $Z-s=1.6875$ and $n=1$. We obtain

$$\epsilon = -1.13\frac{e^2a_0^5}{R_0^6}.$$

If we now take the values $n=0.745$, $Z-s=1$, which occur in the asymptotic form of the wave function we obtain as in the case of the polarizability a somewhat larger value:

$$\epsilon = -1.78\frac{e^2a_0^5}{R_0^6}.$$

The same calculation has been made with the use of the more accurate wave function for He. As a representation of the function R, $\lambda r_j^{\nu} r_k^{\nu}$ was selected. The integrals, similar to those encountered in the calculation of the polarizability, were evaluated graphically. The energy of two helium atoms was computed as

$$\epsilon = -1.59\frac{e^2a_0^5}{R_0^6} = -3.18\frac{E_0}{(R_0/a_0)^6}.$$

This value lies between the two values obtained with the hydrogenic wave function. It is about 30 percent higher than that obtained with values of Z and n determined to give the best energy for the atom and about 13 percent below the value obtained with the asymptotic values of n and Z. Since the wave function which gave the above value also gives a good value of the polarizability, it is likely that the above value is correct within one or two percent. Hassé obtains a value

$$-2.93\frac{E_0}{(R/a_0)^6}$$

which differs from our result by about 8 percent. Both of these values are slightly above the upper limit for the mutual energy of two helium atoms calculated by London:

$$\epsilon = -3/4\alpha^2 V_i/R^6$$

where α is the polarizability and V_j the ionization potential. This has the value

$$-2.65\frac{E_0}{(R/a_0)^6}.$$

The fact that both Hassé's and our values lie above London's upper limit is not to be considered as alarming. For London, in using the second order perturbation method, neglected a factor which has been rather consistently overlooked in such calculations: transitions in which two electrons are excited may contribute appreciably to the dispersion and similar terms, and they are connected with larger energy differences than the ionization potential, so that in the upper limit of such an expression as London's we should really have the highest potential connected with a double jump, much larger than V_i. The relation of our results to London's limit suggests that these double jumps are strong enough to shift the center of gravity of the term system beyond the ionization potential.

A result of considerable interest may be obtained from formulas (16) and (18). While neither of them gives particularly accurate representations of α or ϵ, it is possible to reach through them a correlation between these two quantities. First, it is to be noted that in both formulas only terms arising from electrons in the outer shell of the atoms contribute appreciably to the sums. Terms arising from inner shells (if any), are virtually nullified both through a decrease in the effective quantum number and by an increase in the effective nuclear charge. We may therefore write

$$\alpha = \frac{4.5 \nu_0 a_0^3}{(Z - S_0)^4} \frac{n_0^4 (n_0 + 1)^2 (n_0 + \frac{1}{2})^2}{9}$$

$$\epsilon = -\frac{6.5 \nu_0^2}{(Z - S_0)^6} \frac{e^2 a_0^5}{R_0^6} \frac{n_0^6 (n_0 + 1)^3 (n_0 + \frac{1}{2})^3}{27}$$

where ν_0 is the number of electrons in the outer shell of the atom; n_0 and S_0 are the effective quantum number and screening constant of these electrons. Elimination of n_0 and $(Z - S_0)$ gives

$$\epsilon = -\beta / R_0^6$$

where

$$\beta = 1.36 \nu_0^{1/2} a_0^{3/2} \alpha^{3/2} E_0. \tag{19}$$

Corresponding to the empirically determined polarizability for He, this gives a value $\beta = 3.16 a_0^6 E_0$. This is in excellent agreement with the value 3.18, calculated with the aid of the accurate wave function above.

IV. Correlation with the Equation of State

Although the computation of the last section applied only to atoms for which each electron had a spherically symmetrical distribution, still it is interesting provisionally to compute van der Waals forces in other cases from the polarizability. In cases where the whole atom is spherically symmetrical, though individual electrons are not, this seems fairly reasonable. Thus we obtain values of $\beta / a_0^6 E_0$ for the noble gases as listed in Table I:

Table I.

He	Ne	A	Kr	Xe
3.16	17.0	148	275	582

These values can be tested by calculating the equation of state. Of course, the attractive force is not the only interatomic force; there is also a repulsive force, increasing very rapidly as the atoms approach. This is often represented by assuming the atoms to be rigid, and if the van der Waals attraction is fairly large this is justified. For He, however, large errors are committed by this assumption. The repulsive potential has been computed for atomic hy-

drogen[12] and for helium.[13] It appears possible to represent it in the range of importance in thermal interaction between gas molecules by the approximation formula

$$\epsilon_r = \lambda e^{-cR_0}.$$

It should therefore be possible to write approximately

$$\epsilon = \lambda e^{-cR_0} - \beta/R_0^6$$

for the total interaction energy of two molecules. If the equation of state of a gas is written in the familiar virial form

$$\frac{pV}{RT} = 1 + \frac{B}{V} +$$

where p is the pressure, V the volume, R the ideal gas constant, and T the absolute temperature, it is possible to show that at high temperatures

$$B = 2\pi N \int_0^\infty (1 - e^{-\epsilon/kT}) R^2 dR$$

under the assumption the molecules are spherically symmetrical. Here ϵ is the mutual potential energy of two molecules. If, further the molecules are treated as rigid spheres of diameter σ, and the exponential function in the above integral is expanded, it is found that approximately

$$B = B_0 - A/RT$$

where

$$B_0 = \frac{2\pi N\sigma^3}{3}$$

$$A = -2\pi N^2 \int_\sigma^\infty \epsilon R^2 dR$$

and the equation of state may be written in the van der Waals form

$$p = \frac{RT}{V - B_0} - \frac{A}{V^2}.$$

Moreover, if the repulsive potential is ignored when $R > \sigma$, we may replace ϵ by ϵ_a calculated from Eq. (19). The expression for A then becomes

$$A = 4.76 \times 10^{11}\beta/B_0 \text{ ergs cc/mol} \qquad (20)$$

where B_0 is expressed in cc/mol. It is to be remembered that this is a very rough approximation, for in reality the repulsive potential cannot be adequately represented by a potential wall which rises to infinity when $R = \sigma$. This model is indeed entirely inadequate when the attractive field is very

[12] Heitler and London, Zeits. f. Physik **44**, 455 (1927); Suguira, Zeits. f. Physik **45**, 484 (1927).

[13] J. C. Slater, reference 11.

weak as in the case of helium and hydrogen. This is illustrated in Fig. 1. The interatomic potential

$$\epsilon = \left\{ 7.7e^{-2.43R/a_0} - \frac{0.68}{(R/a_0)^6} \right\} \cdot 10^{-10} \text{ ergs}$$

which we have obtained for helium has been plotted as a function of the separation of the two atoms. The dotted line represents the attractive component alone and the distance marked σ on the R-axis represents the effective atomic diameter calculated from the van der Waals B_0 constant. In a later

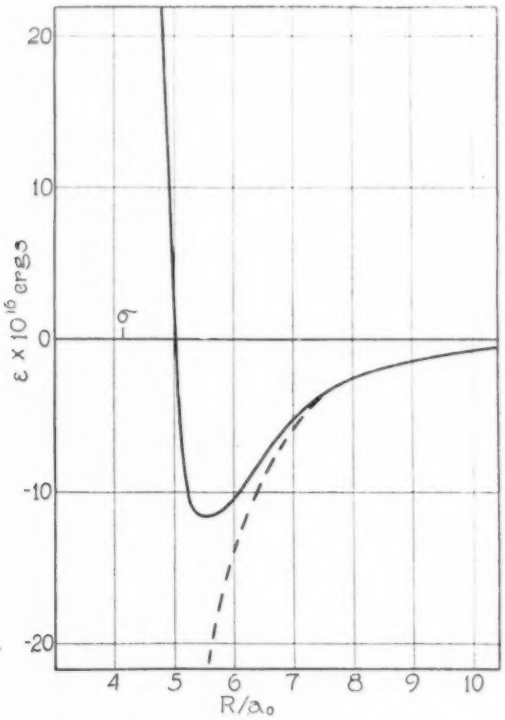

Fig. 1. The mutual energy of two helium atoms plotted as a function of the interatomic distance.

paper a calculation of the second virial coefficient B of helium, based upon the above expression for the interatomic potential, will be presented. It leads to an equation of state and to a description of the thermodynamic properties of helium which are in striking agreement with experiment.

In the present paper, however, we shall content ourselves with the approximation of rigid molecules. We have calculated values of A for several gases by means of Eqs. (19) and (20), from the experimental values of the refractive index and the constant B_0. We have not restricted ourselves to the noble gases, but have included several gases with poly-atomic molecules. The electron configuration in most non-polar molecules resembles that of the noble gases except in the particular case of spherical symmetry. It was thought

that Eq. (19) might still be approximately valid in these cases, since most of the characteristics of the wave function employed in the calculation of α and ϵ were eliminated in the formulation of this relation. The computed values of A are compared with the empirical values of Beattie and Bridgeman[14] in Table II. The A constants for Kr and Xe were computed from viscosity

TABLE II.

	$\alpha \cdot 10^{24}$ (cc)	B_0 (cc/mol)	A(calc) $\cdot 10^{-12}$ (ergs cc)	A(exp) $\cdot 10^{-12}$ (ergs cc)
Ne	0.39	20.6	0.37	0.21
A	1.65	39.3	1.67	1.29
Kr	2.50	52.8	2.33	2.07
Xe	4.12	70.4	3.70	3.86
N_2	1.74	50.5	1.58	1.34
H_2	0.82	21.0	.55	0.20
O_2	1.59	46.2	1.64	1.49
CH_4	2.59	55.9	2.32	2.28

measurements. The agreement appears to be quite satisfactory. The computed values of A are of course somewhat larger than the empirical ones due to the neglect of the repulsive potential outside the sphere $R=\sigma$. However, as A becomes large, the error introduced by this approximation becomes less important just as we should expect. It is to be hoped that a method of calculating the repulsive potential may soon be developed, in order that a more adequate comparison with experiment may be made.

[14] Beattie and Bridgeman, Proc. Nat. Acad. **63**, 229 (1928).

THE SCATTERING OF UNPOLARIZED X-RAYS

By G. E. M. Jauncey and G. G. Harvey
Department of Physics, Washington University

(Received February 4, 1931)

Abstract

Unpolarized x-rays from an x-ray tube excited at 90 to 125 kv and filtered through aluminum and copper were scattered by paraffin at angles of 75°, 97°30′ and 120°. The intensity of the scattered rays was measured by the ionization produced in a chamber containing air saturated with (1) methyl iodide (2) ethyl bromide. It was found very necessary to keep the temperature of the ionization chamber and the voltage on the x-ray tube constant during an experiment. The results are expressed by the ratios of the ionization currents produced at scattering angles of 97°30′ and 120° respectively to the current produced at an angle of 75°. The wave-lengths present in the primary x-rays were determined by measuring the absorption of x-rays in a series of thicknesses of aluminum, the x-rays entering the same ionization chamber as that which was used in the scattering experiment. The absorption curve so obtained was found to consist of two exponential curves which correspond to two wave-lengths, the intensity of the shorter wave-length being much greater than that of the longer. With these wave-lengths and their relative intensities and taking account of the change of absorption in the ionization chamber due to the Compton change of wave-length the theoretical values for the above ratios were calculated by use of (1) the Dirac scattering formula and (2) the Compton formula. The agreement between the ratios calculated from the Dirac formula and the experimental ratios was excellent. The wave-lengths when methyl iodide was in the chamber were 0.205A and 0.39A and when ethyl bromide was in the chamber were 0.26A and 0.47A. At these wave-lengths the difference between the Dirac and the Klein and Nishina formulas is so small that experimental discrimination between them was not possible.

1. Introduction

In 1923, A. H. Compton[1] and Jauncey[2] developed theoretical formulas for the spatial distribution of the intensity of scattered x-rays. The two formulas differ only in the higher powers of α, which is defined by

$$\alpha = h/mc\lambda \tag{1}$$

where λ is the wave-length of the primary x-rays and h, m and c have their usual significance. It is only in the region of γ-rays that the two formulas differ, and as this paper has to do only with the scattering of x-rays and not γ-rays, we shall use the Compton formula as also representing Jauncey's formula with sufficient exactness. According to Compton,[1] the scattering coefficient per unit solid angle in a direction ϕ with the direction of propagation of the primary x-rays is

$$s_\phi = \frac{NZ\rho e^4}{Wm^2c^4} \cdot \frac{1 + \cos^2\phi + 2\alpha(1+\alpha)\,\mathrm{vers}^2\phi}{(1 + \alpha\,\mathrm{vers}\,\phi)^5} \tag{2}$$

[1] A. H. Compton, Phys. Rev. **21**, 491 (1923).
[2] G. E. M. Jauncey, Phys. Rev. **22**, 233 (1923).

where N is Avogadro's number, Z the number of electrons in a molecule of the scattering substance, ρ its density, W its molecular weight and ϕ the angle of scattering. Eq. (2) is Compton's formula for the scattering of unpolarized x-rays. The minimum value of s_ϕ occurs when $ds_\phi/d\phi = 0$, that is, when

$$\cos\phi = -\alpha/2 \tag{3}$$

approximately, the square and higher powers of α being neglected.

In the Thomson[3] theory of the scattering of x-rays, the minimum occurs at $\cos\phi = 0$, or at $\phi = 90°$. In the case of x-rays for which $\alpha = 0.1$, the minimum according to Eq. (3) occurs at $\phi = 92°53'$, which is distinctly different from the position of the minimum on the Thomson theory.

Breit[4] attacked the problem of the theoretical formula for the scattering of x-rays from the point of view of the correspondence principle and obtained a formula differing from Eq. (2). Later Dirac,[5] using the principles of quantum mechanics, obtained a formula identical with that of Breit. The Dirac formula is

$$s_\phi = \frac{NZ\rho e^4}{Wm^2c^4} \cdot \frac{1 + \cos^2\phi}{(1 + a \operatorname{vers}\phi)^3}. \tag{4}$$

According to Eq. (4), s_ϕ has a minimum at

$$\cos\phi = -3\alpha/2 \tag{5}$$

approximately, so that for $\alpha = 0.1$, the minimum occurs at $98°36'$. The minimum according to Dirac therefore occurs at an angle of $5°43'$ greater than according to Compton and Jauncey.

Recently, Klein and Nishina[6] have derived a formula on the basis of the quantum mechanics which is somewhat different from Dirac's formula. The Klein and Nishina formula is obtained from the Dirac formula by multiplying the right side of Eq. (4) by the factor

$$k = 1 + \frac{\alpha^2 \operatorname{vers}^2\phi}{(1 + \cos^2\phi)(1 + \alpha \operatorname{vers}\phi)}. \tag{6}$$

This factor has no effect on Eq. (5) as far as the first power of α is concerned.

In 1924 Jauncey[7] derived a formula for the scattering of polarized x-rays. For scattering in the plane of the electric vector, the position of the minimum is given by

$$\cos\phi = \alpha \tag{7}$$

approximately, so that for $\alpha = 0.1$ the minimum occurs at $84°\ 15'$. The formulas of Breit, Dirac and Klein and Nishina all agree in giving the minimum at $\phi = 90°$, which is in accord with the Thomson classical theory.

[3] J. J. Thomson, Conduction of Electricity through Gases, 2nd. Ed., p. 325.
[4] G. Breit, Phys. Rev. **27,** 362 (1926).
[5] P. A. M. Dirac, Proc. Roy. Soc. **A111,** 405 (1926).
[6] Klein and Nishina, Zeits. f. Physik **52,** 853 (1929).
[7] G. E. M. Jauncey, Phys. Rev. **23,** 313 (1924).

In an early experiment by Jauncey and Stauss[8] on the scattering of polarized x-rays, the experimental position of the minimum appeared to agree with Eq. (7). This experiment was repeated by Barrett and Beardon,[9] who found that the minimum occurred at angles somewhat greater than 90° and within experimental error of 90°. Another repetition was made by Jauncey and Hassler,[10] who found the minimum to be at an angle slightly greater than 90°. The results of these experiments are uncertain due to (1) the difficulty of measuring the exact position of a minimum, (2) the lack of complete polarization, (3) the wide slits which are necessary in order to obtain sufficient intensity, (4) the uncertainty of the wave-length used, and (5) multiple scattering. The wide slits have the effect of flattening the minimum, and on that account making the position of the minimum still more difficult to determine. Referring to Eqs. (3) and (7), it is seen that the Compton-Jauncey formula gives the minimum for unpolarized x-rays at an angle greater than 90°, while their formula gives the minimum for polarized x-rays at an angle less than 90°. It is possible therefore with partially polarized x-rays to obtain a minimum at 90° on the Compton-Jauncey theory. Complete polarization can only be obtained by scattering at 90° or nearly 90° from a slab of some material such as paraffin, when the slab is very thin. Since, in experiments on polarized x-rays, the x-rays are scattered twice, the intensity of the doubly scattered x-rays is quite small unless both slabs of the scattering material are fairly thick. However, multiple scattering increases as the thickness of each slab increases. This multiple scattering increases the lack of complete polarization.

Due to the above objections, the present writers have made the test on unpolarized x-rays and have abandoned the attempt to determine experimentally the position of the minimum. Instead the writers have attempted to measure the relative scattering at the three angles 75°, 97.5° and 120° as accurately as possible and to compare the experimental values with the values predicted by the various theories. It should be mentioned that in 1922 Hewlett[11] published scattering curves for certain organic liquids and that these curves show minima at about 100° to 105°. As we shall show in the present paper, it is very necessary to take account of the Compton change of wave-length in regard to its effect on the ionization produced in the ionization chamber, and this Hewlett did not do, since his paper was published before the discovery of the Compton effect.

2. Experimental Procedure

X-rays from the tube *A*, Fig. 1, after leaving the target almost tangentially and passing through a slit system, fall upon the paraffin slab *B*. Part of the x-rays are scattered by the slab *B* into the ionization chamber *D* and part penetrate through the slab *B* and then fall upon a paraffin slab *C*. Part

[8] Jauncey and Stauss, Proc. Nat. Acad. Sci. **10**, 405 (1924).
[9] Barrett and Bearden, Phys. Rev. **29**, 352 (1927).
[10] Jauncey and Hassler, Phys. Rev. **31**, 1120 (1928).
[11] C. W. Hewlett, Phys. Rev. **20**, 688 (1922).

of the rays falling on slab C are scattered into the ionization chamber E. The slab B is mounted on the axis of an x-ray spectrometer and the ionization chamber D can be rotated about this axis. The angle which the slab C makes with the primary beam and the position of the chamber E remains fixed throughout the experiment. The width of the beam of x-rays entering the chamber E is controlled by the adjustable slit S. The outer electrodes of D and E are connected to $+100$ and -100 volts respectively. The inner electrodes are connected together and to the electrometer as shown in Fig. 1. Doubling and halving the voltages on the chambers E and D had no effect on the observed ionization currents, so that the voltages on the two chambers were always above the voltages necessary for saturation. The chamber D was first filled with air saturated with methyl iodide vapor. Later D was filled with air saturated with ethyl bromide vapor. A reservoir containing either liquid methyl iodide or ethyl bromide was permanently connected to D. The chamber E was filled with air alone. In order that the primary x-rays should be in effect completely unpolarized, the axis of the x-ray tube made an angle of 45° with the plane of scattering.

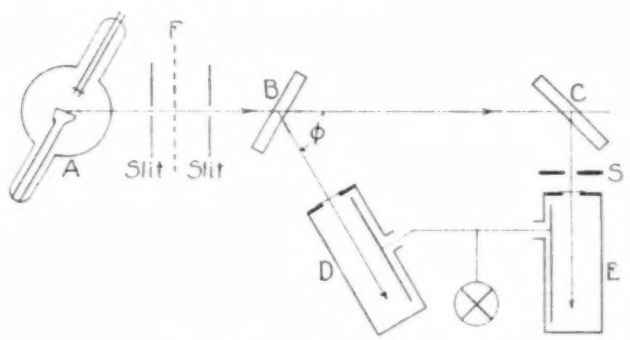

Fig. 1. Diagram of apparatus.

The angular scale of the spectrometer was graduated in quarter degrees so that settings of the ionization chamber could be made with an accuracy of 5 minutes of arc. A pin was mounted on the axis of the spectrometer and it was arranged that, when the primary beam of x-rays was observed by a fluoroscope, the shadow of the pin was in the center of the fluorescence produced by the beam. The target of the tube was turned so that the primary x-rays left the target nearly tangentially, the plane of the target being vertical. Under these conditions it was noted that the edge of the fluorescent image of the slit system as observed in the fluorescope was sharp on one side but was somewhat indefinite on the other. Consequently we could not be certain that the axis of the spectrometer passed through the "center of gravity" of the primary beam. We therefore took readings for a given scattering angle with the chamber D set first on one side of the primary beam and then on the other. Also with a given setting of the ionization chamber we took one set of readings with the paraffin slab B in the Crowther[12] position and

[12] J. A. Crowther, Proc. Roy. Soc. **A86,** 478 (1912).

a second set with the slab B turned through 180°, so that it was again in the Crowther position but with the opposite side presented to the primary beam. For each angle of scattering there were thus two settings of the ionization chamber and four settings of the paraffin slab. In this way, any asymmetry of the primary beam with respect to the spectrometer was corrected.

The primary voltage of the x-ray transformer was supplied by two motor generator sets. The first set consisted of an a.c. motor and d.c. generator operated by Washington University power. By means of a voltage regulator connected to the field coils of the d.c. generator a constant d.c. voltage was obtained, irrespective of variations in the a.c. voltage driving the a.c. motor. This constant d.c. voltage was applied to the d.c. motor of the second set, so that the a.c. generator of the second set gave a constant a.c. voltage. This constant a.c. voltage was applied to the primary of the x-ray transformer. Full wave rectification of the high voltage was obtained by a system of four kenotrons. Care was taken to have the filaments of the kenotrons at a temperature such that the fall of voltage across the kenotrons was too small to produce any detectable x-rays. This was necessary because irregular results were first obtained due to stray x-rays from the kenotrons. In spite of the two motor generator sets, there were occasional variations of the primary voltage across the x-ray transformer and of the milliamperes through the x-ray tube. Accordingly, we placed a choke coil in the primary circuit of the x-ray transformer. By adjustment of the length of the iron core within the coil, any variation of the voltage could be annulled. The tube was operated at maximum voltages between 90 and 125 kilovolts and a current of 7 milliamperes. The voltages were measured by the spark length between spheres of 10 cm radius. The target was of tungsten and was not water-cooled. The corona discharge from the leads to the x-ray tube was reduced by making these leads of $\frac{3}{4}$ inch flexible piping. The x-rays were made more homogeneous by passing them through a filter F of aluminum or copper.

The intensity of the rays scattered by the slab B into the chamber D was compared with the intensity of the rays penetrating the slab B and entering the chamber E. By means of lead shutters, the rays were first allowed to enter D but not E and then were allowed to enter E but not D. Readings of the scattered and primary rays were thus taken alternately. The time for a deflection over a given part of the scale was measured. Due to the fact that the voltages across the chambers D and E were in opposite directions, it was not necessary to ground the electrometer during a set of readings. With a given setting of the chamber, 5 readings on the scattered rays and 5 readings on the primary rays were taken. The slab B was then turned through 180° and the procedure repeated. This was done with a slab of given thickness and with a given voltage on the x-ray tube for the chamber angles of 120°, 97.5°, and 75° on the right side of the spectrometer and 75° 97.5° and 120° on the left side. Thus a total of 60 readings on the scattered rays and 60 on the primary rays were taken, making a total of 120 readings. In an effort to correct for multiple scattering, we then substituted a slab of different thickness and took 120 more readings. The whole of the 240 readings were taken without

interruption. Since the effect of change of temperature on the ionization produced in the saturated methyl iodide or ethyl bromide vapor is quite considerable, we kept the temperature of the room constant during the whole period of the 240 readings. Also, during the same period, the voltage across the x-ray tube and the current through the tube were kept constant.

Readings of the ionization in chamber D were also taken with the slab B removed so as to obtain any effect due to stray rays. Although this effect was small, it was not negligible. The effect was different for different settings of

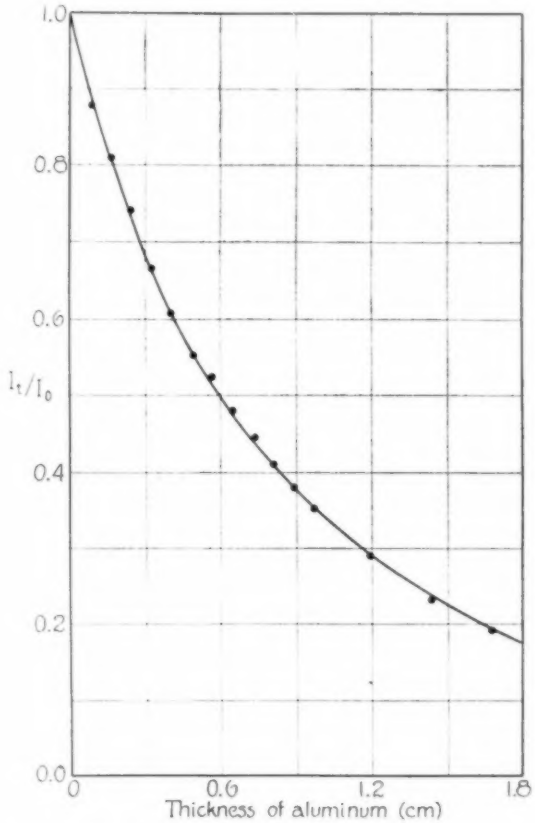

Fig. 2. Absorption in aluminum. Methyl iodide, 90 kv.

the chamber D. For a given chamber angle on one side of the spectrometer and a given thickness of paraffin, the average of the readings for the scattered rays was determined. This average was corrected for the stray rays. The average for the primary rays was also determined. The ratio of this corrected average for the scattered rays to the average for the primary rays is determined for a given scattering angle on each side of the spectrometer. The average of the ratios for the two sides is then determined These are the values shown in Tables I and II.

The linear width of the primary beam when crossing over the axis of the spectrometer was measured with the aid of the fluoroscope and was found to

be 4 mm. Since the distance of the axis to the target of the x-ray tube is 80 cm, the angular width of the primary beam is 17′. The distance from the axis to the window of the ionization chamber D is 15 cm. This window is 1 cm wide. The angle of scattering when the chamber D is set at a given angle therefore has a range of 5° 32′. The angular height of the primary beam is 1° 23′, while the angular height of the scattered rays is 11° 24′. Calculation showed that the angular range of the scattering angle from a thin slab due to the height of the slits was about 30′ at each of the angles 75° 97° 30′ and 120°.

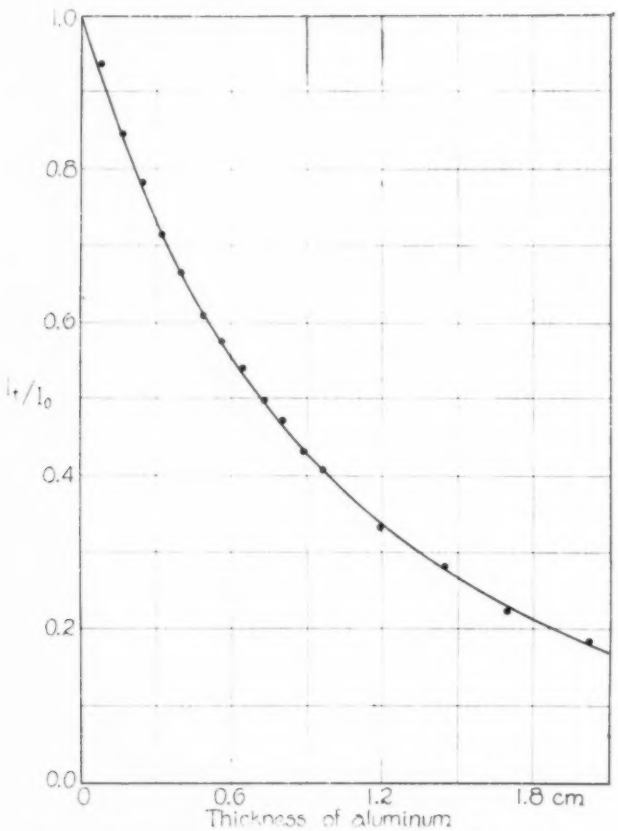

Fig. 3. Absorption in aluminum. Methyl iodide, 125 kv.

The inner electrode of the ionization chamber was placed so that no scattered rays from the slab could strike it. The diameter of the chamber was such that the rays did not strike the sides. The length of the ionization chamber was 43.5 cm.

After completing a run of 240 readings on the scattered rays and meauring the effect of the stray rays, the hardness of the primary rays was measured by placing the chamber D so as to receive the primary rays. In order to cut down the intensity the rays were passed through a pinhole in a sheet of lead. Different thickness of aluminum were placed in the primary. For each thickness several readings alternately with and without aluminum were taken.

The proportion of the rays penetrating each thickness are shown by the black circles in Figs. 2, 3 and 4. The absorption curve was obtained for the same voltage across the x-ray tube and with the chamber D at the same temperature as when the scattered rays were being measured.

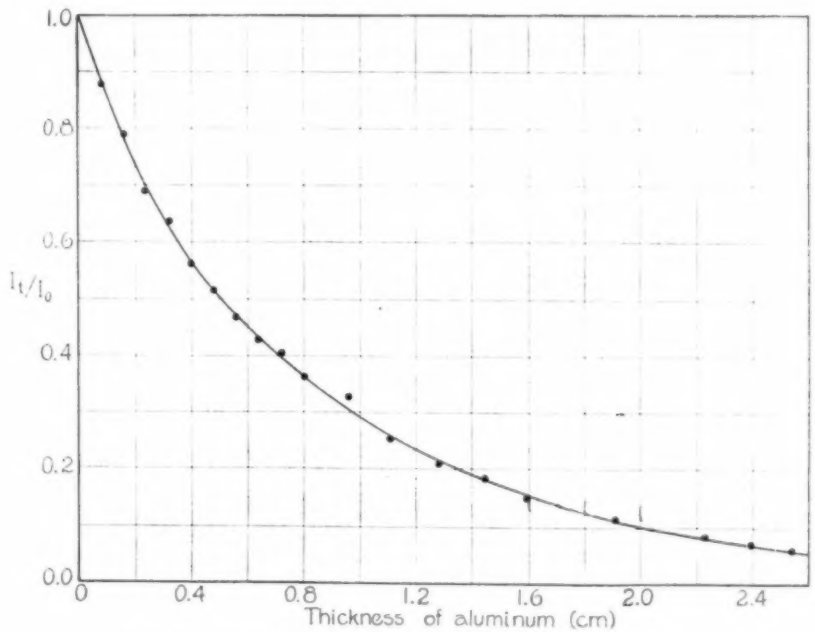

Fig. 4. Absorption in aluminum. Ethyl bromide, 95 kv.

3. Experimental Results

The experiment was first performed with the chamber filled with air saturated with methyl iodide vapor at a temperature of 17°C. The results are shown in Table I. Paraffin slabs of mass per unit area 0.365 gm/cm² and

Table I. *Scattering from paraffin. Methyl iodide in ionization chamber.*

Angle	Potential = 90 kv Mass/Area = 0.365	Scattering ratios 90kv 0.595	125kv 0.365	125kv 0.595
75°	0.531	0.837	0.477	0.760
97° 30′	0.573	0.926	0.550	0.804
120°	0.864	1.414	0.823	1.265

0.595 gm/cm² were used. The values under 125 kv are not comparable with the values under 90 kv. The 90 kv rays were filtered through 2.92 mm and the 125 kv rays were filtered through 7.22 mm of aluminum. The results of the absorption measurements for the 90 kv rays and the 125 kv rays are represented by the black circles in Figs. 2 and 3 respectively.

Later the experiment was performed with ethyl bromide in the chamber and the results shown in Table II were obtained. In this case the rays were

filtered through 0.1 mm of copper and 2.0 mm of aluminum. The temperature was maintained at 24.0°C.

TABLE II. *Scattering from paraffin. Ethyl bromide in ionization chamber. Potential* 95 kv.

Angle	Scattering ratios	
Mass/Area =	0.365	0.595
75°	0.368	0.645
97° 30′	0.397	0.720
120°	0.635	1.150

The results of the absorption measurements with ethyl bromide in the chamber are represented by the black circles in Fig. 4.

4. COMPARISONS WITH THEORY

In order to compare the experimental results with theory it is necessary to obtain the wave-length of the primary rays. Since we used rays of the continuous spectrum filtered through aluminum or aluminum and copper, the rays were only approximately monochromatic.

Smooth curves (not the curves shown) were drawn through the experimental points shown in Figs. 2, 3, and 4. From the smooth curve in a given case values of I_t/I_0 were read off at each successive thickness of 1 mm of aluminum. It was found that after a thickness of about 4 mm the curve was almost exactly exponential. This exponential portion was produced back to zero thickness. Differences were then obtained between this exponential curve and the experimental curve for thicknesses less than 4 mm. It was found that these differences when plotted against thickness gave a fairly exponential curve. Thus the experimental curve appeared to be made up of two exponential portions. The solid curves shown in Figs. 2, 3 and 4 are curves calculated from the formula

$$I_t/I_0 = i_1 e^{-\mu_1 t} + i_2 e^{-\mu_2 t}. \tag{8}$$

The values of i_1, i_2, μ_1 and μ_2 are shown in Table III.

TABLE III.

kv	Vapor in D	i_1	μ_1 cm^{-1}	i_2	μ_2 cm^{-1}	λ_1 A	λ_2 A	I_1	I_2
90	methyl iodide	0.67	0.74	0.33	2.7	0.205	0.39	0.68	0.32
125	methyl iodide	0.815	0.74	0.185	2.7	0.205	0.39	0.82	0.18
95	ethyl iodide	0.806	1.03	.194	4.15	0.26	0.47	0.91	0.09

In Table III, μ_1 and μ_2 are the linear absorption coefficients in aluminum. From these the mass absorption coefficients can be found and the wave-lengths λ_1 and λ_2 can be determined from Compton's table of absorption

coefficients.[13] Now i_1 and i_2 are the proportions of the two wave-lengths present as measured by the ionization produced in the chamber. These are not the proportions present in the primary x-rays. At first, we thought to obtain the proportions present in the primary rays by dividing by the amount of each wave-length absorbed in the gas in the chamber. These proportions are shown in the columns headed I_1 and I_2. However, the energy of the x-rays which are absorbed in methyl iodide does not all give rise to ionization. By far the greater part of the energy goes into iodine K-radiation, and somewhere about 80 to 90 percent of this K-radiation leaves the chamber without producing ionization. According to Compton,[14] the fluorescent yield is independent of the wave-length, so long as it is short enough to excite the fluorescent radiation. Thus the same proportion of the absorbed energy goes into producing ionization in the chamber D for all wave-lengths shorter than 0.375A, the K critical absorption wave-length for iodine. Let m_1 and m_2 be the respective mass absorption coefficients of the wave-lengths λ_1 and λ_2 in the gas of the chamber D. The saturated vapor pressure for methyl iodide at 17°C is 293 mm[15], from which the density of the iodine in the methyl iodide is 0.00206 gm/cm³. The values of m_1 and m_2 for iodine can be obtained from Compton's table of mass absorption coefficients by interpolation and the fraction of the radiation of each wave-length absorbed in the ionization chamber D can be calculated. Let the fractions be represented by k_1 and k_2 for the wave-lengths λ_1 and λ_2 respectively. Of the fractions k_1 and k_2, the fractions p_1 and p_2 respectively appear as ionization. In the case of methyl iodide p_1 and p_2 differ because λ_1 is shorter and λ_2 is longer than the K critical absorption wave-length of iodine. Hence the relative energies in the wave-lengths λ_1 and λ_2 as they enter the chamber D, but not as they are absorbed in the chamber, are i_1/p_1k_1 and i_2/p_2k_2. These are taken as representing the energies of λ_1 and λ_2 in the primary beam.

Now let us consider the scattering experiment. The scattered intensity I_ϕ when the slab B is in the Crowther position is

$$\frac{I_\phi}{I} = \frac{As_\phi t \sec(\phi/2)}{R^2} \tag{8}$$

where I is the intensity of the rays penetrating the slab B and entering the chamber E. This intensity is proportional to the ionization in E, so long as the temperature of the room and the voltage across the x-ray tube is kept constant. s_ϕ in Eq. (8) is the scattering coefficient, t is the thickness of the slab, A the area of the window of chamber D, R the distance of the window from the spectrometer window and ϕ the scattering angle.

Let primed quantities (′) represent values at ϕ' and doubly primed quantities (″) represent values at ϕ''. Then, since the same slab of thickness t is used at both angles, we have from (8)

$$J''/J' = (s''/s') \cdot (\sec \tfrac{1}{2}\phi'')/(\sec \tfrac{1}{2}\phi') \tag{9}$$

where $J = I_\phi/I$.

[13] A. H. Compton, X-Rays and Electrons. p. 184.

[14] A. H. Compton, Phil. Mag. **8**, 961 (1929).

[15] Int. Crit. Tables. III p. 216.

With Eqs. (2), (4) and (6), the various theoretical values of J''/J' for a given wave-length can be found. However, the ratio of the ionization currents produced in chamber D is not J''/J' because of the Compton change of wave-length

$$\delta\lambda = (h/mc) \text{ vers } \phi.$$

Due to this change of wave-length the proportion of the scattered rays of primary wave-length λ_1 which is absorbed in chamber D is different for the scattered rays from the proportion of the primary rays of the wave-length λ_1 absorbed in D in the absorption experiment. The absorbed scattered rays are proportional to i_1k_1'/p_1k_1 where k_1' is the value of k_1 for the scattered rays. The ionization produced is proportional to $i_1p_1'k_1'/p_1k_1$, where p_1' is the value of p_1 for the scattered rays. However, according to Compton,[14] $p_1' = p_1$, so long as the Compton change of wave-length does not cross a critical absorption wave-length. Hence the ionization produced is proportional to i_1k_1'/k_1. The values of i_1/k_1 and i_2/k_2 are shown in the columns respectively headed I_1 and I_2 in Table III.

If we have two wave-lengths, and if the J's of Eq. (9) are to represent ionization currents in chamber D, we have

$$\frac{J''}{J'} = \frac{(i_1k_1''/k_1)s_1'' + (i_2k_2''/k_2)s_2''}{(i_1k_1'/k_1)s_1' + (i_2k_2'/k_2)s_2'} \cdot \frac{\sec(\frac{1}{2})\phi''}{\sec(\frac{1}{2})\phi'}.$$

The values of J''/J' where $\phi' = 75°$ and $\phi'' = 97°\ 30'$ or $120°$ are shown for the various theoretical formula for s_ϕ in Table IV. The experimental values of J''/J' when methyl iodide is in the chamber D are also shown in Table IV.

TABLE IV. *Experimental and theoretical values of J''/J'. Methyl iodide in ionization chamber.*

		90 kv					125 kv				
		Experiment			Dirac	Compton	Experiment			Dirac	Compton
ϕ'	ϕ''	A	B	Mean			A	B	Mean		
75°	97.5°	1.079	1.107	1.093	1.098	1.170	1.152	1.059	1.106	1.103	1.174
75°	120°	1.627	1.690	1.659	1.738	1.898	1.725	1.663	1.694	1.740	1.905

Those values shown under A are for the paraffin slab whose mass per unit area is 0.365 gm/cm² and those under B for the slab whose mass per unit area is 0.595 gm/cm².

During the progress of this research, a paper by DuMond[16] on multiple scattering has appeared. In this paper, DuMond discusses the problem of double scattering from a sphere, and obtains a formula for the ratio of the intensity of doubly scattered rays to that of singly scattered rays. The formula contains a function of ϕ, the scattering angle, but this function is very nearly constant in the range $\phi = 75°$ to $120°$. We have been unable to find any certain direction in which J''/J' changes with the thickness of the

[16] J. W. M. DuMond, Phys. Rev. **36**, 1685 (1930).

slab in our experiments, and this is, we believe, in agreement with DuMond's theoretical finding that the ratio of double to single scattering does not vary with the angle in the range considered. Instead, therefore, of extrapolating the values of J''/J' to zero thickness, we have merely taken the mean values as shown in Table IV.

In calculating the theoretical values, the range of scattering angles at a given setting of the ionization chamber has been neglected and the calculation been made on the assumption that the scattering angle is the angle at which the ionization chamber is set. This is allowed because the correction due to the range of the scattering angle is small since the range of 5° 32′ due to the width of the slits plus 30′ due to the height of the slits only makes a difference in the third decimal place in the theoretical values of J''/J' in Tables IV and V. Further, in calculating the theoretical values it has been assumed that none of the scattered rays at the angles used are of the unmodified type. Compton[17] writes Wentzel's formula [18] for the intensity of the unmodified rays in the form

$$I_{unm} = I_e n^2 \left\{ \int u(r) \frac{\sin kr}{kr} dr \right\}^2 \tag{10}$$

where $k = (4\pi/\lambda) \sin (\phi/2)$ and $u(r)dr$ is the probability that an electron is at a distance r to $r+dr$ from the center of an atom, n is the number of electrons in an atom of the scatterer and I_e is the Thomson value of the scattering from a single electron. In the case of helium, Pauling[19] gives the probability for each of the two electrons as

$$u(r) = 4r^2 \left(\frac{Z - s}{a} \right)^3 \exp \left\{ - (Z - s)r/a \right\} \tag{11}$$

where Z is the atomic number of helium, a is the radius of the normal orbit in the hydrogen atom on the Bohr theory and s is the screening constant. We have applied this formula for $u(r)$ to the case of the K electrons of carbon, putting $Z = 6$, $s = 0.39$ and $a = 0.53$A in Eq. (11) and $n = 2$ in Eq. (10). Performing the integration in Eq. (10), we obtain

$$I_{unm} = 4I_e/(1 + .022x^2) \tag{12}$$

where $x = (4/\lambda) \sin (\phi/2)$. For $\lambda = 0.26$A and $\phi = 75°$, I_{unm} from each carbon atom in paraffin is 0.065 I_e. The average chemical formula for paraffin is $C_{24}H_{50}$. The L electrons of C and the electrons of H do not scatter unmodified rays at $\phi = 75°$, so that the ratio of unmodified rays scattered by paraffin to the total scattering at $\phi = 75°$ is 0.7 percent. We are therefore justified in neglecting the unmodified rays in our calculated values of J''/J'.

In Table III it will be noted that λ_2 for the absorption curves when methyl iodide is just on the long wave-length side of 0.375A, the critical ab-

[17] A. H. Compton, Phys. Rev. **35,** 930 (1930).
[18] G. Wentzel, Zeits. f. Physik **43,** 1 and 779 (1927).
[19] L. Pauling, Proc. Roy. Soc. **A114,** 181 (1927).

sorption wave-length for iodine. We accordingly felt rather doubtful of the reality of this wave-length. For this reason we replaced the methyl iodide with ethyl bromide. The temperature when ethyl bromide was used in the ionization chamber was 24.5°C. At this temperature the density of the bromine in saturated ethyl bromide is 0.00197 gm/cm³. The primary x-rays were filtered through copper as well as aluminum in an attempt to increase the homogeneity of the rays. The absorption measurements are shown by the black circles in Fig. 4. The absorption measurements were carried to a much greater thickness of aluminum than in the case where methyl iodide was in the chamber. This was done in order to obtain the wave-lengths as accurately as possible. The solid curve of the Fig. 4 is constructed with the use of the data shown in Table III. Again as in the case of methyl iodide we have two wave-lengths, but both are on the short wave-length side of the absorption edge from bromine. The experimental and theoretical values of J''/J' are shown in Table V.

TABLE V. *Experimental and theoretical values of J''/J'. Ethyl bromide in ionization chamber. Potential* 95 kv.

		Experiment			Dirac	Klein-Nishina	Compton	Thomson
ϕ'	ϕ''	*A*	*B*	Ave.				
75°	97°30′	1.085	1.110	1.098	1.097	1.102	1.17	1.149
75°	120°	1.755	1.795	1.775	1.740	1.755	1.89	1.860

5. Discussion

The agreement of the experimental values of J''/J' with the Dirac or Klein and Nishina values as shown in Table V is excellent. At the wave-lengths used the Dirac or Klein and Nishina Formula is a much better description of the experimental facts than the Compton or Thomson Formula. The agreement of the experimental values of J''/J' with the Dirac values as shown in Table IV is also good for the 90 kv x-rays. The agreement for the 125 kv x-rays, however, is not so good although the agreement of the mean values with the Dirac values is good. The corona discharge when the x-ray tube was excited with 125 kv was considerable and this seemed to introduce irregularities into the electrometer readings. This difference between the *A* and *B* values for $\phi'' = 97°\ 30'$ is due to the irregularities.

In calculating the theoretical values of J''/J', two wave-lengths have been used. In the case of ethyl bromide, the longer wave-length was 0.47A. This wave-length is perhaps somewhat fictitious and we feel that the reality of the wave-length 0.26A is greater because by far the larger part of the absorption curve in Fig. 4 is due to this wave-length. If it is supposed that only this wave-length is present in the primary rays, the Dirac values in Table V become 1.098 and 1.753 for $\phi'' = 97°\ 30'$ and 120° respectively, while the Klein and Nishina values become 1.103 and 1.771. Also it might be objected that even the wave-length 0.26A is an average wave-length. We have therefore calculated the Dirac values in the case of ethyl bromide for $\lambda = 0.22$,

0.24, 0.28, 0.30A in addition to 0.26A. The values of J''/J' vary from 1.098 to 1.108 at $\phi''=97°\ 30'$ and from 1.73 to 1.76 at $\phi''=120°$. The Dirac theoretical values of J''/J' are therefore practically constant for a wave-length range of 0.08A about 0.26A. The Compton values are also practically constant over the same range. This is our justification for using the average wave-length 0.26A in the calculation of the theoretical values.

If the effect of the Compton change of wave-length on the ionization produced in the chamber is neglected, the Dirac theoretical values of J''/J' for 0.26A become 1.035 at $\phi''=97°\ 30'$ and 1.540 at $\phi''=120°$ in total disagreement with the experimental values. The ionization produced by the photoelectrons ejected from the brass wall at the end of the chamber and the aluminum window were neglected because with the length of chamber used this ionization is only a small fraction of the total ionization in the chamber. The aluminum window was 0.005 cm thick and the absorption in it was neglected.

We observed a rather curious effect during these experiments. The hardness of x-rays as determined by absorption in aluminum depends upon (a) the angle at which the rays leave the target of the x-ray tube (b) the nature of the gas in the ionization chamber, and (c) the temperature of the chamber if saturated vapor is used in the chamber. The length of the ionization chamber is such that the x-rays are incompletely absorbed. It is quite possible to apply a higher voltage to an x-ray tube and yet obtain less penetrating x-rays.

For the wave-lengths used in this research it is not possible to discriminate between the Dirac and the Klein and Nishina formulas. Recently, Chao[20] using γ-rays of wave-length 0.0052A has shown that the Klein and Nishina Formula fits the experimental facts much better than the Dirac Formula. This research was assisted by a grant from the Science Research Fund of Washington University.

[20] C. Y. Chao, Phys. Rev. **36**, 1519 (1930).

APPEARANCE OF EXTRA LINES IN X-RAY DIFFRACTION PATTERNS OF MIXTURES AND ABSENCE OF SOME LINES PECULIAR TO THE COMPONENTS OF THE MIXTURES

By Roy W. Drier

Department of Metallurgy
Michigan College of Mining and Technology
Houghton, Michigan

(Received February 2, 1931)

Abstract

Abnormalities in x-ray spectra of mechanical mixtures of minerals are described. The spectra of some show the presence of extra lines, and in the spectra of others some lines peculiar to the components are missing. Some possible reasons are briefly considered.

THE x-ray, useful in the solution of many problems, has revealed the existence of others. Among these are the appearance in x-ray diffraction patterns of mechanical mixtures, of lines not peculiar to either of the components of the mixtures, and the disappearance, in the spectra of the mixtures, of some of the lines peculiar to the components.

It is not the purpose of this paper to offer any definite explanation of these phenomena of the disappearance of spectral lines and the appearance of new lines but rather to record them and to mention a few possible reasons for them.

The diffraction patterns are composed of spectral lines produced in Debye-Scherrer or Hull type cameras. These lines are indicative of interplanar spacings in the crystal structure.

These effects were first noticed by the writer while he was working with Dr. G. L. Clark, of the Department of Chemistry, of the University of Illinois. The mixture which drew attention to this phenomenon was one of rutile (TiO_2) and barite ($BaSO_4$).

The two minerals, rutile and barite, were rayed separately for their diffraction patterns. Mixtures of the two were made, and diffraction patterns of the mixtures were then obtained. These were simple mechanical mixtures, mixed on glazed mixing paper and placed in capillary tubes for raying. No heat or pressure entered into the process of sample preparation.

The apparatus used was a G. E. diffraction unit. It supplied 30,000 volts R.M.S. to a molybdenum target, water-cooled Coolidge tube operating at 20 m.a. The films were held in a cassette in the form of an arc 8 inches in radius. The samples (-200 mesh) were contained in small, capillary, Pyrex glass tubes about 2 inches long and approximately 0.03 inches in internal diameter. This tube is held in the center of the circle of which the film mentioned above is an arc. By means of a ZrO_2 filter placed in the cassette between the sample and the film, practically all but the $MoK\alpha$ radiation is filtered out, the film registering this monochromatic beam only.

A comparison of the spectra of the components and of the mixture revealed that some of the lines peculiar to the constituents were missing in the mixture pattern and that some of the mixture lines were not included in the spectra of the constituents.

Several series of mixtures were then made up and rayed, for the purpose of investigating this "extra line" phenomenon. The mixtures were Cu-Zn, Cu-Ag, Cu-NaCl, and Cu-Ni. Each series was composed of members whose proportions varied from 0% A-100% B to 100% A and 0% B. The Cu-Zn series had the following mixtures: 100% Cu-0% Zn, 95% Cu-5% Zn, 75% Cu-25% Zn, 50% Cu-50% Zn, 25% Cu-75% Zn, 5% Cu-95% Zn, and 100% Zn. This series was proportioned according to weight, but the rest of the mixtures were proportioned according to volume, which was approximated by eye. Although a more accurate method of proportioning and making the mixtures could have been followed, it was felt that each series would yield samples which would vary approximately as desired.

The Cu-Zn series was the most outstanding of the five. A few of the lines appearing in the Cu did not appear in the mixtures, and several of the lines of the zinc patterns were not a part of the composite spectrum. In each of the mixture-spectra there were found eight distinct lines which occurred in neither the Cu nor the Zn spectrum.

The extra lines in the Cu-Zn series agreed fairly well with the spectrum of alpha-brass, a fact which seems to indicate the occurrence of interfacial diffusion. In an attempt to reproduce this reaction, a sheet of zinc was ground to a knife edge. This knife edge was pressed into −100 mesh copper filings and held there for 24 hours. It was then removed; the copper filings were brushed off, and the knife edge was placed in an x-ray beam. The resulting spectrum contained only the lines which were in the spectrum of an untreated piece of the same zinc. If interfacial diffusion occurred in the powder mixture, it was probably due to a catalytic action, possibly of the x-rays themselves.

Spectra of pure Ag and pure Cu and of a 50-50 mixture showed no new spectral lines in the mixture, but did show that the (100) 4 copper line was missing in the mixture and that there was a slight gradual shift to the right (i.e., shortening) in the mixture as compared to the copper. Some slight traces of impurities were indicated in the spectra of the Ag and Cu.

The Cu-Al series seemed to be regular; there were neither extra lines nor any lines missing. In the mixtures which had a low aluminum content many of the Al lines were faint and some had disappeared, but such a disappearance is to be expected of reflections from an element of comparatively low atomic number. E. C. Bain[1] noticed the appearance of extra lines in mixtures of Cu and Au heated to the sintering point. His spectrogram of the mixture before heating indicated merely the composite spectrum of Au and Cu. The writer is inclined toward the opinion that when the mixture was heated to the sintering temperature some such sort of reaction as diffusion or solid solution took

[1] E. C. Bain, Chem. Met. Eng. **28,** 2 (1923).

place which would account for the new lines. Davidson and Aborn,[2] in their research on the structure of ZnO and CuO catalysts, carried on at 360°C, noticed "extra lines." It might be that the temperature obtaining during the experimentation was near enough to the melting point of zinc to make possible the occurrence of a reaction between the ZnO and the CuO, or it might be that the oxides were reduced and formed conditions which permitted the reaction to take place. Davidson and Aborn favor this latter possibility, especially since the extra lines seemed to agree fairly well with the spectrum for gamma brass.

There is a possibility, too, that if reduction did occur, the tendency for zinc to become brittle between 200°C and 300°C, indicating a possible change in atomic arrangement, might account for their extra lines. In working with mixtures of ZnO and Cr_2O_3, G. R. Griffin,[3] noticed in the mixture-spectra the disappearance of some lines peculiar to the components. Tamman,[4] has predicted the appearance of "overstructure lines." Hull,[5] while interpreting the spectra of a number of minerals, noticed the absence of some of the spectral lines which theoretically should have been present.

For these phenomena there are several possible causes. It is conceivable that the extra lines are due to a secondary reflection; this hypothesis, however, is not in accord with the fact that some of the extra lines are those of a solid solution or other phases of the system. The appearance of new lines might be explained by interfacial diffusion. But the disappearance of regular lines could not be so effected. A possible explanation of such disappearance is interference. Research on this problem is being continued in an attempt to determine the cause or causes of the phenomena.

[2] Davidson and Aborn, J. Phys. Chem. **34,** 522 (1930).
[3] G. R. Griffin, Inst. in Geol. U. of Ill. Paper not published.
[4] Tamman, Lehrbuch der Metallographie 3 ed. p. 450.
[5] A. W. Hull, Phys. Rev. **17,** 571 (1921).

THE DEPENDENCE OF X-RAY ABSORPTION SPECTRA UPON CHEMICAL AND PHYSICAL STATE

By J. D. Hanawalt*
University of Michigan

(Received January 30, 1931)

Abstract

The x-ray absorption spectra of As, Se, Br, Zn, Hg, Xe, and Kr, and of compounds of some of these elements have been photographed for both the solid and the vapor states at a dispersion of about 5 X.U. per mm. The effect of the chemical and physical state of the absorbing atom upon the secondary structure which lies to the short wave-length side of the main absorption edge was investigated. It was found that: (1). The monatomic vapors Zn, Hg, Xe, and Kr exhibit no secondary structure at distance from the main edge greater than the ionization potential of the atom. (2). Polyatomic vapors usually, though not necessarily, have a secondary structure similar to that which is exhibited by the same molecule in the solid state. (3). For a polyatomic molecule in the solid state there is often an additional structure observed which is absent when the molecule is in the vapor state. (4). There is an additional structure in the secondary absorption of solid $NaBrO_3$ which is not observed in a solution of $NaBrO_3$. (5). Completed electron shells of atoms in the solid state do not necessarily mean the absence of secondary absorption edges as has been suggested. In order to account for this dependence of secondary absorption on molecular and physical state it is suggested that perhaps the secondary discontinuities correspond to the excitation energies of the structure electrons postulated by O. W. Richardson.

Introduction

A STUDY of the x-ray absorption spectrum of a substance shows that there are sharp discontinuities in the absorption at wave-lengths corresponding to the energies of the Bohr levels of the atom. These absorption discontinuities do not always have the same appearance for different elements. The absorption edge may be what is known as "simple," or there may be some absorption discontinuities of lesser magnitude associated with the principal absorption edge. Fig. 2 (a) and (b) illustrate respectively a simple edge and one with secondary absorption. This secondary absorption falls to the short wave-length side of the main edge and therefore means the absorption of quanta of greater energy than that which produces the main edge. In some cases the difference in energy between a secondary discontinuity and the main edge may be more than 300 volt electrons. Experiments show that the wave-length of the main edge and the type of the absorption are functions of the chemical state of the absorbing atom. Experiments also show that the chemical state of an atom affects the emission spectrum of the atom. These latter experiments are complicated by the fact that one can not be sure of the chemical state of atoms on the anode of an x-ray tube, so it seems that absorption experiments have an advantage in this respect. An excellent and

* National Research Fellow.

complete presentation of the researches on the influence of chemical combination on the x-ray absorption and the x-ray emission spectra of an atom has been given by A. E. Lindh.[1] However, because of the complexity of the results, no unified picture of the work can be as yet formed.

There are two general questions, probably more or less related regarding absorption spectra to be considered. What are the factors which govern the position of the main edge; and, what is the origin or interpretation of the secondary absorption structure? The suggestions regarding the first question, as given by Wentzel, Coster, Stelling, Aoyama, Kimura and Nishina, are summarized by A. E. Lindh.[1] The latest work is that of Pauling[2] who was able to calculate quantitatively the shifts in the position of the K absorption edge in the alkali chloride series and in the potassium halide series. The answer to the second question as given by Coster,[3] Lindsay,[4] Ray,[5] and others, has been in terms of the simultaneous transitions of two or more electrons within the atom, due to the absorption of a single quantum. This suggestion does not give any idea as to why secondary absorption is a function of chemi-

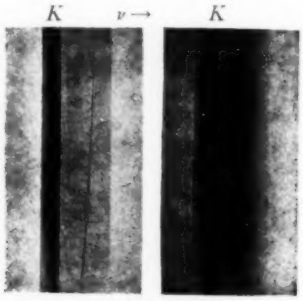

Fig. 1. (a) Simple edge. (b) Edge with secondary absorption.

cal state, though Coster and Wolf[6] have postulated that multiple jumps will be less probable in an atom which has completed electron shells. On the side of emission spectra, the suggestion of F. K. Richtmeyer[7] of simultaneous transitions of electrons to account for x-ray satellites seems to be the most acceptable at present in view of the recent experiments of Du Mond and Hoyt.[8,9] This fact no doubt makes the same hypothesis more probable as an explanation of secondary absorption. The writer simply wishes to bring out here that with the present knowledge regarding secondary absorption one can not make much use of the experimental data, whereas, because of its pene-

[1] Handbuch der Experimental Physik XXIV 2. Teil (1930).
[2] L. Pauling, Phys. Rev. **34,** 954 (1929).
[3] D. Coster, Zeits. f. Physik **25,** 83 (1924).
[4] G. A. Lindsay and H. R. Voorhees, Phil. Mag. **6,** 910 (1928).
[5] B. B. Ray, Nature **122,** 771 (1928).
[6] Coster and Wolf, Nature **124,** 652 (1929).
[7] F. K. Richtmyer, Journ. Frank. Inst. **208,** 325 (1929).
[8] Du Mond and Hoyt, Phys. Rev. **36,** 799 (1930).
[9] Du Mond, Phys. Rev. **36,** 1015 (1930).

trating power, it seems that the x-ray has the possibility of giving interesting information about the atom in the solid state. It was thought that a study of the x-ray absorption of vapors, where one is concerned with isolated atoms or molecules, would be of help to the problem.

Apparatus

In order to study absorption in vapors one must have a cell which will transmit the radiation, which will stand the requisite temperature to secure sufficient vapor pressure, and which will not react with the hot vapors. One is practically limited to a study of those vapors which have their characteristic x-ray absorption in the region from about one to two and one-half angstroms, since at shorter wave-lengths the energy dispersion becomes too small, and at longer wave-lengths nothing can be found to use for a cell. Fig. 2 shows the arrangement which was used. *S* is the slit, *C* is the calcite crystal, and *P* is the photographic plate. The furnace *B* is for controlling the vapor pressure, and the furnace *A* is for superheating the vapor. The furnace box is

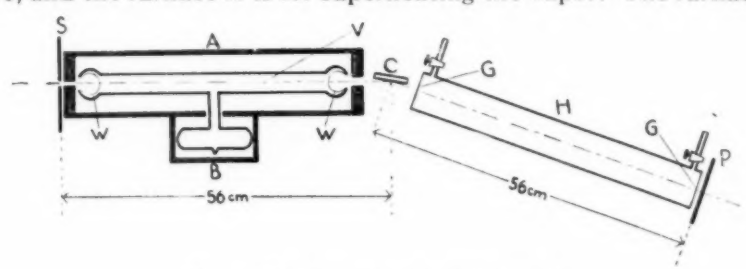

Fig. 2. Diagram of x-ray spectrograph.

made of transite. The vapor cell *V* is made of Pyrex or of quartz, and the concave windows *W* may be drawn as thin as 0.005 mm in Pyrex,[10] and to 0.003 mm in quartz, and yet maintain a vacuum and stand temperatures to the melting points. In order to prevent any vapor condensation on the windows *W*, the openings in the ends of furnace *A* were covered with three sheets of Al foil or mica with air spaces between the sheets. *H* is a glass tube with gold-beater's skin windows. The air is flushed out with hydrogen simply to reduce the air path of the radiation. The dispersion of this spectrograph in the region worked varies from 4.9 to 5.3 X.U. per mm. The usual slit width was 0.05 mm, though for special cases it was narrowed to 0.025 mm or widened to 0.1 mm. The x-ray tube was an extra large size of the Siegbahn type. The current was usually about 30 m.a., and exposure times varied from 4 to 30 hours depending on the absorbing material.

Preparation of Materials

The substances which were investigated in this work were As, Se, Br, Zn, Hg, Xe, and Kr, and compounds of some of these elements. When it was possible, each substance was studied in both solid and vapor forms. In the solid form the absorption spectrum was secured for various thicknesses of screen, while in the vapor state all degrees of absorption could easily be se-

[10] Slack, J.O.S.A. **18,** 123 (1929).

cured by regulating the vapor density through the temperature. After thorough cleaning and baking of the cell V, the material was inserted, and the cell sealed-off under high vacuum conditions. The cell was about 40 cm long. With this length of path a few cm pressure of vapor was usually sufficient to produce the maximum contrast in the absorption spectrum. The vapor was always superheated so that there would be no condensation on the ends of the tube. When studying Zn, the vapor was superheated to 950 degrees C, though all of the other vapors could be studied at temperatures much lower than this. Attention must be paid to the fact that polyatomic molecules dissociate at certain temperatures, so that this temperature must not be exceeded. The fact that the x-radiation itself decomposes some molecules did not cause any difficulty in this work since, for example with AsH_3, the As atoms froze on the walls of the cell and left only AsH_3 in the path of the radiation.

In studying solids, if it is possible, the simplest method is to soak cigarette paper in a solution of the material and let it dry. A metal like Zn may be rolled to a thin sheet. Thin sheets of metallic As were formed by passing AsH_3 through a Pyrex tube heated to 500 degrees C. The AsH_3 decomposes, depositing a silvery mirror of As which can be peeled off of the tube. Because of its surface tension, it is hard to get a thin sheet of Hg. A screen of finely divided Hg was formed by reducing mercurous nitrate by formic acid held in gelatine. This gives an emulsion containing very densely packed mercury globules of about 10μ diameter.[11] The compound $NaBrO_3$ can not be had in the vapor form so it was studied as a solid and in solution. Solutions varying from saturated to 1/3 normal were put in cells from 0.7 to 2.0 mm thick. These cells had thin mica windows.

Experimental Results

Due to the character of secondary absorption, there has been no uniformity among different workers in the methods of recording measurements. The absorption regions may vary in width from the slit width of a few volts to as much as 40 volts. The tables in this paper record the distances of both sides of every absorption band, or the distance of the center of the absorption bands from the principal edge. The secondary discontinuities near to the principal edge are always sharper than those farther from the edge. This diffuseness of those farther out, makes it impossible to state their position to closer than about 10 volts.

B. B. Ray[12] has introduced two definitions which it will be convenient to use for purposes of classification and of discussion. Any absorption discontinuities which exist at energy distances from the principal edge of less than the ionization potential of the atom will be called "fine structure" while the term "secondary absorption" will be used to designate absorption discontinuities which occur at greater distances than this from the main edge.

An inspection of Table I shows the following facts: The secondary absorption of As in the solid and vapor states is radically different. $AsCl_3$ in the solid

[11] M. Wolf, Zeits. f. Physik **53,** 72 (1929).
[12] B. B. Ray, Ind. Journ. Phys. **3,** 477 (1929).

form shows an additional structure near the main edge which does not occur for the vapor. The same statement applies to the spectra of As_2O_3 in solid and in vapor form. AsH_3 shows no secondary structure. In the vapor state, the principal edges agree within the experimental error, while in the solid state there are differences as great as 5.2 ± 1.5 volts.

The results of the study of Br_2 and its compounds are uncertain in a few cases because one can not get rid of the effect due to the AgBr in the photographic plate. All of the solids and the $NaBrO_3$ solution show an extensive secondary absorption structure. A comparison of the $NaBrO_3$ solid and the solution shows the same type of additional structure which appeared in the solid As compounds here occurring for the solid $NaBrO_3$. There are shifts in the positions of the main edges of as much as 6.9 ± 2.3 volts.

The positions of the main edges of the Se compounds were not determined. Se_8 vapor exhibits one very close fine structure line but no secondary absorption. Se solid has a white line absorption at the main edge and perhaps an indication of a fine line like that shown by the vapor. SeO_2 solid and vapor both show a secondary absorption, and, as in the cases of the As and Br compounds, there is an additional structure in the absorption spectrum of the solid which does not appear in that of the vapor.

TABLE I.

Substance	Temperature °C.#	Main Edge X. U.	ΔV (volts)	Distances of both sides, or, of center of absorption bands from the main edge. (volts)
Solids				
As		1042.49	0	0–3.6, 10–12, 40–58, 75–92, 130–152, 168–?
$AsCl_3$		1042.41	0.9	0–7.6, 14–22, 33–38, 48–92, 145–?
As_2O_3		1042.22	3.1	0–5.1, 12–18, 55–97, 140–?
As_2O_5		1042.03	5.2	0–5.4, (54–30)*, 60–118, 150–?
Vapors				
As[4]	350 270 95	1042.31	2.0	0–4.4, 57–102, 135–?
$AsCl_3$	35	1042.31	2.0	0–3.8, 57–82, 125–?
As_2O_3	320 260	1042.34	1.7	0–5.2, 55–93, 160–?
AsH_3	20	1042.43	0.7	0–3.0
Outer levels of Se atoms				12., 61., 160., 236.
Solids				
AgBr		918.23	4.1	0–6, 23.5, 52., 93., 129.
NaBr		918.04	6.9	0–9, 27.7, 60–?
$NaBrO_3$		918.09	6.1	0–7, 15–23, 35, 52–110, 180–?
Solution				
$NaBrO_3$		918.09	6.1	0–23, 55–110, 170–216
Vapors	20			
Br_2	−20	918.51	0	0–6
HBr	20 170	918.41	1.5	
$AsBr_3$	120	918.44	1.0	0–6.
Outer levels of Kr atom				13., 28., 96., 212., 295

TABLE I (*Cont'd.*)

Substance	Temperature°C	Main edge X.U.	ΔV (volts)	Distances of both sides, or, of center of absorption bands from the main edge. (volts)
Solids				
Se				0–4.
SeO_2				0–5.4, 12–18, 53–108, 159–?
Vapors				
Se_x	510			0–5.5, 10–12
	470			
SeO_2	330			0–32., 72–108, 159–?
	280			
Outer levels of Br atom				11., 23., 80., 183.
Solid				
Zn		1280.5	0.0	0–5.8, 9.7–16., 23., 28–43, 72–87, 113–145, 175–214, 252–280, 310–?
Vapor				
Zn	950	1280.7	−1.5	0–4, 5.8–9.
	750			
Outer levels of Ga Atom				10., 22., 106., 158.
Vapor				
Kr	20	863.72		
Vapor				
Xe	20	L_{III} 2587.2		0–3.9
		L_{II} 2424.1		0–3.9
		L_I 2269.1		
Liquid		L_{III} edges		
Hg		1006.7	−2.5	
Solid				
$HgCl_2$		1006.4	+1.2	0–6, 18, 50, 115
HgO		1007.1	−7.4	0–8, 16–66, 80–?
Vapor				
Hg	250	1006.5	0.0	
	200			
$HgCl_2$	330	1006.9	−4.9	0–6, 18, 50, 115
	230			

* Faint absorption.

The upper temperature is the superheated vapor temperature, the lower is the temperature at which the vapor would be saturated.

No compounds of Zn were studied. The metal itself shows a very extended secondary absorption which is absent in the absorption spectrum of Zn vapor at 950°C. There is a very faint fine structure line at 5.8 volts from the main edge for Zn vapor. The data given on the secondary absorption of Zn are the results of observations on a number of different plates obtained under different conditions. Plates were taken using slit widths of 0.025, 0.05, and 0.1 mm. The fine structure close to the edge is just detectable with the narrowest slit, but with this slit the radiation is so faint that it would take too long a time to secure the secondary absorption farther from the edge. The $WL\beta_1$ line falls close to the K edge of Zn, so that some plates were taken using a Pt filament with a Mo, and also a Pt target to eliminate any uncertainties due to the presence of emission lines.

The K edge of Kr proves to be a simple edge without even a white line at the edge. The wave-length of the K edge of Kr is measured using $SrK\alpha_1$ (873.37 X.U.) as a reference line.

The L edges of Xe show no secondary absorption, but at the L_{III} and L_{II} edges there is a white line absorption which is 3.9 volts in width. The positions of the L_{III}, L_{II}, and L_I, edges of Xe were measured from the $WL\beta_1$ (1279.17 X.U.), $WL\beta_2$ (1242.03 X.U.), and $WL\gamma_5$ (1129.2 X.U.) lines, respectively.

The data on mercury show that there is no secondary absorption for the liquid or the vapor, but there is for the Hg compounds. However, the structure is very faint and the values given are only approximate. The L_{II} edges of $HgCl_2$ solid and vapor also show a very faint secondary structure which has the same energy separations from the main edge as has that associated with the L_{III} edges. No secondary structure was found for any L_I edges. Noting the positions of the main edges, it is seen that $HgCl_2$ solid has the shortest, and HgO solid the longest wave-length. These edges can be determined to about 4 volts.

Summary and Discussion

A consideration of the experimental results permits a number of generalizations to be made.

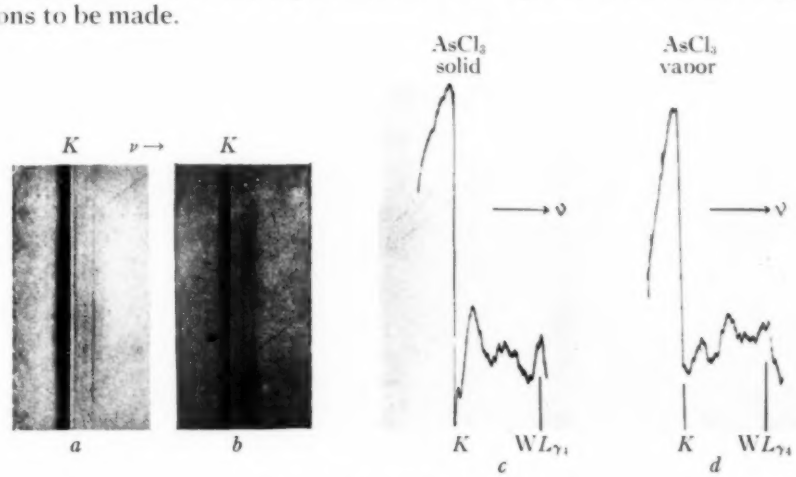

Fig. 3. $AsCl_3$ (a) solid; (b) vapor.

1. The secondary absorption of a polyatomic vapor usually has the same main characteristics as that of the solid, though the solid shows some additional structure, near the main edge, not found for the vapor. The examples of this are $AsCl_3$, As_2O_3, and SeO_2. Fig. 3 shows the data for $AsCl_3$. The microphotometer trace records clearly the dark line which splits the first white region, but it does not resolve the next dark region into the two close dark lines which can be seen on the original plate.*

* One may feel some assurance that statement No. 1. is a *bona fide* effect because of the fact that due to its perfect homogeneity the vapor makes as good, and probably a better absorbing screen for displaying secondary absorption than does the solid.

2. The Br secondary absorption shown by $NaBrO_3$ in the solid form has the same characteristics as that of $NaBrO_3$ in solution except that there is an additional structure near the main edge for the solid which is not observed for the solution. This same experiment has been performed by Meyer[13] for both

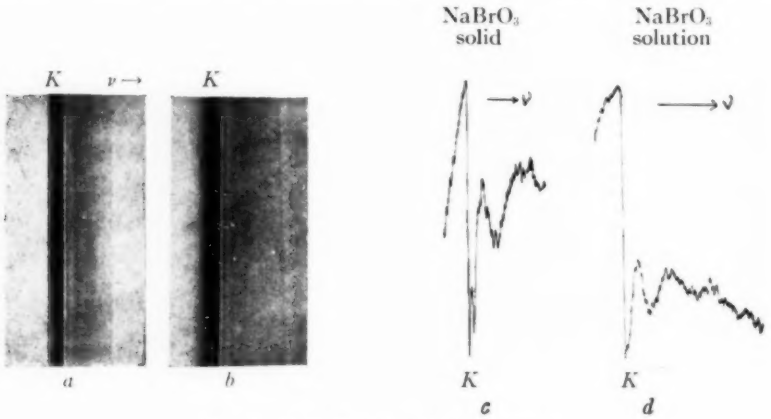

Fig. 4. $NaBrO_3$ (a) solid; (b) vapor.

$KBrO_3$ and $NaBrO_3$. He did not observe any additional structure in the absorption spectra for the solid state. Yost[14] found no detectable difference in the K absorption of manganous and chromate ions in crystals and in aqueous solutions.

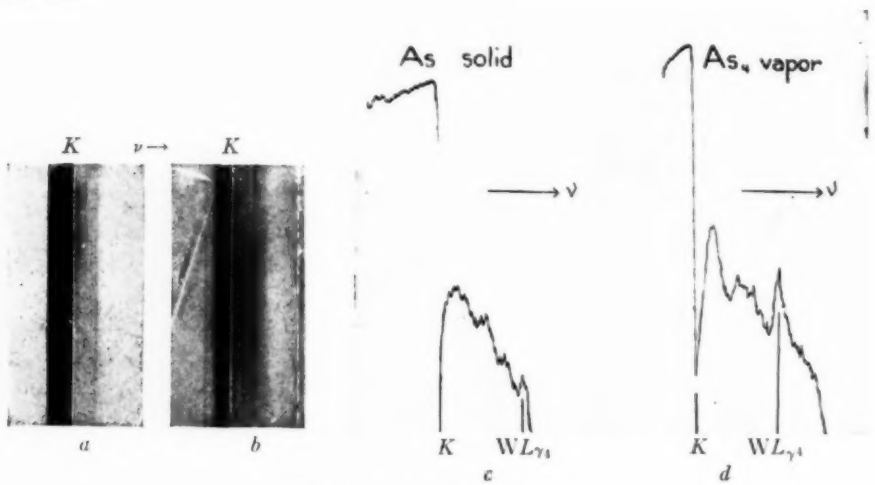

Fig. 5. As (a) solid; (b) vapor.

3. The secondary absorption of a polyatomic vapor may differ entirely from that of the solid. This effect is shown by As and illustrated in Fig. 5. As is tetratomic in the vapor state.

[13] H. Th. Meyer, Wissenschaftliche Veröffentlichungen aus dem Siemens-Konzern **7**, 101 (1929).

[14] D. M. Yost, Phil. Mag. **8**, 845 (1929).

4. The secondary absorption of a compound may differ from that of the element. Every case investigated in this work corroborates this statement. Also, this effect is well known from previous work with the lighter elements, and has recently been shown by Lindh[15] for Cu and Ni.

5. Secondary absorption is not observed for any monatomic vapor. Hg vapor, Zn vapor, Xe, and Kr are the examples of this; and one may also include Coster's and Van derTuuk's[16] case of argon. Xe and Kr were not studied in the solid form. Liquid Hg showed no secondary absorption, but Zn in the solid state exhibited the extensive structure shown in Fig. 6.

6. A monatomic vapor may show a fine structure a few volts from the main edge. Zn vapor has a faint absorption at 5.8 volts from the principal edge, though it is too faint to be seen in Fig. 6. Coster and Van der Tuuk found an absorption line for A at 1.7 volts from the main edge. They inter-

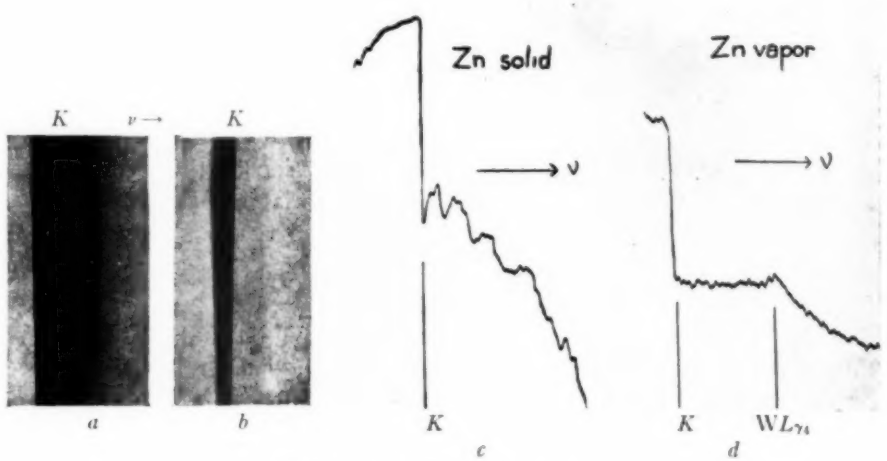

Fig. 6. Zn (a) solid; (b) vapor.

preted this as due to the transitions of the electron to different virtual orbits of the A atom, since the 1.7 volts coincides exactly with the resonance potential of K which is the next higher atom in the periodic table. The 5.8 volts for zinc does not coincide with the resonance potential of Ga, which is only 3.06 volts and would not be resolved. However, the ionization potential of Ga is 5.97 volts. This might mean that the electron stops either at the first virtual orbit, causing the main edge, or travels entirely out of the atom causing the fine structure line.

The L_{III} and L_{II} absorption edges of Xe showed a white line absorption at the main edges. The widths of these white lines were 3.9 volts. The short wavelengths edges were quite diffuse. Lepape and Dauvillier[17] have studied Xe and found a white line absorption only at the L_{III} edge. The width of their

[15] A. E. Lindh, Zeits. f. Physik **63,** 106 (1930).
[16] Coster and Van der Tuuk, Zeits. f. Physik **37,** 367 (1926).
[17] Lepape and Dauvillier, Comp. Rend. **177,** 34 (1923).

white line was about 13 volts which they related to the ionization potential of Xe. (11.5 volts). However, with the K electron absent, the outer field of Xe should compare with the next higher atom which is Cs, and which has an ionization potential of 3.88 volts. The reason for there being no white line absorption at the L_I edge may be that according to the selection rule $\Delta l = \pm 1$, transitions to the first virtual orbit could take place from the L_{III} and L_{II} orbits, but not from the L_I orbit. The absorption edges of Hg and of Kr were 'simple' without the white line at the edge. However, this may simply be because the energy dispersion in this wave-length region is from 70 to 90 volts per mm. while in the Xe L region it is 9.7 volts per mm.

7. Secondary absorption is not exhibited by all polyatomic vapors. Se_8 vapor and AsH_3 are two examples of this.

8. Completed shells of the atom in the solid state need not necessarily be associated with the absence of secondary absorption. The Br absorption in both AgBr (in the photographic plate) and NaBr shows a secondary structure. Meyer[13] has reported that secondary absorption is absent for these compounds, and several people[6,18] have remarked that secondary absorption will not be exhibited by atoms with completed shells such as Br^-.

The points at which the results of these experiments differ from those of other workers can be attributed to higher dispersion and better resolution. The resolution is such that the $WL\gamma_4$ line, which is measured in Siegbahn's laboratory as 1025.8 X.U., is here separated into two components 15 mm apart. This is 0.79 X.U. and gives 0.68 ν/R units or 9.25 volts for the separation of the O_{II} and O_{III} levels of W. The results of Meyer,[13] for instance, that there is no structure in the K edge of Br in the photographic plate, and that the secondary absorption of $NaBrO_3$ solid and solution are identical, were gotten if the experiments were performed with an 18 cm radius Siegbahn spectrograph using a calcite 100 face (dispersion 16.6 X.U. per mm); or using a calcite 111 face (dispersion 7 X.U. per mm). This latter dispersion should be high enough to observe the additional structure but it is apparent from the pictures obtained that the 111 face does not allow the resolution which can be gotten with the 100 face.

It is not apparent as yet how successful the idea of multiple electron transitions will be in explaining the effects of physical and chemical state on secondary absorption. Several workers have quantitatively correlated the energies of the secondary discontinuities with the energies of certain chosen multiple electron jumps. In the table are shown the energies of *double* electron jumps simply calculated from the energy levels of the atom next higher in atomic number. There is an approximate agreement with at least one compound of each element. A more precise calculation such as that of Kievit and Lindsay[19] was not attempted because the discontinuities here measured could not be located more accurately than about 10 volts unless the discontinuities were close to the main edge, where they are always sharper. It seems that if

[18] R. Swinne, Phys. Zeits. **30,** 523 (1929).
[19] Kievit and Lindsay, Phys. Rev. **36,** 648 (1930).
[20] G. Wentzel, Ann. d. Physik **66,** 437 (1921); **73,** 647 (1924).

secondary absorption is due to double electron transitions, then those discontinuities occurring more distant from the main edge represent transitions of electrons from deeper levels of the atom and so would be expected to be sharper, rather than more diffuse, than the discontinuities occurring close to the main edge and representing transitions of outer electrons.

The suggestion of transitions of electrons in multiply ionized atoms which has been made by Wentzel[20] to account for x-ray satellites, and applied also to absorption spectra[21,22] does not seem suited to explain secondary absorption, because the number of quanta of radiation of sufficient energy for ionization which are produced by the x-ray tube is so small that the number of ionized atoms in the absorbing screen at any time is a negligible fraction of the total number present.

The data as it appears in this work would seem to favor the idea of relating the secondary absorption to some characteristic of the structure of the molecule or solid. One might suppose that the secondary edges correspond to the energies of excitation of the vibrational states of "structure electrons" such as postulated by O. W. Richardson[23] to account for the facts observed in experiments both on the secondary electron emission of substances and the soft-x-ray production of substances. The relation between the secondary absorption discontinuities and the kinks in the secondary electron curves can not be carried very far at present because the sensitivity is so much less for the x-ray secondary absorption determinations of energies. However, there are some points of similarity between the observations made in the study of x-ray absorption spectra, and in the study of secondary electron emission.

The kinks in the secondary electron curves correspond to the Bohr energy levels of the atom when the experiment is done roughly, but with increased sensitivity many more kinks are discovered which can not be related to the Bohr levels of the atom. The range in which these kinks occur is from zero to about 500 volts. Above this range one finds only kinks which agree with Bohr levels. These facts are exactly paralleled by the study of x-ray absorption spectra. Also, the present experiments indicate a close relation between the occurrence of secondary absorption and the structure of the substance. Turning to the study of secondary electron emission, it is found that the number and positions of the kinks which are not related to Bohr levels are functions of the structure of the substances which the primary electron beam bombards. For example, the kinks obtained using a polycrystalline substance seem to be the sum of those from the faces of a single crystal of the substance studied separately. (This is presumably not a diffraction phenomenon.) There are enough of these kinks so that Richardson was able to see that they could all be included in tables like sets of bands, and this fact led to the idea of relating them to the excitation energies of the vibration levels of some oscillating system.

An obvious experiment to check the validity of such an idea to account for

[21] E. C. Stover, Phil. Mag. **2,** 97 (1926).
[22] H. R. Robinson, Phil. Mag. **4,** 763 (1927).
[23] O. W. Richardson, Roy. Soc. Proc. **A128,** 63 (1930).

secondary absorption would be to study the absorption spectra of both elements of a chemical compound and see in how far the secondary absorption is a function of the individual elements and in how far a function of the compound. Satisfactory data for such a check do not exist at present.

In order to be certain that the absence of secondary absorption for zinc vapor at high temperature is not simply a temperature effect, experiments are now being carried out on the effect of high temperature on the secondary absorption exhibited by solids.

The writer wishes to express his warm appreciation for the excellent and ample facilities for research which have been available at the Department of Physics of the University of Michigan. He is particularly indebted to Professor G. A. Lindsay for much helpful advice, and to Mr. G. Kessler for his part in the difficult task of making the thin quartz windows.

INFRARED ABSORPTION BANDS IN HYDROGEN SULPHIDE

By Harold H. Nielsen and Ernest F. Barker
Department of Physics, University of Michigan

(Received January 30, 1931)

Abstract

Absorption spectrum of H_2S in the region from 1.0μ to 10.0μ.—The absorption spectrum of hydrogen sulphide in the infrared has been investigated with a prism spectrometer from 1.0μ to 10.0μ. Two regions of absorption, one at 2.6μ and another 3.7μ were located, both of which revealed fine structure when examined under high dispersion.

Structure of the 2.6μ absorption band of H_2S.—The band at 2.6μ was found to consist of P, Q, and R branches, the P and R branches being made up of somewhat irregularly spaced lines and the Q branch broadened unsymmetrically, sloping off more steeply toward lower frequencies. The separation between the most prominent lines in the P and R branches was found to be about 10 cm^{-1}. A slight convergence was observed toward higher frequencies.

Structure of the 3.7μ absorption band of H_2S.—The 3.7μ band was found to consist of but one branch, made up of several prominent lines with weaker satellites on either side. The average spacing between these is about 9.0 cm^{-1}, and no convergence was discernable.

Qualitative quantum mechanical discussion of structure of absorption bands of H_2S.—Only a qualitative discussion of the structure of the observed bands is given, based on the classical quantum mechanical solution of an asymmetric rotator due to Witmer. The band at 2.6μ is accounted for by a vibration of the electric moment along the least axis of inertia while the band at 3.7μ is shown to arise from a vibration along the intermediate axis. It is pointed out that the rigorous quantum mechanical solutions of asymmetric rotators confirm the conclusions drawn herein and in addition satisfactorily explain the broadening of the Q branch.

RECENT quantum mechanical studies of asymmetric rotators[1] have emphasized the importance of investigating the vibration rotation spectra of molecules belonging to this class. The water-vapor absorption bands measured by W. W. Sleator[2] and again by Sleator and Phelps[3] are characteristic of this kind, and they have suggested that a study of the infrared spectrum of hydrogen sulphide might prove fruitful.

W. W. Coblentz[4] has mapped the spectrum of hydrogen sulphide in the region from 3μ to 12μ with a prism spectrometer. More recently A. H. Rollefsen[5] has published two bands in hydrogen suphide at 4.2μ and 8.0μ. In the present work an absorption cell forty centimeters long with mica windows was used, and the spectrum carefully remapped from 1.0μ to 10.0μ with a Wadsworth type prism spectrometer. It was, however, impossible to dupli-

[1] Kramers and Ittman, Zeits. f. Physik **53,** 553 (1929); Wang, Phys. Rev. **34,** 243 (1929); Klein, Zeits. f. Physik **58,** 730 (1929).
[2] Sleator, Astrophys. J. **48,** 125 (1918).
[3] Sleator and Phelps, Astrophys. J. **62,** 28 (1926).
[4] Coblentz, Pub. Carnegie Inst. No. 35, pp. 52 and 178.
[5] Rollefsen, Phys. Rev. **34,** 604 (1929).

cate any of the bands previously reported, but two other absorption maxima were located, lying at 2.6μ and 3.7μ. The prism curve of the absorption spectrum of hydrogen sulphide as determined in this investigation is shown in Fig. 1 A. The maximum near 4μ reported by Coblentz and Rollefsen was found in the first trial, but upon careful purification of the gas it disappeared and almost certainly is to be ascribed to carbon dioxide as an impurity. Likewise in another series of observations when a cell with rock salt windows was used, the band reported by Rollefsen at 8.0μ was found. In all other trials, mica windows were used and although this spectral region was carefully searched, the 8μ band could not be found. It appears that this band can not be due to the hydrogen sulphide molecule, for on all occasions before searching for it, the presence of the absorption maxima at 2.6μ and 3.7μ was first confirmed. It is suggested that the 8.0μ band may be characteristic of some substance formed by the interaction of hydrogen sulphide with the rock salt windows.

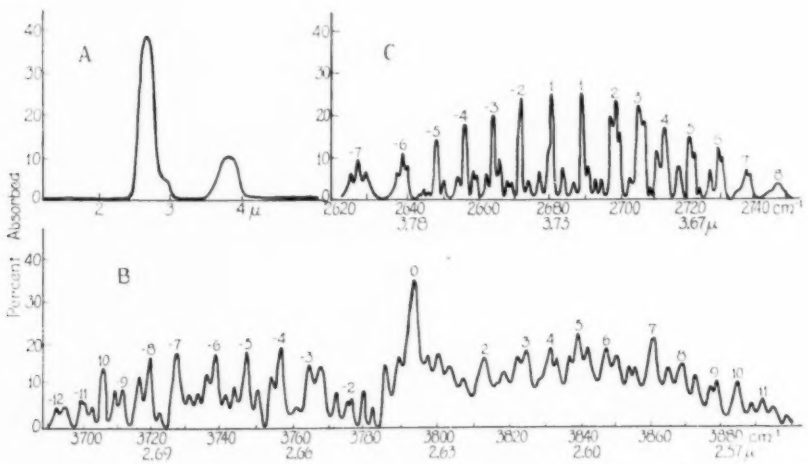

Fig 1. Absorption bands in hydrogen sulphide. *A*, Prism curve with low dispersion. *B*, Fine structure in the band at 2.6μ. *C*, Fine structure in the band at 3.7μ.

A prism grating spectrometer designed by C. F. Meyer was available for further investigation of the hydrogen sulphide spectrum under high dispersion. The apparatus was equipped with a vacuum thermopile constructed by Meyer and was used in conjunction with a Moll thermal relay and a Leeds and Northrup high sensitivity galvanometer. This gave a sensitivity sufficiently high to make the use of slit widths of 16 angstrom units feasible. The grating used in both regions was one with a spacing of 7200 lines per inch (2834 lines per centimeter) ruled on a copper-nickel surface. The calibration of this grating was obtained from a table prepared by A. A. Levin for this spectrometer, based upon the positions of the -3 and -4 lines of hydrogen chloride determined by Colby, Meyer and Bronk.[6]

Two lengths of absorption cell were used, the H_2S being at atmospheric

[6] Colby, Meyer and Bronk, Astrophys. J. **57**, 7 (1923).

pressure in each. For the band at 2.6μ, a length of ten centimeters was found most advantageous. This cell was double, one side being filled with dried air to compensate for the water-vapor absorption in the atmosphere. At 3.7μ a cell twenty five centimeters long was used. Compensating windows were not necessary here since the diminution of the energy due to the mica could satisfactorily be taken into account by making a preliminary run with the cell empty, and no atmospheric absorption occurs in this region.

The hydrogen sulphide gas was obtained in ordinary lecture bottles from the Matheson Company, their analysis showing a purity of 99.7 percent. In order to remove any carbon dioxide, carbon disulphide and hydrogen chloride,

TABLE I. *Wave numbers and intensities of lines in the band at 2.7 μ.*

Intensity	Wave No. (cm^{-1})	Line No.	Intensity	Wave No. (cm^{-1})	Line No.
2.0	3692.5	−12	6.5	3786.0	
2.0	3694.7		7.0	3789.5	
2.5	3700.0	−11	15.0	3793.9	0
2.0	3701.3		6.5	3797.7	
6.0	3706.5	−10	6.5	3800.5	
3.5	3709.6	− 9	6.0	3804.1	
3.5	3712.0		5.0	3808.2	
5.0	3716.6		7.0	3813.7	2
7.0	3720.1	− 8	5.0	3819.9	
1.0	3722.5		6.5	3822.9	
7.0	3728.0	− 7	7.5	3825.0	3
2.5	3731.8		7.5	3831.8	4
2.5	3733.4		6.5	3834.0	
5.0	3736.0		6.5	3837.7	
7.0	3737.6	− 6	8.0	3840.3	
3.0	3740.3		6.5	3843.6	
3.0	3743.1		6.5	3848.5	6
7.0	3746.6	− 5	6.4	3851.5	
3.0	3750.7		5.0	3855.6	
5.0	3754.0		5.0	3757.1	
8.0	3756.2	− 4	7.5	3861.2	7
1.0	3760.8		5.5	3866.1	
6.0	3764.5	− 3	6.0	3870.5	8
6.0	3768.0		5.0	3873.3	
3.0	3772.6		4.0	3878.5	
2.5	3775.1		4.5	3879.7	9
2.5	3776.9	− 2	4.5	3886.0	10
3.0	3780.1		2.0	3889.9	
2.0	3782.5		2.5	3892.5	11
			2.0	3895.8	

the gas was passed through three successive wash bottles each of which contained a solution of potassium hydrosulphide (KHS). After drying over phosphorus pentoxide, the gas was gathered by freezing with liquid air and finally purified by partial distillation. This was done immediately before each run.

The two absorption maxima which had been located prismatically, reveal fine structure when examined under high dispersion. They are distinctly different in type, but are both characterized by an irregularity of structure suggestive of water vapor bands. When only the most intense lines are considered however, the patterns resemble the bands due to certain symmetrical molecules.

The 2.6μ region. The 2.6μ band shows distinct *P*, *Q* and *R* branches, the *P* and *R* branches being made up of irregularly spaced lines. The average spacing for those of greatest intensity is about 10 cm^{-1}. Moreover, proceeding from the center outward it seems possible to identify the various lines in the *P* branch with corresponding lines in the *R* branch. A slight convergence is noticeable toward higher frequencies, and the *Q* branch is broadened unsymmetrically, sloping off more steeply toward lower frequencies. Curve B shows those details of this band which repeated themselves in the many sets of data taken. Original circle settings have been replaced for convenience by a scale of frequencies, and in Table I the frequencies and approximate relative intensities of the lines are given.

TABLE II. *Wave numbers and intensities of lines in the band at 3.7μ.*

Intensity	Wave No. (cm^{-1})	Line No.	Intensity	Wave No. (cm^{-1})	Line No.
2.5	2624.3		10.0	2690.1	1
3.5	2626.9	−7	2.0	2692.2	
2.5	2629.7		1.0	2693.3	
3.0	2636.5		1.0	2694.6	
5.0	2637.8	−6	8.8	2697.8	
3.5	2638.9		9.5	2698.7	2
.3	2642.6		8.0	2701.2	
.4	2643.7		1.5	2704.1	
.3	2645.2		9.0	2706.6	3
6.2	2647.8	−5	8.5	2707.0	
2.2	2650.2		.5	2709.8	
2.2	2654.4		5.0	2712.7	
7.5	2656.6	−4	7.5	2714.4	4
2.2	2658.6		3.5	2719.1	
2.1	2660.6		6.0	2721.9	5
2.1	2663.2		4.0	2722.8	
8.7	2665.1	−3	.5	2724.5	
2.5	2666.6		2.5	2727.0	
1.0	2669.5		5.0	2729.5	6
1.0	2670.9		3.0	2730.5	
10.0	2673.8	−2	.8	2737.7	
1.0	2675.6		3.0	2738.4	7
2.0	2679.4		2.0	2739.4	
10.0	2682.5	−1	.8	2743.3	
2.0	2684.9		2.0	2745.3	8
1.0	2687.8		.8	2746.7	

The 3.7μ region. The 3.7μ band is of the type which shows an envelop with but one maximum. It also has been resolved, at least partially, revealing a number of prominent lines, characterized in general by accompanying satellites of lesser intensity on either side. No apparent convergence is discernible and the most prominent lines are separated by an average spacing of about 9.0 cm^{-1}. Details repeating themselves in all sets of data are shown in curve C where as before a frequency scale replaces the original circle settings. Table II gives the frequencies and relative intensities of the lines measured in this region.

INTERPRETATION OF THE OBSERVED BANDS

It is hoped in a later communication to give a complete description of this spectrum in terms of the rigorous quantum mechanics of an asymmetrical

rotator model. At present, it seems better, however, to consider qualitatively only the general characteristics of the two observed bands.

A solution for the asymmetrical rotator by a perturbation method is given by E. E. Witmer[7] in the classical quantum mechanics where the perturbation function involves the third moment of inertia. Taking A, B, and C as the three principal moments of inertia where $A<B<C$, the energy levels are shown to be of two kinds, A-levels arising when the molecule rotates principally about the least axis of inertia, and C-levels, arising when the molecule rotates principally about the largest axis of inertia; their combined number being $J+1$. The energy values of A-levels are those of a symmetric rotator rotating about the A-axis plus a certain perturbation component to the energy involving C. The C-levels are similarly determined by the energy expression of a symmetric top rotating about the C-axis plus another perturbation component involving A.

Hund[8] and Dennison[9] have shown that isosceles triatomic molecules have three fundamental modes of vibration, two of which are along the bisector of the apex angle, and a third perpendicular to this. If the three absorption bands corresponding to these three vibrations can be observed, the dimensions of the triangle (i.e., the apex angle and the lengths of the sides) may be calculated, from which the three moments of inertia may in turn be determined. In hydrogen sulphide only two bands have been observed, however; hence this means of determining the shape and moments of inertia is not available. The indeterminancy of the shape of the molecule introduces the further limitation that one can not know whether the bisector of the apex angle will be the least or the intermediate axis of inertia, since this depends upon the magnitude of the angle. Consequently the appearance of the third fundamental, were it observable, cannot be predicted, for if the bisector of the apex angle were the least axis of inertia, there would be two identical bands of one kind, while if it is the intermediate axis of inertia there would be two identical bands of the other type.

In hydrogen sulphide the electric moment vibrates in the plane of the three atoms, i.e., along either the A-axis or the B-axis. When the electric moment changes along A, and the rotation is principally about the same axis, quantum transitions occur among the A-levels governed by the rules (retaining the nomenclature of the symmetric rotator) $\Delta J=\pm 1, 0; \Delta K=0$. When, however, the rotation is principally about C, quantum transitions occur among the C-levels and are determined by the rules, $\Delta J=\pm 1, 0; \Delta K=\pm 1$. This gives rise to a band having P, Q and R branches, the P and R branches originating from the transitions $\Delta J=\pm 1, 0; \Delta K=\pm 1$; and $\Delta J=\pm 1, \Delta K=0$; and the Q branches from $\Delta J=0, \Delta K=0$. The band observed at 2.6μ having distinct, P, Q and R branches, is consequently due to a vibration of the electric moment along the least axis of inertia; i.e., the A-axis.

Vibrations of the electric moment along the B axis are perpendicular to

[7] Witmer, Proc. Nat. Acad. **12**, 602 (1926).
[8] Hund, Zeits. f. Physik **31**, 81 (1925).
[9] Dennison, Phil. Mag. **1**, 195 (1926).

rotations about both the A and C-axis, hence quantum transitions among both A and C-levels must be governed by the selection rules $\Delta J = \pm 1, 0$; $\Delta K = \pm 1$ alone. It may easily be seen that the resulting band is of the type observed at 3.7μ with no Q-branch. The regularity in spacing and intensity of the lines of bands of symmetric rotators is due to the fact that many transitions are over the same frequency range giving rise to lines which are precisely superposed. In the case of asymmetric rotators the positions of successive energy levels are altered by the asymmetry, but with no definite order; hence no regularity of line structure is here to be expected since only rarely do two or more lines fall at the same place.

The general characteristics are borne out also in the rigorous quantum mechanical solutions of the asymmetric rotator given by Kramers and Ittman and by Wang. One of the main differences is the splitting up of the $J+1$ levels of the old theory into $2J+1$ levels on the basis of the new. The magnitude of this doubling as given by Wang is:

$$\Delta\nu = \left\{ \frac{1}{2} \frac{\left(\frac{1}{C} - \frac{1}{B}\right)}{\frac{1}{A} - \frac{1}{2}\left(\frac{1}{C} + \frac{1}{B}\right)} \right\}^{K} \left\{ \frac{h\left[\frac{1}{A} - \frac{1}{2}\left(\frac{1}{C} + \frac{1}{B}\right)\left((J+K)!\right)\right]}{2^{3K}\pi^2 (J-K)!(K-1)!^2} \right\}$$

This is seen to be small when K is small and the rotation is almost entirely about either A or C, but becomes large for those levels which mark the transition from rotation principally about one axis to rotation principally about the other. It is this doubling of the levels that accounts for the broadening of the Q branch. In the symmetric rotator, the Q branch arises from transitions from a rotational level in one vibrational state to the corresponding rotational level in another vibrational state. In the asymmetric case each rotational level save one is a doublet, and transitions now occur from the one doublet component of such rotational levels in one vibrational state to the other doublet component of the corresponding rotational level in another vibrational state. The Q branch thus arising is not a sharp maximum, but consists of many lines near the center of the band.

The kind cooperation and support given to this work by Professor H. M. Randall, and Professor D. M. Dennison's many helpful suggestions in the interpretation of these bands are gratefully acknowledged.

NOTE ON THE INTERPRETATION OF CERTAIN $^2\Delta$, $^2\Pi$ BANDS OF SiH

By Robert S. Mulliken
Ryerson Physical Laboratory, University of Chicago

(Received February 4, 1931)

Abstract

It is shown that Jackson's $^2\Delta$,$^2\Pi$ SiH bands have a *regular* $^2\Pi$ state and thus are closely analogous to the λ4300 bands of CH. The orbit-spin coupling coefficient A is determined for the $^2\Pi$ state of SiH and shown to agree closely with A of the ^3P state of the Si atom, from which the $^2\Pi$ molecular state is supposed to be derived. This is a new example of a relation which seems to be universal. Another new example of the same relation, found in BeH, is also cited.—The coefficients A and B of the $^2\Delta$ state and B of the $^2\Pi$ state of SiH are also discussed.

C. V. JACKSON has obtained some SiH bands near λ4100 and has shown by a skilful analysis that they have a structure corresponding to a $^2\Delta$,$^2\Pi$ transition.[1] Because of the analogy of Si to C, there is a very strong presumption that these bands are analogous to the $^2\Delta$,$^2\Pi$ bands of CH near λ4300. In the case of CH the $^2\Delta$ doublet is very narrow and inverted ($A/B \sim -0.07, B = 14.57$), while the $^2\Pi$ is regular ($A/B = +2.0, B = 14.2$). According to Jackson, the $^2\Delta$ state of SiH is narrow and *regular*, but the $^2\Pi$ *inverted*, with $A/B \sim -10$, $B = 7.4$. From a consideration of electron configurations, however, it is clear that if the $^2\Pi$ state of SiH is inverted it cannot be at all analogous to that of CH, since in such simple molecules[2] an inverted Π state implies a group of three equivalent π electrons, whereas a regular Π state implies only a single π electron outside of closed shells. In the case of the $^2\Delta$ state, however, the existence of a reversed sign of A in SiH, while rather unexpected, has no such important implications. For the $^2\Delta$ state of CH is attributed to an electron configuration $\cdots \sigma\pi^2$, in which the small observed doubling can be ascribed to the small interaction of the spin of the σ electron with the orbital angular momenta of the two π electrons.[2] In similar cases in atomic spectra, we know that doublets of this kind may be either regular or inverted.

A study of Jackson's analysis shows that, while the fact that the $^2\Delta$ is regular is incontrovertible, the only evidence that the $^2\Pi$ is inverted comes from an application of Van Vleck's theoretical work[3] on Λ-type doubling. [The question whether a given $^2\Pi$ level is regular or inverted can in general also be decided by determining the lowest J value in each of the two sets of levels supposed to be $^2\Pi_{1/2}$ and $^2\Pi_{1\ 1/2}$, but this method could not be used in the present instance because of the complexity of the band and the weakness of the lines having low J values.] Van Vleck's theory demands that in case a the Λ-type

[1] C. V. Jackson, Proc. Roy. Soc. **126A**, 373 (1930).
[2] R. S. Mulliken, Phys. Rev. **33**, 730 (1929).
[3] J. H. Van Vleck, Phys. Rev. **33**, 496–7 (1929).

doublets shall be much wider in the $^2\Pi_{1/2}$ than in the $^2\Pi_{1\,1/2}$ levels, and if we assume case *a*, this criterion applied to the experimental data indicates an inverted $^2\Pi$. This was the basis of Jackson's conclusions.

But, as is mentioned in another forthcoming paper,[4] we have in the $^2\Pi$ of SiH a state which is case *a* for the lowest J values but goes over to case *b* with increasing J. In such a case the $^2\Pi_{1/2}$ Λ-type doublets, although they should at first be wider than those for $^2\Pi_{1\,1/2}$, should soon get narrower again and their widths should pass through zero, while the $^2\Pi_{1\,1/2}$ doublets should begin to widen rapidly under the influence of the approach to case *b*.[3] This would give on the whole wider doublets for $^2\Pi_{1\,1/2}$ than for $^2\Pi_{1/2}$, and would require that we reverse Jackson's conclusions and interpret the $^2\Pi$ state as regular. In order to prove that this interpretation is correct we should show that the Λ-type doublets change sign with increasing J in what is here considered to be the $^2\Pi_{1/2}$ state (Jackson's $^2\Pi_{1\,1/2}$ state). Now according to Jackson, the levels which we call $^2\Pi_{1/2}$ show measurable doubling only beginning with $K=14$, while in the $^2\Pi_{1\,1/2}$ levels doubling becomes appreciable at $K=8$. But Jackson remarks that lines going to the levels $K=5$ and 6 of $^2\Pi_{1/2}$ also show a doubling, which he classifies as a perturbation. If, however, we suppose that the Λ-type doubling in the $^2\Pi_{1/2}$ state first increases to a maximum, which is just large enough to be measurable, at $K=5$ or 6, then decreases again, passes through zero at about $K=11$ or 12, and again increases with opposite sign until at $K=14$ it is again large enough to be detected experimentally, all the observed relations are explained, and we have surely a regular $^2\Pi$ state. Table I, based on Jackson's Table VIII, gives the values of the Λ-type doublet separations.

TABLE I. *Λ-type doublet widths* (cm^{-1}) *in* $^2\Pi$ *state of* SiH.*

K	$^2\Pi_{\frac{1}{2}}$	$^2\Pi_{1\frac{1}{2}}$	K	$^2\Pi_{\frac{1}{2}}$	$^2\Pi_{1\frac{1}{2}}$	K	$^2\Pi_{\frac{1}{2}}$	$^2\Pi_{1\frac{1}{2}}$
4	—	—	9	—	0.66	14	0.33	1.61
5	−0.30	—	10	—	0.80	15	0.60	1.91
6	−0.27	—	11	—	0.99	16	0.84	2.12
7	—	—	12	—	1.0	17	0.99	2.42
8	—	0.38	13	—	1.35	18	1.32	—

* Most of these values are weighted averages of values obtained from P, Q, and R branches as given by Jackson in his Table VIII. The negative signs for the low numbered K values of $^2\Pi_{\frac{1}{2}}$ and the positive signs for all other values are of only relative significance here, and furthermore are based only on the fact that according to Van Vleck's theory, the sign of the doubling should be the same in case *b* (high K values) for $^2\Pi_{\frac{1}{2}}$ as for $^2\Pi_{1\frac{1}{2}}$. Empirically there is no way of deciding, from data on Δ, Π bands, whether the T_a or the T_b levels of the Π state are higher. (In the case of a Π, Σ transition this *can* be decided empirically).

Thus we have a regular $^2\Delta$ and a regular $^2\Pi$ state in SiH, and there is every reason to believe that these are analogous to the similar states of CH. It is of interest to determine the magnitudes of the coefficients A of the coupling between Λ and S for the two states of SiH. The value of A/B for the $^2\Pi$ state can be estimated most accurately by fitting Hill and Van Vleck's formula[5] for the general intermediate case between cases *a* and *b* to the data on

[4] R. S. Mulliken and A. Christy, forthcoming Phys. Rev.

[5] E. L. Hill and J. H. Vleck, Phys. Rev. **32**, 250 (1928).

the term *differences* between $^2\Pi_{1/2}$ and $^2\Pi_{1\ 1/2}$ states of the same K values (cf. Jackson's Table IX). This and a further use of Jackson's data on ΔF's in order to determine B more accurately, give $A/B=+19.5$ and $B=7.35$.[6] [$A/B=-15.5$ would do equally well if we did not know from Van Vleck's theory of Λ-type doubling that $A>0$.] In a similar way one obtains for the $^2\Delta$ state the values $A/B=+0.6$ and $B=7.3$ [$A/B=+3.4$ would equally well explain the observed spectrum, but since we expect a very small A for a $\sigma\pi^2$ $^2\Delta$ state, and since $A/B\sim-0.07$ is very small in $^2\Delta$ of CH, the value $A/B=+0.6$ is the more probable].

We thus have $A=+4$ for the $^2\Delta$ state and $A=+143$ for the $^2\Pi$ state, which may be compared with the values $A=-1$ and $A=+28$ for the corresponding states of CH. In the case of CH there is an interesting relation between A in the $^2\Pi$ state of the molecule and A in the ^3P state of the carbon atom from which the $^2\Pi$ of CH is supposed to be derived by the addition of a hydrogen atom.[2] For a $\cdots p^2\ ^3P$ atomic state, we know that for normal coupling the over-all width of the triplet, i.e., $^3P_2-{}^3P_0$, is $1\frac{1}{2}A$. For the normal state of carbon, $^3P_2-{}^3P_0=42$ cm^{-1}, giving $A=+28$ in exact agreement with A as obtained from the $^2\Pi$ state of CH. [Similar, although usually less exact, agreements are found in many other hydrides. Usually the A from the molecule is somewhat *less* than that from the atom.[2]] A similar comparison is of interest for the normal ^3P of the silicon atom and the $^2\Pi$ of SiH. For the atom, $^3P_2-{}^3P_0=223$, giving $A=+149$, in excellent agreement with the value $A=+143$ from SiH. The significance of such agreements has been discussed in a previous paper.[2]

In connection with the comparison of A values of atoms and their hydrides, a recent result of Watson and Parker[7] is of interest. These authors find $A=+1.97$ for the presumably $1s\sigma^2 2s\sigma^2 2p\pi$, $^2\Pi$ state of BeH, which agrees well with the value $A=+2.08$ from the triplet separation ($^3P_2-{}^3P_0$, $\Delta\nu=3.12$) of the $1s^2 2s2p$, ^3P state of the Be atom.

[6] No attempt has been made to obtain very accurate values of A and B, but it is believed that the A value of the $^2\Pi$ state is fairly accurate, the calculations having been made by means of the Hill and Van Vleck formula in such a way as to make the best use of the experimental data.

[7] W. W. Watson and A. E. Parker, Phys. Rev. **37**, 167 (1931).

COLLISIONS OF THE SECOND KIND AND THEIR EFFECT ON THE FIELD IN THE POSITIVE COLUMN OF A GLOW DISCHARGE IN MIXTURES OF THE RARE GASES

By L. B. Headrick and O. S. Duffendack
University of Michigan
(Received January 24, 1931)

Abstract

A study was made of the collision processes in the uniform positive column of a glow discharge in mixtures composed of two of the rare gases, helium, neon and argon and a mixture of each of these gases with mercury vapor, by means of measurements of the electric field and by spectroscopic observations. The discharge tube was of cylindrical form, 4.4 cm in diameter, with plane parallel electrodes The electrode distance could be varied from zero to 32 cm by means of an external electromagnet. The phenomena were studied with currents from 20 to 40 m.a. and pressures from 5 to 30 mm of mercury. The mixtures were circulated through the discharge tube and a purifying system during the entire time that observations were being made. It was very important to maintain extreme purity of the gases. The results show that the electrical and spectral characteristics of the uniform positive column in mixtures of monatomic gases can be explained principally in terms of collisions of the second kind between the ions or metastable atoms of one gas and the neutral atoms of the other. The effect of limitation of electron velocities is insufficient to explain the results, and its effect is shown to be negligible as compared with collisions of the second kind when the concentration of one gas is very small. The necessary condition for a large effect to be produced in the electrical and spectral characteristics of the positive column by a small percentage of one gas added to another is that a close resonance exists between the metastable states of the main gas and the ionization potential or excited states of the added gas atom or ion. By the introduction of as little as 0.4 percent neon or argon into helium, a marked increase in the electric field is produced, and the spectrum emitted is changed almost completely from the arc spectrum of helium to that of neon or argon respectively. The addition of mercury vapor at room temperature to neon caused a decrease of 45 percent in the field while the addition of mercury to either argon or helium produced a small increase. In the cases where the excitation and ionization potentials of the added gas were above the metastable states of the main gas, no reactions between the two gases could occur to affect the concentration of metastable atoms. In these cases practically no change in either the spectral or electrical characteristics were observed upon adding a small amount of one gas to another. However, in larger proportions the change produced in the field was proportional to the amounts of the two gases and the difference between the field in each of the pure gases. This result is accounted for mainly by the difference in the energy of the ionization processes in the two gases by electron impact.

Introduction

THE phenomena occurring when electricity passes through a gas are many and complicated. The various phenomena have been the subject of many investigations and a great deal is known about the electrical and spectral characteristics of the different types of electrical discharges. Until the development of the Bohr theory of the atom, the beginning of the classification of spectroscopic data, and the measurements of critical potentials by means of

electrons of controlled velocity, very little was known about the mechanism of the elementary processes involved in the discharge of electricity through gases. With the information obtained from the classification of spectroscopic data, the spectroscopic study coupled with measurements of the electrical characteristics of a discharge gives a very powerful means of studying the elementary processes taking place. This method has been used by the writers to study the collision phenomena occurring in the positive column of a glow discharge in mixtures of the rare gases.

Klein and Rosseland[1] suggested that since a collision between an electron and a molecule may result in the excitation of the molecule, due to its absorption of the kinetic energy of the moving electron, the reverse of this process should also take place; that is, the change of excitation energy of a molecule to kinetic energy of an electron at a collision between an excited atom and a slowly moving electron. This type of collision is called a collision of the *second kind*. The former process is called a collision of the *first kind*. Franck[2] has shown that the theory of Klein and Rosseland may be extended to include impacts of the second kind between excited atoms and neutral atoms.

Nearly all gases, unless very carefully purified, contain small amounts of other gases as impurities. It has been observed from spectroscopic studies that, in certain regions of a discharge and for certain gases as impurities, the spectra of the impurities were often stronger than that of the main gas. These observations led to spectroscopic investigations of discharges in mixtures of gases.

Duffendack[3,4,5,6] and a number of his pupils have made spectroscopic studies on the excitation in a low voltage arc in mixtures of the rare gases with nitrogen, carbon monoxide, and various metal vapors in a tungsten furnace. The limits and maxima of excitation observed were explained on the basis of collisions of the second kind between the excited atoms or rare gas ions and the neutral gas or metal molecules.

Sawyer,[7] Takahashi,[8] Naudé,[9] Kruger,[10] Frerichs[11] and others have used the hollow cathode discharge with the rare gases to excite the spectra of various metals and have explained the observed maxima and limits of excitation on the basis of collisions of the second kind.

Penning[12,13] has shown that certain phenomena regarding the sparking potentials of mixtures of the rare gases and also other gases can be explained by means of collisions of the second kind.

[1] Klein and Rosseland, Zeits f. Physik **4,** 46 (1921)
[2] J Franck, Zeits. f. Physik **9,** 259 (1922).
[3] O S. Duffendack and H. L. Smith, Phys. Rev. **34,** 68 (1929).
[4] O. S. Duffendack and R. A. Wolfe, Phys. Rev. **34,** 409 (1929).
[5] O. S. Duffendack and J. G. Black, Phys. Rev. **34,** 35 (1929).
[6] O. S. Duffendack, C. L. Henshaw and Marie Goyer, Phys. Rev. **34,** 1132 (1929).
[7] R. A. Sawyer, Phys. Rev. **36,** 44 (1930).
[8] Y. Takahashi, Ann. d. Physik **3,** 49 (1929).
[9] S. M. Naudé, Ann. d. Physik **3,** 1 (1929).
[10] G. Kruger, Phys. Rev. **34,** 1122 (1929).
[11] R. Frerichs, Ann. d. Physik **85,** 376 (1928).
[12] F. M. Penning, Zeits. f. Physik **46,** 335 (1928).
[13] F. M. Penning, Zeits. f. Physik **57,** 723 (1929).

In the present investigation the study of the effect of collisions of the second kind on discharge characteristics has been extended to the positive column of a glow discharge. Mixtures of the three rare gases, helium, neon and argon and mixtures of each of these with mercury vapor were used. The study of collision phenomena and the processes of production of ions was made by observing simultaneously the changes in excitation and in the electric field in the positive column with the change in the proportion of the two gases in a mixture.

Theory of the Uniform Positive Column

The phenomena occurring in the positive column are independent of the material and form of the electrodes and depend only on the properties of the gas, the current density, and the tube diameter. For pure monatomic gases the positive column is uniform under almost all conditions. In diatomic gases or in mixtures, for certain limits of current and pressure, the positive column is striated. The electric field in the uniform positive column is uniform. In the striated positive column a slight sinusoidal variation is superimposed upon the uniform field. This variation has a wave-length equal to the distance between striations. The field reaches a maximum value at the cathode end of the luminous region of each striation. The theory of the uniform positive column will be discussed in detail since practically all of the work in this investigation was done with a uniform column. While most of the data on this part of the discharge are qualitative, some approximate empirical relations have been worked out for a considerable range of the variables. For a tube of cylindrical form, the field is directly proportional to the pressure and inversely proportional to the radius of the discharge tube. At a small current density, for which the positive column does not completely fill the tube, the field increases with an increase in current. The field reaches a maximum value when the column just fills the tube and then decreases slowly until the current density reaches a high value, corresponding to nearly one hundred percent ionization of the gas, after which the field increases quite sharply and rapidly with further increase in current. This condition of practically complete ionization has never been attained in large discharge tubes. It has been studied by Langmuir[14] in capillary tubes with a current density of the order of 40 amp/cm^2.

Schottky[15] has made a study of diffusion currents to the tube walls in the positive column and has developed a theory on the basis of the results obtained. The assumptions made for a cylindrical discharge tube are the following:

(1) The field in the positive column is the source of the energy necessary to maintain a certain degree of ionization which is required for a given discharge condition. (2) Ions are lost by diffusion to the walls where recombination occurs. (3) The current density and concentration of positive ions and electrons is constant throughout the length of the column. (4) The

[14] I. Langmuir, G. E. Rev. **27,** 762 (1924).
[15] Schottky, Phys. Zeits. **25,** 342 and 635 (1924).

radial component of the positive ion current is equal to the radial component of the electron current. (5) The concentration of positive ions and electrons is zero at the walls and reaches a maximum at the tube axis. (6) The dimensions of the tube are large compared to the mean free path of the molecules. (7) Sufficient collisions occur to give both the positive ions and electrons a Maxwellian distribution of velocity.

The equation obtained from these assumptions without the use of Poisson's equation is given below.

$$G = \frac{2.4}{R}\left(\frac{V_i}{H}(B^+ + B^-)\frac{K^+ \cdot K^-}{(K^+ + K^-)^2}\right)^{1/2}.$$

Where G is electric field in volts per cm; R is tube radius in cm; V_i is ionization potential of the gas in volts; H is an efficiency factor of ionization; B^+ is energy of random motion of positive ions in volts; B^- is energy of random motion of negative ions in volts; K^+ is mobility of positive ions; and K^- is mobility of negative ions.

This expression for the dependence of the field on the tube radius checks the empirical relation. The field will however not be equal to zero for R increased indefinitely but will reach a minimum value. The above form of the equations results from the assumption that ions are lost only by diffusion to the tube walls and therefore does not hold for large values of R where recombination in the body of the gas becomes important. This theory does not give the dependence of the field on current density or on pressure.

Morse[16] has developed an equation for the electric field in the positive column, giving its dependence on both the tube radius and the pressure, but not on the current density. He assumes that the relations for mobility and average number of ions produced by an electron under given conditions are known and uses the results of Schottky to determine the diffusion currents to the tube walls. The calculations are based on three general differential equations which represent the conditions for a stable discharge in a tube of unit cross section. The following result is obtained.

$$E = 5.76\epsilon V_r \frac{Gp}{r}.$$

Where E is field in the positive column in volts/cm; G is a constant inversely proportional to the mobilities of positive ions and electrons; p is gas pressure in mm of mercury; r is tube radius in cm; and V_r is ionization potential of the gas, or if metastable states are formed, the first critical potential.

The value of the field given by this equation satisfied the empirical relation for its dependence on both the tube radius and the pressure, but still leaves the dependence on current density to be explained qualitatively. The field increases with the current for small current densities where an increase in current increases the diffusion to the tube walls, but the field decreases slowly for large current densities where the increase in current decreases the

[16] P. M. Morse, Phys. Rev. **31**, 1003 (1928).

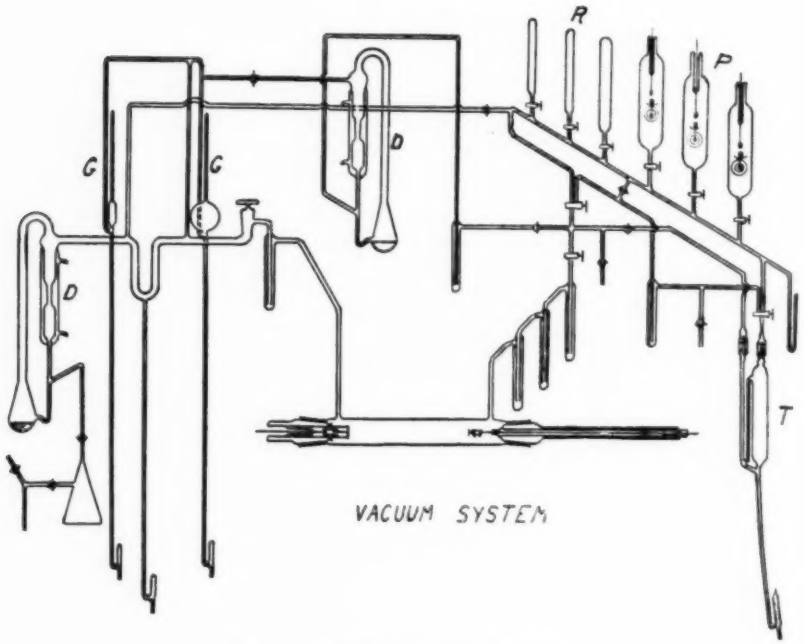

Fig. 1. Diagram of vacuum system.

percent of diffusion to the tube walls. In order to obtain an expression for the field as a function of the current it would be necessary to determine the diffusion current to the tube walls as a function of the current density in the tube.

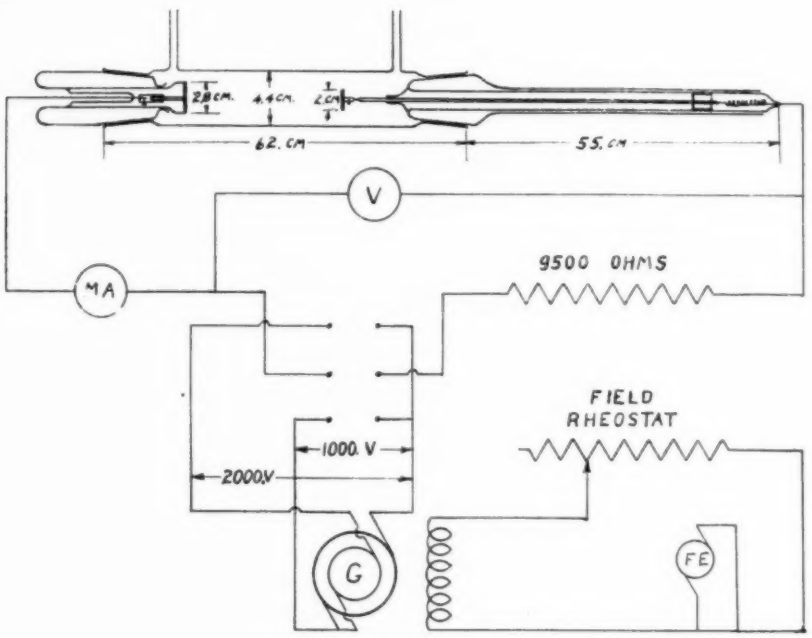

Fig. 2. Diagram of apparatus.

Apparatus

A detailed diagram of the entire vacuum system is shown in Fig. 1. *R* represents the gas storage reservoirs, *P* the gas purifying tubes, *D* diffusion pumps, *G* the McLeod guage and *T* a Toepler pump. Fig. 2 shows a drawing of the discharge tube and a diagram of the electrical circuit used.

Purification of the Gases

Since the results of this investigation depended largely on the purity of the gases used, each gas was very carefully purified before being admitted to the discharge tube. The helium, free from neon, was obtained from the Ohio Chemical Company in a steel bomb under high pressure and was purified by circulating it with a Toepler pump through a charcoal trap immersed in liquid air. The pure gas was stored at a little less than atmospheric pressure in a liter glass reservoir which had been well baked and evacuated.

The neon, of spectroscopic purity, was obtained from Linde Air Products Co., Buffalo, N. Y., in liter glass bulbs. It was further purified in the same manner as described above for helium and stored in a liter glass reservoir. In most cases both of these gases were purified again just before being admitted to the tube by circulating slowly through charcoal in liquid air for about one hour. However, no difference could be found by spectroscopic means or by changes in the electrical characteristics of the discharge when the gases were admitted to the tube directly from the storage reservoirs.

The argon, of commercial grade, was obtained in small metal bombs at high pressure. It contained more impurities than either the helium or the neon, and was the most difficult of the three gases to purify, since, because of its absorption of argon, charcoal in liquid air could not be used. The argon was purified by maintaining an arc of about 2 amperes between a mischmetal and an iron electrode in the gas at a pressure of 10 to 15 cm. The arc was run continuously for from one to two days with the argon in one purifier, then the gas was transferred to another purifier and run under the same conditions for about a week. After this treatment it was still found to contain a very small trace of nitrogen. It was then stored in a reservoir containing well-degassed charcoal where it was allowed to stand for several days at room temperature. When admitted to the tube from this reservoir it was found to be very pure with the exception of a small trace of hydrogen. Most of this hydrogen was removed from the argon by admitting a very small amount of oxygen, generated by heating potassium permanganate, to the gas and circulating the mixture through the discharge tube and liquid air traps. The argon was again stored over well-degassed charcoal for several days, after which time it was found to be very pure.

Preparation of the Tube

The electrodes were well-outgassed by heating with an induction furnace before being mounted in the tube. Before each set of experiments with mixtures of two of the gases the whole system was pumped for several hours and allowed to stand over night, evacuated and with liquid air on the traps, to

test for leaks. In case the system was tight the tube was baked at from 300 to 350°C for four hours while being pumped. At the same time the charcoal trap and the mischmetal getter trap, in the circulating system, were baked at 400°C. This part of the system, including the tube, was then pumped for about 4 hours while the tube and traps cooled. The whole system was allowed to stand over night, evacuated and with liquid air on the traps, to test again for leaks. After pumping again for about two hours the system was ready for use.

Procedure

After the gases were purified and the tube prepared as described above, one of the gases to be used was admitted to the tube very slowly by means of a slow leak grooved stopcock, through the system of traps, Fig. 1, until the desired pressure was obtained and was then circulated for about 20 minutes through the discharge tube and traps with a discharge running at the desired current. The rate of circulation was then decreased to a very low value and the pressure adjusted accurately to the value desired. The current was kept constant, and voltage readings were taken at short time intervals in order to determine when conditions were constant for the taking of data as described below. Pressure measurements were taken at various intervals to see that the pressure and rate of circulation remained constant.

If a very small amount of another gas was to be mixed with the gas already in the tube, the gas in the tube was pumped out with the mercury circulating pump backed by a Toepler pump and stored in an empty reservoir or in a charcoal trap in liquid air. The tube was well pumped out with the mercury pump and a small amount of the other gas admitted to the tube to the pressure necessary to give the percentage mixture desired. The gas previously used was readmitted to the tube slowly in the same manner as before. The process described above of circulating the gases was repeated to insure a homogeneous mixture of the gases and the data were taken as described in the next section. For adding larger amounts of one gas to another, a separate system including a guage with its volume calibrated with respect to the tube volume was used. In this way by starting with one pure gas, mixtures with another gas could be studied in any proportions from very small percentages up to a 50 percent mixture. The results obtained were found to be repeatable within a few percent at any time. For each gas mixture studied a spectrogram of the light emitted from the positive column was taken in order to observe the change in excitation produced with changes of the gas mixture and to check the purity of the gas.

Method Used in Measuring the Potential Gradient in the Positive Column

The method consisted in measuring the total drop in potential across the tube at various electrode distances, while the current was kept constant by varying the e.m.f. in the circuit. The anode was moved by magnetic control from outside the tube. Before any measurements were taken, the discharge was run with the maximum electrode distance for from one to two hours at

constant current until the maintaining voltage across the tube remained constant. The maximum electrode distance was 32 cm. The anode was moved from this point, 2 cm at a time, to within 10 cm of the cathode and back to 32 cm again. Readings of the total voltage across the tube were taken every two cm at intervals of one minute as the electrode distance was decreased and then increased again. The voltage readings for increasing electrode distance checked those for decreasing electrode distance to within less than one percent.

This method of measuring the field is applicable since a uniform cylindrical tube was used, and only the uniform positive column was studied. Since the current density and the concentration of ions and electrons remain constant throughout the length of the uniform positive column, the anode drop in potential does not change with the anode position along the column. The tube was run long enough before any data were taken so that the cathode drop in potential remained constant while observations were being made. The time required to take a complete set of observations was 24 minutes. The voltage readings, taken with decreasing electrode distance, when plotted against electrode distance, gave a straight line very accurately. The slope of this line gave the potential gradient or electric field in the positive column in volts/cm.

RESULTS

The results of the investigation are shown by the data given in Tables I and II and by the curves in Figs. 3 to 8 inclusive. The values of the electric field in the positive columns are given in Table I for the pure gases, helium, neon, argon and for mixtures of each of these gases with mercury vapor at

TABLE I. *Electric field in the positive column for the rare gases and mixtures of each with mercury vapor.* Current, 40.0 m.a. Pressure, 14.0 mm. Tube diameter, 4.4 cm.

Gas	pure He	He-Hg	pure Ne	Ne-Hg	pure A	A-Hg
Positive column (Field in volts/cm)	17.0	18.4	4.0	2.2	3.8	4.5

about 0.005 mm pressure. It can be seen from this table that mercury vapor added to neon causes a large decrease in the field but when added to either helium or argon causes a slight increase.

Table II gives the results of spectrograms taken from the positive column of the discharge in the various gas mixtures studied. It will be noted that a very small amount of argon added to either helium or neon completely subdues the helium or neon spectrum and only the argon is excited. Mercury has the same effect on either argon or neon; while with mixtures of small amounts of neon or of mercury with helium, the spectra of both gases appear. When argon, containing a trace of nitrogen, is added to neon in amounts up to 2.0 percent the neon spectrum disappears and the argon spectrum appears strong with the nitrogen spectrum weak. As more of the argon, containing a trace of nitrogen, is added to the neon the argon spectrum becomes weak and the nitrogen spectrum strong until with more then 5.0 percent only the nitrogen spectrum appears.

TABLE II. *Results of spectrograms taken of radiation from the positive column of a glow discharge in the various mixtures of the rare gases and mercury vapor studied.*

Gas mixtures	Percentage of added gas greater than the amount given below		Spectrum obtained
Helium—Neon	0.4%	Neon	Helium and Neon
Helium—Argon	0.2%	Argon	Argon only
Neon—Argon	0.15%	Argon	Argon only
Neon—{Argon with a trace of nitrogen}	0.5% 2.0%	{Argon with a trace of nitrogen}	Argon and Nitrogen
Neon—{Argon with a trace of nitrogen}	5.0%	{Argon with a trace of nitrogen}	Nitrogen only
Helium—Mercury	0.03%	Mercury	Helium and Mercury
Neon—Mercury	0.03%	Mercury	Mercury only
Argon—Mercury	0.03%	Mercury	Mercury only

Fig. 3 shows the variation with pressure of the electric field in the positive column for pure helium and for a mixture of neon with helium. These curves show that the field varies directly as the pressure for both the pure gas and the mixture. They also show that the effect on the field produced by adding a small percentage of neon to helium does not change appreciably with the total pressure over a considerable range of pressure.

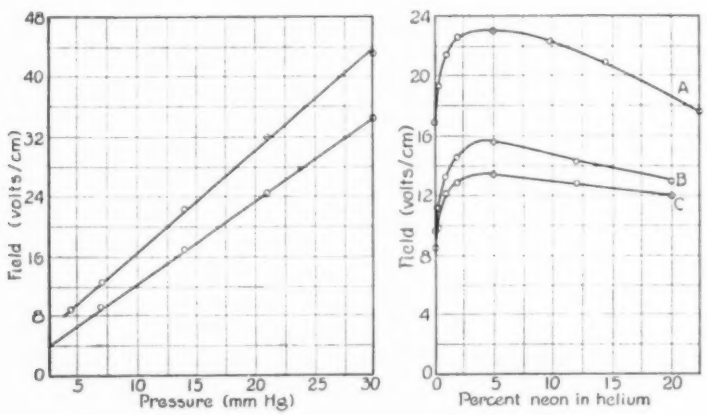

Fig. 3. Variation of electric field with pressure for pure helium A and a mixture of 99.0 percent helium and 1.0 percent of neon B. Current, 40 m.a.

Fig. 4. Variation of electric field with percent of neon added to helium. A, current 40 m.a., pressure 14 mm; B, 20 m.a., 7 mm; C, 40 m.a. 7 mm.

These curves of Fig. 4 show the variation of the electric field in the positive column with small amounts of neon added to helium under different conditions of pressure and current. The interesting point to note here is that the maximum field is a function only of the percent of neon in the helium and is independent of the pressure or of the current density. These curves also show that a large change in the field is produced by a very small amount of neon in helium.

Fig. 5, 6, and 7 show the variation of the field in the positive column with all possible mixtures of the three gases helium, neon, and argon taken only two together.

The curve of Fig. 5 shows that a small amount of neon in helium has a large effect on the field while a small amount of helium added to neon has very little effect on the field.

It can be seen from the curve of Fig. 6 that argon-helium mixtures have about the same characteristics as those of neon-helium except that a smaller amount of argon is more effective in helium than in neon in changing the field. The discontinuity in the curve is probably due to the difference in mobility and large difference in ionization potential of the two gases. For pure argon

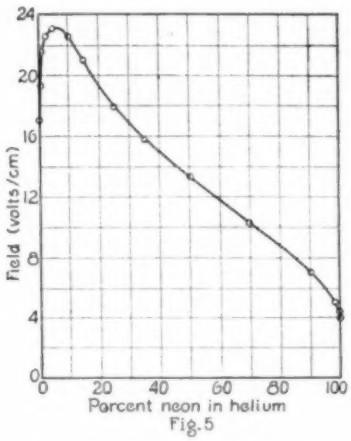

Fig. 5

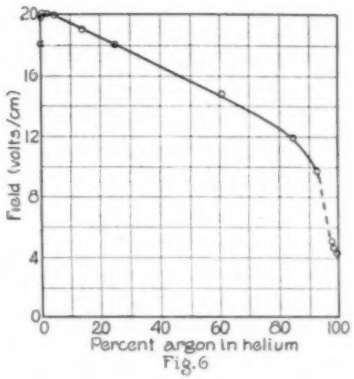

Fig. 6

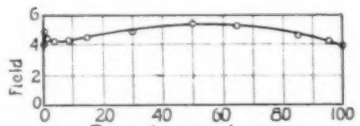

Fig. 7

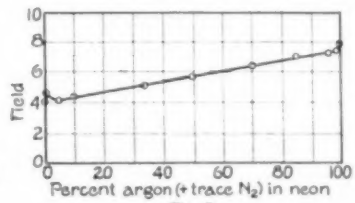

Fig. 8

Fig. 5. Variation of electric field with percent of neon in helium. Current 40 m.a., pressure 14 mm.

Fig. 6. Variation of electric field with percent of argon in helium. Current 40 m.a., pressure 14 mm.

Fig. 7. Variation of electric field with percent of argon in neon. Current 40 m.a., pressure 14 mm.

Fig. 8. Variation of electric field with percent of argon, containing trace of nitrogen, added to neon. Current 40 m.a., pressure 14 mm.

and for mixtures of argon with small amounts of helium the discharge did not fill the tube completely but concentrated toward the axis of the tube. For from 2 to 7 percent helium in argon the discharge was unstable and could not be maintained at the current and pressure desired without changing the resistance of the circuit. For mixtures containing more than 7 percent helium the discharge filled the tube uniformly. The sudden increase in field produced is due to the change in the current density distribution over the cross section of the positive column. Where the current density is large at the tube axis

there is less diffusion of positive ions to the tube walls and therefore a smaller field, than in the case of a more nearly uniform distribution of current over a cross section of the column.

From Fig. 7 it can be seen that small amounts of argon have much less effect on the field in neon than of that in helium and that neon in small amounts has practically no effect on the field in argon.

Fig. 8 shows how the field in neon-argon mixtures is affected by a small trace of nitrogen in the argon.

Discussion and Interpretation of Results

The interpretation of the electrical and spectral characteristics of the positive column in the gas mixtures studied is based principally upon collisions of the second kind between the excited metastable atoms or the ions of one gas and the neutral atoms of the other gas. The effect of limitation of electron velocities observed when a considerable amount of a gas of lower ionization and excitation potentials is added to another gas is insufficient to explain the large effects obtained with the very small percentages of the added gas. With a formula given by K. T. Compton,[17,18] calculations were made of the number of collisions an electron would make with gas atoms in a mixture of helium with 0.1 percent neon under the discharge conditions which obtained. It was found that an electron would make in the order of 1000 collisions with gas atoms and hence, on the average, one collision with a neon atom while gaining the energy represented by the difference between the ionization potential of helium and the lowest excited state of neon. Since the probability of excitation by electron impact under these conditions is far from certainty, an increase in the field of 26 percent could hardly be attributed to limitation of electron velocities by collisions with neon atoms. With the mixture of less than 0.03 percent mercury vapor with neon the field is reduced by 45 percent which is entirely too large an effect to be explained by limitation of electron velocities. Therefore we must turn to collisions of the second kind for a satisfactory explanation of the observed results.

Collisions of the second kind. The following list of reactions, 1 to 6, inclusive, show the possible ways by which collisions of the second kind may take place between two gas atoms X_1 and X_2 where the energy of excitation is transferred from X_1 to X_2. The resultant products of each of the first six reactions may be represented by any one of the expressions 7 to 10, depending upon the relative ionization and excitation potentials of X_1 and X_2.

1. $X_1' + X_2 \rightarrow$
2. $X_1^+ + X_2 \rightarrow$
3. $X_1' + X_2' \rightarrow$
4. $X_1^+ + X_2' \rightarrow$
5. $X_1' + X_2^+ \rightarrow$
6. $X_1^+ + X_2^+ \rightarrow$

7. $X_1 + X_2' + KE$
8. $X_1 + X_2^+ + KE$
9. $X_1 + X_2^{+\prime} + KE$
10. $X_1 + X_2^{++} + KE$

[17] K. T. Compton, Phys. Rev. **32**, 433 (1923).
[18] K. T. Compton, Revs. of Mod. Phys. **2**, 220 (1930).

X' is an excited gas atom, X^+ a gas ion, $X^{+\prime}$ an excited gas ion, X^{++} a doubly ionized ion, and KE is kinetic energy.

The reactions represented by the initial conditions 1 or 2 resulting in 7, 8, or 9 are of most common occurrence in discharges in mixtures and are most important in explaining the effects observed.

Processes of ionization and excitation. The processes of ionization and excitation in the positive column in pure monotomic gases having metastable states can be represented by the following reactions.

Reactions by which ions are produced by electron impact.

$$e_f + X = X^+ + 2e + KE \tag{1}$$

$$e_s + X_m' = X^+ + 2e + KE \tag{2}$$

where e_f is a fast moving electron with sufficient kinetic energy to ionize the neutral gas atom X, and e_s is a slow moving electron with sufficient kinetic energy to ionize an excited metastable atom X_m'.

Reactions by which metastable atoms are produced.

$$e_f + X = X_m' + e + KE \tag{3}$$

$$X' - \text{radiation} = X_m', \tag{4}$$

$$X' + X \rightarrow X_m' + X + KE, \tag{5}$$

where X_m' is an excited metastable atom, and X' is an excited atom in a non-metastable state.

Reactions producing excitation of non-metastable states of atoms.

$$e_{f_1} + X = X' + e + KE. \tag{6}$$

$$e_{s_1} + X_m' = X' + e + KE, \tag{7}$$

where e_{f1} is a fast moving electron with sufficient energy to excite a neutral atom, and e_{s1} is a slow moving electron with sufficient energy to excite a metastable atom.

In gas mixtures composed largely of one gas with a small amount of gas of lower ionization and excitation potentials than those of the main gas, other processes of ionization and excitation take place by collisions of the second kind.

Let X_1 = atoms of the main gas and X_2 = atoms of the gas present in small amounts.

Reactions of the second kind which produce ionization and affect the concentration of metastable atoms in a discharge in gas mixtures are the following.

$$X_{1m}' + X_2 = X_2^+ + e + X_1 + KE \tag{8}$$

$$X_{1m}' + X_2 = X_2^{+\prime} + e + X_1 + KE \tag{9}$$

$$X_{1m}' + X_{2m}' = X_2^{+\prime} + e + X_1 + KE. \tag{10}$$

A reaction of the second kind which decreases the concentration of metastable atoms of the main gas and therefore affects the ionization processes in a discharge in a gas mixture is the following

$$X_{1m}' + X_2 = X_2' + X_1 = X_1 + X_2 + \text{radiation}. \tag{11}$$

The reactions involving collisions of the second kind between ions of the main gas and excited or neutral atoms of the mixed gas, do not tend to increase the number of ions. Therefore, they will in general have very little effect on the field in the positive column. Reactions of this type will be discussed only in a few particular cases.

It was shown in the discussion of the theory of the positive column that the electric field gives a measure of the energy necessary to produce the concentration of ions required by the current passed through the tube and includes the energy lost in radiation as well as the heat conducted away by the tube walls. It was also shown that, for a pure gas, the electric field in the positive column is proportional to the ionization or excitation potentials of the gas. It can also be shown that the electric field in the positive column will be a function of the excitation potentials of the gas and proportional to the ratio of the energy emitted as radiation to that producing ionization.

If any process is introduced into the positive column which will change the ratio of the energy expended in radiation to that expended in ionization the field should change. A process which increases the efficiency of ionization will decrease the electric field in the positive column, since for a given current and pressure the concentration of ions remains constant. A process which decreases the efficiency of ionization or increases the energy expended in radiation will cause an increase in the electric field.

By adding a small amount of one gas to another gas the processes of ionization and excitation may be considerably changed. In case the added gas has lower ionization and radiating potentials than the main gas, very large changes in the field may be produced by very small amounts of added gas. When the added gas has higher ionization and excitation potentials than the main gas the field is only changed slightly, the change being proportional to the amount of gas added.

Helium-Neon Mixtures

Consider the case of helium with a small amount of neon added. The variation of electric field in the positive column with the percent of neon added to helium is shown in Fig. 4, for amounts of neon up to 20 percent. The maximum of the field curve comes at 5 percent neon for different values of current and pressure. The amount of increase in the field over that for pure helium caused by the addition of 5 percent neon is 28.3 percent, for curve *A*; 60.8 percent for curve *B*; 61.8 percent for curve *C*. This shows that the effect of the neon on the field of helium is practically independent of the current, but varies with the pressure.

The following table gives the term values of the normal and metastable states, the ionization potentials and excitation potentials of the metastable states of the gases used in this investigation.

To explain the rise in the field produced by adding neon to helium the reactions producing ionization and excitation in the mixture must be considered.

TABLE III. *Metastable states and ionization potentials.*

Atom	Normal state (term in cm^{-1})	Ionization potential (volts)	Metastable (term in cm^{-1})	States excitation potential (Volts)
He	$^1S_0$ 198298.0	24.47	2^3S_1 38454.7	19.73
			2^1S_0 32032.5	20.51
Ne	$^1S_0$ 173930.0	21.47	3^3P_2 39887.0	16.54
			3^3P_0 39110.0	16.64
A	$^1S_0$ 127103.8	15.69	4^3P_2 33996.7	11.50
		15.87	4^3P_0 32557.79	11.67
Hg	$^1S_0$ 84178.5	10.39	6^3P_2 40138.3	5.43
			6^3P_0 46536.2	4.66

First consider the processes for production of ions occurring in pure helium.

$$\underset{>24.47}{e_f} + \mathrm{He} = \underset{24.47}{\mathrm{He^+}} + 2e + KE \tag{1}$$

$$\underset{>4.74}{e_s} + \underset{\substack{20.51\\19.73}}{\mathrm{He_m'}} = \underset{24.47}{\mathrm{He^+}} + 2e + KE. \tag{2}$$

The numbers represent the energy of the state in equivalent volts.
Reactions producing the excitation of the arc spectrum of helium.

$$\underset{>19.73<24.47}{e_f} + \mathrm{He} = \underset{>19.73<24.47}{\mathrm{He'}} + e + KE \tag{3}$$

$$\underset{<4.74}{e_s} + \underset{\substack{20.51\\19.73}}{\mathrm{He_m'}} = \underset{>19.73<24.47}{\mathrm{He'}} + e + KE \tag{4}$$

$$\underset{>19.73<24.47}{\mathrm{He'}} - \text{radiation} = \mathrm{He} \text{ or } = \underset{\substack{19.73\\20.51}}{\mathrm{He_m'}} \tag{5}$$

When a small amount of neon is added to helium the excitation of the helium arc spectrum is reduced to some extent while the neon arc spectrum is developed very strongly. Therefore the following reaction is considered to take place in the helium-neon mixture.

$$\underset{\substack{20.51\\19.73}}{\mathrm{He_m'}} + \mathrm{Ne} = \underset{19.69 \text{ to } 20.62}{\mathrm{Ne'}} + \mathrm{He} \pm KE \tag{6}$$

These results in Table IV show very close resonance between the metastable levels of helium and a large number of excited states of neon. The excess energy to become kinetic energy is very small for the excitation of a large number of the excited states of neon by impacts with metastable helium. Therefore, this reaction should have quite a high probability of occurrence in helium containing a small amount of neon.

This reaction (6) shows that the presence of a small amount of neon in helium will greatly reduce the concentration of metastable helium atoms, and practically eliminate the reaction (2), one of the processes of producing ions

TABLE IV. *Excitation of neon by metastable helium.*

Helium I Metastable states term (cm^{-1})	excitation potential (Volts)	Neon I Excited states term (cm^{-1})		excitation potential (Volts)	Energy difference in equivalent volts
		$^3P_0$	14395	19.69	0.04
		$^1P_1$	14549	19.67	0.06
2^3S_1 38454.7	19.73	$^3P_0$	20958	18.78	0.95
		$^3P_1$	22891	18.65	1.08
		$^3P_2$	23071	18.62	1.11
		$^1P_1$	23012	18.63	1.10
		8 levels	12419.0	19.91	0.60
			12228.0	19.96	0.55
		10 levels	11520.0	20.05	0.46
			10529.0	20.17	0.34
2^1S_0 32032.5	20.51	$^1P_1$	10272.1	20.20	0.31
		$^3P_2$	10220.8	20.21	0.30
		$^3P_0$	9643.5	20.28	0.23
		8 levels	6961.8	20.61	−0.10
			6880.8	20.62	−0.11

in helium. Therefore, due to the presence of neon, a large amount of energy supplied by the field is transformed into radiation by reaction (6) which would have gone into ionization in the case of pure helium. Thus we see that the presence of a small amount of neon in helium greatly decreases the efficiency of ion production and therefore the field increases. The field decreases again when the concentration of neon atoms becomes large enough so that a considerable amount of the ionization is produced by direct electron impact with neon atoms. After the maximum in the field is reached at 5 percent neon the field gradually decreases to that of pure neon. A small amount of helium has no abnormal effect on the field in neon, as shown by Fig. 5. No collisions of the second kind take place between excited neon and neutral helium because the excited states of helium are all above the metastable states of neon. The spectrum of helium disappears between 10 percent and 5 percent helium in neon, for less than 5 percent helium in neon only the neon spectrum is obtained. This shows that when only a small amount of helium is present in neon, only very few helium atoms are excited by direct electron impact.

The phenomena at this end of the curve show the effect of limitation of electron velocities in mixtures but here the gas of the lower excitation potentials is present in the larger amount. The fact that the helium spectrum is developed quite strongly in mixtures containing as much as 85 percent neon shows that neon is not very effective in limiting the electron velocities even when present in more than 50 percent. Thus limitation of electron velocities sufficient to cause a 20 percent increase in field could not be considered to occur with less than 1 percent neon in helium. Therefore, the effect of the limitation of electron velocities is negligible as compared to collisions of the second kind where neon is present in only a few percent.

Helium-Argon Mixtures

Fig. 6 shows that the maximum value of the field for the mixture is produced with 1.5 percent argon which is less than the amount of neon required to produce the maximum effect in helium. However, the maximum increase in the field for the mixture over that of pure helium is only 17.6 percent for argon, as compared with an increase of 28.3 percent caused by the addition of 5 percent neon to helium. The results of spectrograms given in Table II show that with 0.2 percent argon in helium the arc spectrum of helium is completely surpressed and only the argon arc spectrum is developed. These facts would indicate that argon is more effective in removing metastable helium atoms than neon but that part of the energy of these metastable helium atoms is converted into ionization of argon and not entirely lost in radiation, as was the case of neon. These results are particularly interesting because neither the helium ion nor the metastable states of the helium atom are in close resonance with any of the known excited states of neutral argon or of the argon ion. The lowest excited state of argon II is the term ^2s 108730 cm^{-1} or 13.41 volts above the normal state of argon II. The first ionization potential of argon is 15.69 volts. Thus to ionize and excite argon would require at least $15.69+13.41=29.10$ volts. The highest metastable state of helium is 2^1S_0 32032.5 cm^{-1} or 20.51 volts above the normal state, which is 8.59 volts too low to ionize and excite argon. The ionization potential of helium is 24.47 volts, which is 4.63 volts too low to ionize and excite argon.

Spectrograms taken of the positive column in mixtures of a small amount of argon in helium show that the spark spectrum of argon is not excited in mixtures with helium. The spectrogram of argon alone shows only the arc spectrum of argon. The spectrograms of helium-argon mixtures also show only the arc lines of argon and the strongest arc line of helium. However, there are a large number of strong argon spark lines in the region photographed which would have appeared if an appreciable amount of excitation of the argon ion had occurred. Therefore, the only possible reactions between metastable helium and neutral argon are the following:

$$\underset{\substack{19.73\\20.51}}{\mathrm{He}_m'} + \mathrm{A} = \underset{\substack{15.69\\15.87}}{\mathrm{A}^+} + \mathrm{He} + \underset{3.86 \text{ to } 4.82}{KE} + e \qquad (1)$$

$$\underset{\substack{19.73\\20.51}}{\mathrm{He}_m'} + \mathrm{A} = \underset{19.0 \text{ to } 20.5}{\mathrm{A}'} + \mathrm{He} + KE. \qquad (2)$$

TABLE V. *Table for reaction* (1).

Helium Term (cm^{-1})	Excitation potential of metastable state	Argon Term	Ionization potential (volts)	Energy difference in equivalent (volts)
2^3S_1 38454.7	19.73	$4^2P_0 0$	15.69	4.04
2^1S_0 32032.5	20.51	$4^2P_0 0$	15.69	4.82
2^1S_0 32032.5	20.51	4^2P_1 1430.	15.87	4.64
2^3S_1 38454.7	19.73	4^2P_1 1430.	15.87	3.86

The amount of energy going into kinetic energy is too large to make reaction (1) very probable. However, the results indicate that this reaction does occur to some extent in helium-argon mixtures.

From the results obtained with mixtures of a small amount of argon with helium it would appear that reaction (2) has a high probability of occurrence. The outer electron configuration of argon is $3s^2$, $3p^6$. It seems probable that two of the p electrons could be excited simultaneously by a collision of an argon atom with a metastable helium atom, which would excite negative terms in argon I. Negative terms have not been observed in the argon I spectrum, but there is no reason to expect negative terms to be excited under normal discharge conditions in argon when practically all of the excitation is by electron impact, However, if negative terms exist which are in close resonance with the metastable states of helium, reaction (2) should be highly probable in mixtures of a small amount of argon with helium. Reaction (2) will account for the strong excitation of the arc spectrum of argon in helium-argon mixtures and also will account for the increase of the field in helium produced by the addition of small amounts of argon. The negative terms which could be excited by reaction (2) would lie between three and four volts above the ionization potential of argon I. It would be interesting to make an extended spectroscopic study of the excitation of argon by metastable helium in the positive column to see if such negative terms could be observed.

Neon-Argon Mixtures

In this case the field in the positive column is small and nearly the same for each pure gas. Under the existing conditions of current, pressure, and tube diameter, the field in neon was 4.0 volts/cm; in argon 3.8 volts/cm. However, the curve in Fig. 7 shows that a small amount of argon added to neon causes a small increase in the field while neon in small amounts has practically no effect on the field in argon.

The possible reactions for argon mixtures are the following

$$\underset{16.54}{\overset{16.64}{Ne_m'}} + A = \underset{15.87}{\overset{15.60}{A^+}} + Ne + e + \underset{0.67 \text{ to } 0.95 \text{ volts}}{KE} \qquad (1)$$

$$\underset{16.54}{\overset{16.64}{Ne_m'}} + A = \underset{16.54 \text{ to } 16.64 \text{ volts}}{A'} + Ne + KE. \qquad (2)$$

Reaction (1) tends to decrease the field and (2) tends to increase the field. Reaction (1) would not have a high probility due to the large residual energy to be transformed to kinetic energy. The probability of transitions to the negative term states demanded by reaction (2) is also small. This is in agreement with the fact that argon has only a small effect on the field when added to neon.

The curve Fig. 7 shows that a maximum field is reached at about equal proportions of argon and neon due to the fact that there are more possible excited states in a mixture of the two gases than in either gas separately. Therefore, a greater part of the total energy of the field is expended in radia-

tion than would be the case for either gas separately. The fact that the field in pure argon is only slightly less than that in pure neon even though the ionization potential of argon is much less than that of neon must be due to a proportionally greater amount of the total energy supplied by the field going into radiation and heat in argon than in neon.

Helium-Mercury Mixtures

TABLE VI. *Excited states of mercury I and II which result from reactions with helium, neon and argon.*

Mercury II		Mercury I	
Term from normal state of Hg II (cm^{-1})	Equivalent volts from normal state of Hg II	Term from ionized state of Hg I (cm^{-1})	Equivalent volts from normal state of Hg I
$^2D_3$ 119695	14.75	6^3P_0 −7860	11.36
$^2D_5$ 134732	16.62	6^3P_1 −9798	11.60
2^2P_1 135666	16.71	6^3P_1 −9798	11.60
2^2P_2 144789	17.85	Ionization Potential	10.39
3^2P_2 196151	24.20	6^1S_0 84178.5	normal state
Hg^{++} 235461	29.06		

The possible reactions which can occur in helium-mercury mixtures are the following:

$$\underset{\substack{20.51\\19.73}}{He_m'} + Hg = \underset{17.85}{Hg^{+\prime}} + He + e + \underset{\substack{1.88\text{ volts}\\2.66}}{K.E.} \qquad (1)$$

$$\underset{24.47}{He^+} + Hg = \underset{24.20}{Hg^{+\prime}} + He + e + \underset{0.27\text{ volts}}{K.E.} \qquad (2)$$

The probability of reaction (1) occurring is low since the residual kinetic energy is too high for close resonance. Reaction (2) has a higher probability of occurrence but will have very little effect on the ion concentration.

From the results of spectrograms of this mixture given in Table II it can be seen that both the spectra of helium and mercury are developed, which indicates that the mercury is not very effective in eliminating the metastable states of helium. The results given in Table I show that mercury has very little effect on the field in the positive column of helium. Both of these facts are in agreement with the low probability of the occurrence of reaction (1) in helium-mercury mixtures.

Neon-Mercury Mixtures

The case is quite different for neon and mercury mixtures. The only possible reaction for neon-mercury mixtures is the following.

$$\underset{\substack{16.64\\16.54}}{Ne_m'} + Hg = \underset{\substack{16.71\\16.62}}{Hg^{+\prime}} + e + \underset{\substack{0.02\text{ or }-0.07\\-0.08\text{ or }-0.17}}{K.E.} + Ne \qquad (1)$$

This is the only reaction which can occur in neon-mercury mixtures that will affect the field in the positive column and which has a high enough probability of occurrence to be considered. This reaction has a very high prob-

ability due to the close resonance between the metastable states of neon and the excited states of the mercury ion.

Since most of the energy of the metastable neon atoms goes into ionization of mercury this reaction greatly increases the efficiency of the ionization processes in neon-mercury mixtures over those of pure neon. This is shown by the fact that the field in the positive column of neon is reduced to almost one half of its original value by the addition of less than 0.03 percent mercury vapor. The results of spectrograms of the neon-mercury mixture given in Table III show that the mercury arc spectrum is developed strongly while the neon arc spectrum is completely absent. This would be expected according to the above reaction which would greatly reduce the concentration of metastable neon atoms in the mixture over that for pure neon. If the results were attributed to the effect of limitation of electron velocities, mercury vapor would be expected to have the same effect on helium as it has on neon and possibly to a greater extent, but instead mercury vapor causes a slight increase in the field for helium. This fact is strong evidence that the observed effects, where one gas is present in a small percent of the total volume, are correctly attributed to the action of collisions of the second kind.

Mixture of Argon and Mercury

The possible reactions in argon containing a small amount of mercury are

$$\underset{\substack{11.50\\11.67}}{A_m'} + Hg = \underset{10.39}{Hg^+} + A + \underset{\substack{1.11\\1.28}}{K.E.} + e \qquad (1)$$

$$\underset{\substack{11.50\\11.67}}{A_m'} + Hg = \underset{11.36}{Hg'} + A + \underset{\substack{0.14,\ -0.10\\0.31,\ \ 0.07}}{K.E.} + e \qquad (2)$$

$$\underset{\substack{15.69\\15.86}}{A^+} + Hg = \underset{14.75}{Hg^{+\prime}} + A + \underset{\substack{0.94\\1.11}}{K.E.} + e. \qquad (3)$$

Reaction (1) has a low probability of occurrence due to the rather high residual kinetic energy. Reaction (2) has a high probability due to the quite close resonance, the residual kinetic energy being small. This reaction corresponds to the excitation of negative terms of the mercury arc spectrum which have been observed with hollow cathode excitation of mercury by impacts of the second kind.[19] Reaction (3) is not very probable and would not have much effect on the electric field in any case.

The results of spectrograms given in Table II show that the mercury spectrum is very much stronger than the argon spectrum in the mixture. This fact is in good agreement with the probability of reaction (2) being much greater than that of reaction (1). The fact that the field in the argon mercury mixture is higher than in pure argon shows that reaction (2) occurs with greater probability than reaction (1).

By comparing curves in Figs. 7 and 8 the effect of a trace of a diatomic gas as an impurity in one of the gases can be seen. Only a trace of nitrogen

[19] F. Paschen, Preuss Akad. p. 3, 1928; also Naudé (reference 9).

was sufficient to more than double the field in pure argon. This large increase was due to the excitation of the nitrogen bands by collisions of the second kind with argon metastable atoms. In diatomic gases also a larger proportion of the energy of electron impacts goes into radiation than in monatomic gases and this causes an increase in the field. The spectrograms taken of these mixtures show that the nitrogen band spectrum begins to be developed strongly where the field in this mixture becomes larger than the corresponding mixture of pure argon and pure neon.

Birge and Hopfield[20] give the energy-level system for the positive bands of nitrogen. There are three states at 8.1, 8.5 and 9.4 volts, respectively. Each of the states have a large number of vibration levels. These vibrational levels extend from 8.1 to 14 volts. The ionization potential of nitrogen is given as 16.7 volts. The metastable states of argon at 11.50 and 11.67 volts will be in very close resonance with a large number of excited states of the nitrogen molecule. The metastable states of neon at 16.58 and 16.67 are in close resonance with the ionization potential of the nitrogen molecule. Therefore one would expect a very strong excitation of the positive bands of nitrogen in a mixture of neon and argon containing a trace of nitrogen, by impacts of the second kind between the metastable states of argon and neon and the neutral nitrogen molecules. From the curves in Figs. 7 and 8, it can be seen that the field in a mixture of neon and argon is greatly increased by the addition of a trace of nitrogen. This result is in good agreement with the fact that the metastable states of argon are in very close resonance with many excited states of the nitrogen molecule. Thus the concentration of metastable argon and neon atoms is very effectively decreased by the presence of only a trace of nitrogen.

Conclusion

The results show that the electrical and spectral characteristics of the uniform positive column in mixtures of monatomic gases can be explained principally in terms of collisions of the second kind between the ions or metastable atoms of one gas and the neutral atoms of the other. The effect of limitation of electron velocities is wholly inadequate to explain the results obtained for mixtures containing a fraction of 1 percent of one gas and is negligible as compared to the effect of collisions of the second kind. The limitation of electron velocities does occur in mixtures where both gases are present in large amounts and produces an appreciable effect.

The necessary condition for a large effect to be produced in the electrical and spectral characteristics of the positive column by a small percentage of one gas added to another is that there exists a close resonance between the metastable states of the main gas and the ionization potential or excited states of the added gas atom or ion.

[20] R. T. Birge and J. J. Hopfield, Astrophys. J. **68**, 257 (1928).

RELATIVE INTENSITIES OF THE MAGNETIC AND ELECTROSTATIC ILLUMINATION COMPONENTS IN THE ELECTRODELESS DISCHARGE

By Charles T. Knipp
Department of Physics, University of Illinois

(Received January 22, 1931)

Abstract

Recent theory indicates that a considerable portion of the illumination in the electrodeless discharge is due to the electrostatic field. A discharge vessel was constructed to test this point experimentally. Obstructions were set in it with the idea that each type of discharge would cast its own shadow. Distinct shadows were obtained for both discharges when acting separately. When the magnetic field predominated and the ring discharge was fully formed no evidence was obtained of shadows due to electrostatic discharges, and conversely, as is shown by the photographs that accompany the article. The intensities of the two illuminations, as judged by the times of exposure, varied about as 1 to 50. The photographs seem to support the calculations of Sir J. J. Thomson.

RECENT theory indicates that a considerable portion of the illumination in the electrodeless discharge is due to the electrostatic field; that under favorable conditions of gas pressure and position of the energizing coil and electrodes this illumination may amount to a considerable part of the total. This result is in addition to the calculations made a few years back by Sir J. J. Thomson.[1]

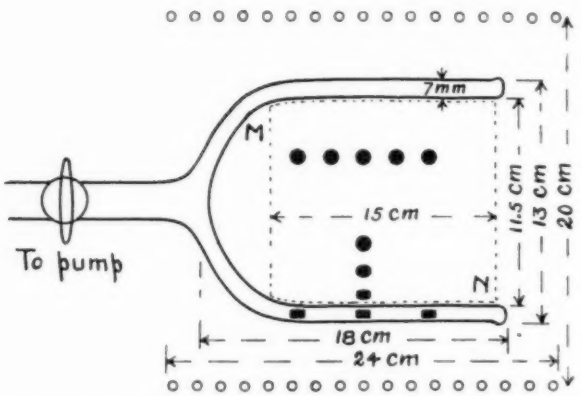

Fig. 1. Sketch of discharge vessel. Similar to a large Dewar vacuum test tube. Asbestos obstructions are shown. These appear in the four photographs that follow. A cylinder, MN, of black paper screened off high lights on opposite side. The position of energizing coil is shown.

A tube was designed by the writer with which it was hoped to test this point experimentally, at least qualitatively. In appearance the discharge ves-

[1] J. J. Thomson, Phil. Mag. **4**, 1128 (1927).

sel was not unlike a wide-mouthed Dewar vacuum flask. Two Pyrex beakers of 1.5 and 2 liters capacity, respectively, were used in its construction. Its length when completed was 18 cm, its diameter 13 cm, and the interspace about 7 mm. Asbestos disks about 8 mm in diameter were placed at regular intervals throughout the interspace similarly to the spacing disks in a vacuum bottle. Fig. 1 shows a section through the vessel and coil.

The idea in mind was that these obstructions should cast shadows, similar to the Malteze cross experiment in a Crookes tube, and thus under proper conditions it was hoped that the direction of the discharge due to either field would be made visible.

The study was made with residual air at pressures of about 0.2 mm of mercury. The discharge vessel was energized by damped oscillations from a motor-generator high-voltage high-frequency set. The maximum voltage was about 25 kv operating on a frequency of about 800 kc.

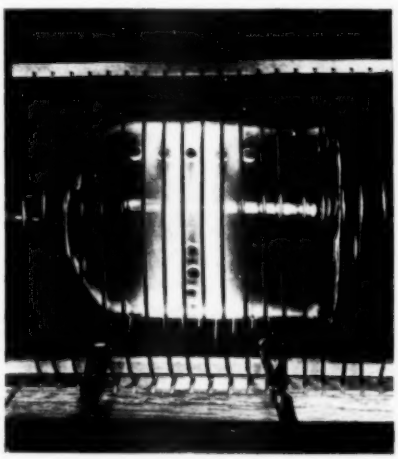

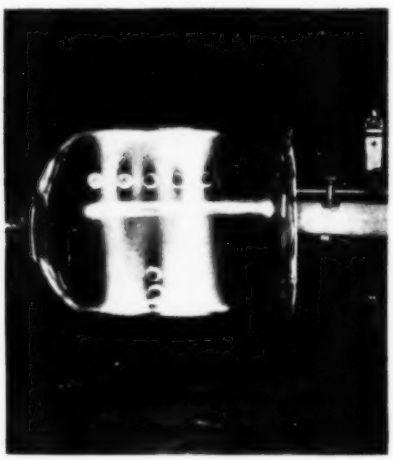

Fig. 2. Electrodeless discharge completely formed by using 8 turns of energizing coil. Residual air, pressure about 0.2 mm Hg. Illumination intense white. Time of exposure 6 seconds, followed by a photoflash to get apparatus. Shadows are in plane of coil. No shadows due to electrostatic field are discernable.

Fig. 3. Electrodeless ring discharge completely formed when an energizing coil of 8 turns was placed inside of vessel. Illumination intense white. Time of exposure 6 seconds followed by a photoflash. Again shadows due to the asbestos obstructions plainly show the paths of the carriers. No electrostatic effects are visible.

To give prominence to the magnetic field the energizing coil should be compact and of comparatively few turns—6 or 8 in this instance. This may be placed either round the vessel as indicated in Fig. 2, or the coil may be replaced by one of smaller diameter and placed within the discharge vessel as shown in Fig. 3. If an outside coil of too large a diameter, or of too many turns, is employed the ring discharge will not form.

On the other hand to give prominence to the electrostatic field a long solenoid, as shown by the extended coil turns in Fig. 1, should be used. Better still is to place external electrodes consisting of a band conductor to the right

and to the left of the medial line as shown in Fig. 4. To prevent heavy sparking with the attending danger of disrupting the vessel a parallel coil of about 10 turns should be inserted. By adjusting the number of turns included in this parallel circuit a wide range of electric field intensities may be obtained.

The two fields may indeed be obtained simultaneously by simply using a long energizing coil of from 20 to 30 turns and of about 1 cm pitch. For the electrostatic field to predominate it is only necessary to make connections at the ends of this solenoid, Fig. 4. To localize the magnetic field (as is necessary in order to have the ring discharge form) the connecting leads should now be transferred to include 4 to 6 turns at the center of the solenoid, Fig. 2. Moving the leads from the ends to the center does not seem to reduce the resultant electrostatic field very greatly, but it does serve to localize the ring dis-

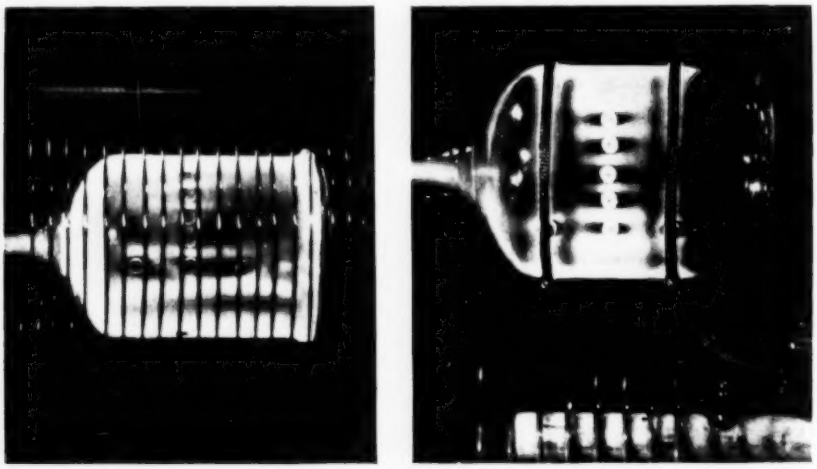

Fig. 4. Electrostatic discharge only. Electrostatic field obtained by using full length of energizing solenoid. Illumination faint (compared with that in the ring discharge). Time of exposure about 2 minutes. Overhead lights to get outline of apparatus. The direction of field is clearly shown by the streamers. Magnetic field not intense enough to form the ring discharge.

Fig. 5. Electrodeless discharge only. The band electrodes are looped across a coil of 8 turns (this coil was placed on the inside of vessel in Fig. 3). Illumination a faint purplish red glow. Time of exposure 130 seconds. The direction of field is clearly shown by the shadows cast. Overhead lights to finish exposure.

charge due to the magnetic field. It should be added that at no time, even with the electrodes most favorably placed, was it possible to get the characteristic ring discharge by means of the electrostatic field alone.

Summary

1. To form an intense ring discharge required but a comparatively few turns of the energizing coil. Figs. 2, 3.

2. The paths of the carriers in the ring discharge were in the *plane* of the coil as is distinctly shown by the *shadows cast*. Figs. 2, 3.

3. The illumination was very intense. It required but 6 to 8 seconds to make an exposure.

4. The electrostatic discharge may be produced by either external electrodes, or by a long solenoid. Figs. 4, 5.

5. The paths of the carriers in this case, as one should expect, were parallel to the axis of figure as is distinctly shown by the *shadows cast.* Figs. 4, 5.

6. The illumination was very weak, a purplish red, as compared with the intense white of the ring discharge. It required 2 to 3 minutes to make an exposure of the density shown in Figs. 4 and 5.

7. At no time while the ring discharge was formed were the electrostatic effects visible. These, however, may have been masked by the greater intensity of the former.

SUPERSONIC INTERFEROMETERS*

By Elias Klein and W. D. Hershberger
Naval Research Laboratory, Bellevue, D.C.

(Received January 26, 1931)

Abstract

The methods of applying high frequency sounds to small scale measurements are discussed. An interferometer was constructed and used to measure the velocity of sound in gases, liquids, and solids at frequencies ranging from about 10 to 700 kc. Three types of sources were tried, viz: quartz and Rochelle-salt crystals and magnetostrictive rods. The determination of the velocity of sound in solids is based upon: (1) optimum transmission of sound through a partition whose thickness is an integral number of half wave-lengths; (2) relative displacement of the nodal planes in a given liquid due to the immersion of a solid slab in the acoustical path. In the same manner, a small quantity of an unknown liquid is placed in a parallel walled cell and the latter is immersed in a liquid of known acoustic properties. Reactance and effective resistance of the interferometer (with a liquid medium) as a function of the reflector distance from the sound source were investigated. Approximate values of the impedance, power factor and watts dissipated in the instrument were thus computed. An improved circuit for use in absorption measurements in gases is described as well as the extended use of the interferometer employing two identical sound generators.

Introduction

CERTAIN physical and thermodynamic properites of various substances may be deduced from their sound transmission and absorption characteristics. The latter are usually determined experimentally by employing some form of standing wave system. The Kundt's tube and its diverse interesting modifications have provided a large amount of useful data relating to the velocities of sound in gases,[1] liquids[2] and solids.[3] However, velocities measured by these so-called "tube methods" at audible frequencies require special corrections due to the yielding of the walls of the tube.[4] The disturbing effects caused in this way may be eliminated by increasing the frequency of the source to the extent that the emitted waves within the tube are plane. Under such circumstances the velocity of sound in a confined fluid, when calculated from a standing wave system is independent of the size or shape of the container. Practically, these conditions obtain when the ratio of the diameter of the radiating surface to that of the emitted wave-length is greater than 12. Furthermore, to be reliable, the measurements should be taken at a considerable number of wave-lengths from the source, particularly if the radiator is

* Published with permission of the Navy Department.

[1] Behn and Geiger, Ber. deut. Phys. Ges. **5**, 657 (1907); Partington and Shilling, Phil. Mag. **45**, 416 (1923); Shilling and Partington, Phil. Mag. **5**, 920 (1928).

[2] Dorsing, Ann. d. Physik **25**, 227 (1908); V. Ionescu, J. de Physique et le Radium **5**, 377 (1924).

[3] H. O. Taylor, Phys. Rev. **2**, 270 (1913); E. C. Wente and E. H. Bedell, Bell System Techn. J. **7**, 1 (1928).

[4] L. G. Pooler, Phys. Rev. **35**, 832 (1930).

composed of many elements, such as a mosaic of piezoelectric crystals. In general, the energy radiated by a circular plate emitting longitudinal waves is confined mainly to a central beam, the width of which is found by the expression

$$\sin \theta = 1.22\lambda/D$$

where θ is the angle between the axis of the radiator and the boundary of zero intensity of the central beam, D is the diameter of the aperture or radiating surface; λ is the wave-length of the emitted wave.

Langevin[5] was the first to make wide application of supersonic waves by utilizing the piezoelectric properties of quartz. In 1916 in an experimental water tank he demonstrated supersonic beam reflection at 100 kc. Since the original investigations of Langevin, Boyle[6] and his collaborators have done a great deal of work in supersonics (or "ultrasonics" as they called it) by the aid of quartz-steel generators. Among their researches are measurements on the velocities of sound in a number of liquids and solids by the stationary wave method. A separate detector was required to indicate the nodal or antinodal planes in their standing wave system.

The present paper deals with supersonic stationary waves in which the source also detects the nodal and antinodal planes of the system. Therefore, an instrument in which stationary plane waves of high frequency sound are generated and detected shall be termed a *supersonic interferometer*.[7]

During the past few years several investigators have applied this type of interferometer to the study of sound in fluids. Pierce[8] was the first to use it in his determination of the velocities of sound in air and CO_2 at high frequencies. His method employed an oscillating quartz crystal serving a threefold purpose; namely, to control the frequency in a vacuum tube circuit; to generate sound waves from one face to a movable piston which is plane and parallel to the radiating face; and to detect the sound waves reflected from the piston. A stationary wave system is thus set up between the crystal and reflector. As the latter is moved through a series of nodal planes periodic maxima and minima are indicated on a microammeter suitably connected in the plate circuit. By these changes in the electrical circuit Pierce was able to measure the wave-length to a very high degree of precision. With this method, several other researches have been reported,[9] in which the velocity as well as the absorption of supersonic waves in gases and vapors are measured.

[5] International Hydrographic Bureau **3,** (1924); La Nature, January 1921 and August 1921.

[6] Boyle and others, Roy. Soc. Canada Trans. **19,** 167 (1925); **20,** 245 (1926); **21,** 79 (1927); **21,** 115 (1927); **22,** 371 (1928).

[7] This type of self-detecting interferometer has been variously described as a sonic interferometer by Wood and Loomis and an acoustic interferometer by Crandall and others. In the opinion of the authors, neither of these terms distinguishes the instrument from a tube resonator used at audio frequencies.

[8] G. W. Pierce, Am. Acad. Proc. **60,** 271 (1925).

[9] W. H. Pielemeier, Phys. Rev. **34,** 1184 (1929); **36,** 1005 (1930); G. E. Thompson, Phys. Rev. **36,** 77 (1930); C. D. Reid, Phys. Rev. **35,** 814 (1930).

Hubbard and Loomis[10] developed a compact interferometer with which they determined accurately the velocity of sound in various liquids. Their arrangement differs from that of Pierce in that the quartz crystal does not control the frequency of the oscillating circuit but is driven by an alternating e.m.f. whose frequency is far removed from that of the crystal. One surface of the quartz disk radiates sound directly into the liquid which is being studied. The production of stationary waves in the liquid and their measurements are effected by the aid of a plane reflector attached to a micrometer screw. Here also the nodal and antinodal planes are located by their reactions on the crystal source.

In all work with supersonic interferometers heretofore recorded quartz was used as the source of high frequency sound, and the investigations were limited to fluids. The present experiments deal with methods for using Rochelle-salt crystals or magnetostrictive rods as well as quartz for the interferometer source. It is further shown that the same interferometer can be used to determine the velocity of supersonic waves in solids and minute quantities of liquids.

Apparatus

The interferometer employed in the present investigation is composed of three principal units as shown in Fig. 1. The upper part, (a), consists of a specially constructed micrometer screw whose spindle has a maximum movement of four inches and whose barrel is graduated every 0.025 inches for the entire travel of the spindle. The least count of the instrument is 0.001 inch. To the lower end of the spindle is attached a plane brass reflector which is accurately machined so that its reflecting surface always remains normal to the axis of the cylinder in which it is traveling. The lowest portion of (a) is a threaded cap to fit the various fluid containers.

The central section, (b), may be a cylindrical or rectangular fluid container, each end of which is threaded so as to fit the adjoining units, (a) and (c), interchangeably.

Part (c) represents one of several holders for the elements used as sources of supersonic waves. The side tube at the bottom accomodates the leads to the electrodes of the crystal or groups of crystals used. The dimensions of (b) and (c) differed according to the range of frequency and substance studied. The fluid containers, (b), varied from four to sixteen inches in length and from three to nine inches in diameter. Among the elements used as sources are: a single disk of quartz 2.5 inches in diameter and 0.25 inch thick; a similar disk of Rochelle-salt; several rectangular slabs of the above crystals about $1\times1\times3/16$ inches; a mosaic of quartz about four inches in diameter and one of Rochelle-salt 2.5 inches in diameter; several magnetostrictive rods 0.5 inch in diameter and 4 to 10 inches in length.

In the photographs of Fig. 1 may be seen an assembled interferometer with a rectangular container, one side removed; the three separate units; and three of the generating elements.

[10] Hubbard and Loomis, Phil. Mag. **5**, 1177 (1928); Loomis and Hubbard, J.O.S.A. **17**. 295 (1928); J. C. Hubbard, Phys. Rev. **35**, 1442 (1930).

The circuit employed for impressing an alternating e.m.f. upon the source of the interferometer when the latter is used in conjunction with liquids and solids is shown in Fig. 2. A quartz crystal controls the driver frequency when extreme constancy is required. For work in which a continuously variable

Fig. 1. Diagram of interferometer.

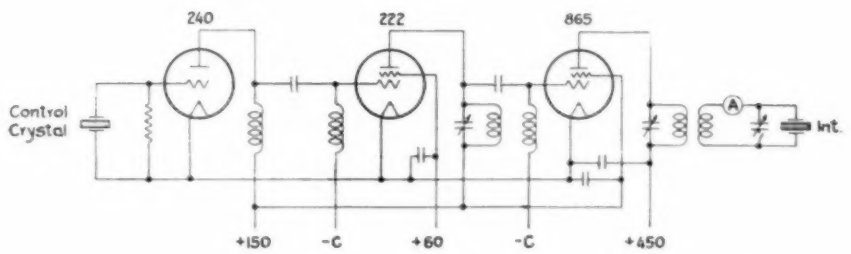

Fig. 2. Electrical driving circuit used with interferometer for work with liquids and solids.

frequency is desired a tuned-grid circuit is employed in the master oscillator stage. Extremely loose inductive coupling is used between the interferometer and the plate coil of the last tube. The circuit is designed to eliminate any effect of a variable load upon the frequency of the exciting e.m.f. The actual power drawn by the interferometer is a very small fraction of the available output power of the last tube.

Methods of Detection

There are numerous methods available for detecting the variations in impedance of the interferometer caused by changes in the position of the reflector. One of the simplest is to note changes in the series current. When the quartz disk is used as a sound source, it is essential to tune the output circuit sharply by means of the small variable capacity in parallel with the interferometer in order that the relatively small changes in impedance may become evident. The quartz interferometer at frequencies far removed from the resonant frequency of the disk reacts very nearly as a pure capacity which permits sharpness of tuning. On the other hand, when Rochelle-salt is employed the current through the instrument leads the voltage across its terminals by angles varying from 30° to 60° depending upon the reflector position, thus making sharp tuning impossible. The greatest fractional change in current observed with the quartz disk is about 15 percent, while if Rochelle-salt is used the fractional change in current ranges from 40 percent to 60 percent. To measure the series current, a vacuum thermocouple and microammeter with a full scale deflection of 200 microamperes was employed.

A novel method for detecting these impedance variations due to change in the reflector position is utilized by Hubbard and Loomis.[10] They actually permit the variations in load on the last tube to affect the driving frequency, then readjust the tuning condenser which varies the frequency so as to compensate for this change. The curves obtained are condenser settings plotted against reflector position.

A number of alternative methods were tried. In one set of experiments not only was the series current through the interferometer measured, but simultaneously the potential difference across its terminals was determined with a thermionic voltmeter. Again, instead of employing inductive coupling between the driving circuit and the interferometer, resistance-capacity coupling was used. The reactions, though much feebler than those obtained with inductive coupling, were in entire agreement with them.

The exact nature of the impedance changes taking place as the reflector position is varied was examined in detail by bridge measurements of the effective capacity and resistance of the interferometer (with a liquid medium). The circuit of the bridge is shown in Fig. 3. Two of the arms were equal capacities of 500 micromicrofarads each. The Rochelle-salt interferometer was placed in one arm and a calibrated air capacity in series with a resistance in the remaining arm. A thermionic voltmeter indicated the state of balance of the bridge. Simultaneously, the series current through the interferometer was measured. No high degree of accuracy is claimed for these measurements,

due to the large phase angles encountered and due to difficulties with the shielding. The result of a set of observations at 122 kc is shown in Fig. 4. These curves show resistance, reactance, net impedance, power factor, phase angle, series current, potential difference across the interferometer terminals and milliwatts dissipated in it as a function of the position of the reflector.

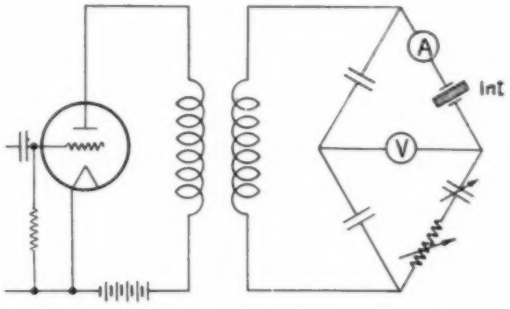

Fig. 3. Circuit used in bridge measurements of effective capacity and resistance of interferometer.

Examining the curves in detail, it is noted that to a first approximation, the capacitative reactance may be expressed by the equation:

$$X = X_0 + A \sin \alpha$$

and the resistance by

$$R = R_0 + A \cos \alpha$$

where $\alpha = 4\pi(l\text{-}L)/\lambda$; l is the micrometer reading; L is a reference point on the micrometer scale, and λ is the wave-length of sound in the medium. Also, it may be shown that to a first approximation:

$$Z = Z_0 + A \cos (\alpha - \theta)$$

where $Z_0 = (X_0^2 + R_0^2)^{\frac{1}{2}}$ and $\theta = \tan^{-1}(X_0/R_0)$. That is, the impedance of the instrument may be represented by the vector sum of one impedance whose magnitude and direction is constant and a second impedance whose magnitude is very nearly constant but whose direction depends upon the position of the reflector. In general, the impedance of the interferometer may be expressed by the equation:

$$Z = Z_0 + \sum_{n=1}^{n=\infty} A_n \cos (n\alpha - \theta_n)$$

The impedance diagram obtained on plotting X against R possesses some similarities to those observed by Kennelly and Pierce[11] in their work on the motional impedance of telephone receivers and to those obtained by Black[12] in his work on magnetostrictive rods. However, in these particular cases the driving frequency is varied while the resonant frequency of the driven

[11] A. E. Kennelly and G. W. Pierce, Am. Acad. Proc. **48,** 113 (1912).
[12] K. C. Black, Am. Acad. Proc. **63,** 49 (1928).

remains constant. In the present case, the driving frequency is held constant, and the resonant frequency of the driven is varied by altering the length of the liquid column. Each time the length of this column is changed by a half wave-length, the set of observed points encircle the diagram once. By external mechanical means Kennelly, Pierce, and Black prevented any displacement on the part of the device whose motional impedance was being measured while here the motion of the crystals is never zero but is aided or impeded by sound reflected from the movable piston.

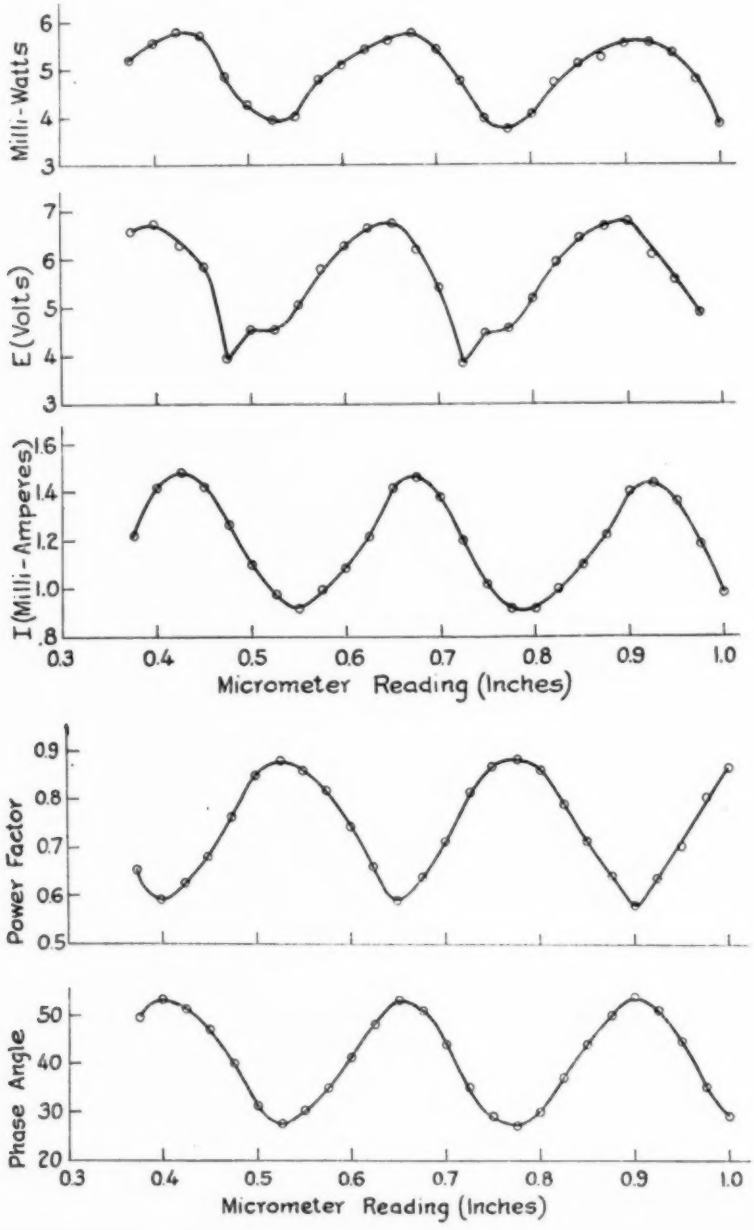

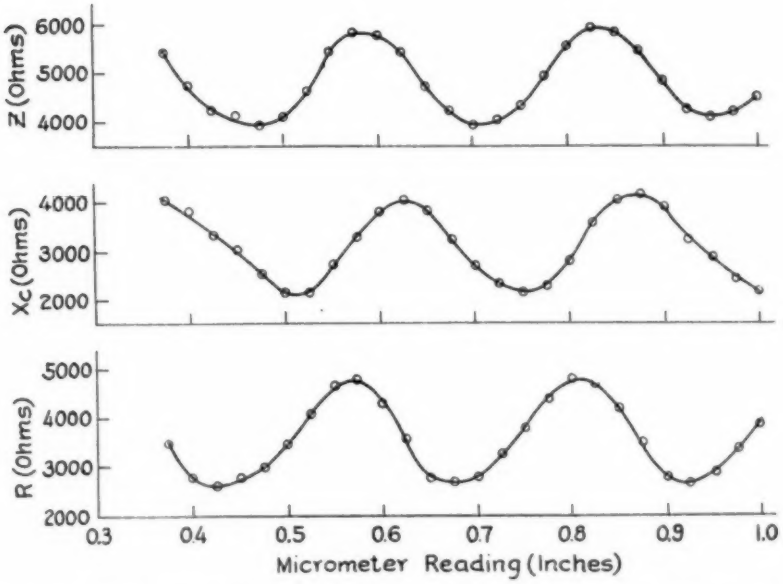

Fig. 4. Curves showing relationship between reflector position and resistance, reactance impedance, phase angle, and power factor of interferometer as well as current through it, e.m.f across its terminals, and watts dissipated in it.

Let ϕ denote the angle between the axis of resistance and the vector joining the center of the impedance diagram to any point on the perimeter. If the value of $d\phi/dl$ is constant around the diagram the simple set of resistance and reactance curves shown in Fig. 4 is obtained. In case $d\phi/dl$ varies around the diagram, the current curve no longer approximates a cosine function. It will be noted in Fig. 5 that the curves taken at 130 kc and 148 kc differ markedly from those taken at 122 kc. The constancy of $d\phi/dl$ and the shape of the curves are very closely dependent upon frequency. It is suspected that the sharpness of resonance in the liquid column is related to the selective transmission of the reflector.

Experimental Procedure

Liquids.—The velocity of sound in a number of liquids was measured by means of this instrument using different types of generators. The set of curve shown in Fig. 5 are typical for the Rochelle-salt interferometer. The liquid used was a high grade of transformer oil. Half wave-lengths were determined with an accuracy of 0.1 percent. Frequencies were measured to 0.03 percent. Hence a relatively high degree of accuracy may be obtained in velocity calculations. Curves possessing "fine structure" may be obtained by driving the interferometer at lower frequencies and favoring higher harmonics by the selection of proper coupling coils. Such a curve is shown in Fig. 6. The driving frequency was 45 kc while the third harmonic was emphasized by tuning. This curve is of interest in showing particularly the complexity which may arise in the standing wave system.

Solids.—In order to measure the velocity of supersonic waves in solids a suitable liquid (oil) was chosen as the medium for the solid under considera-

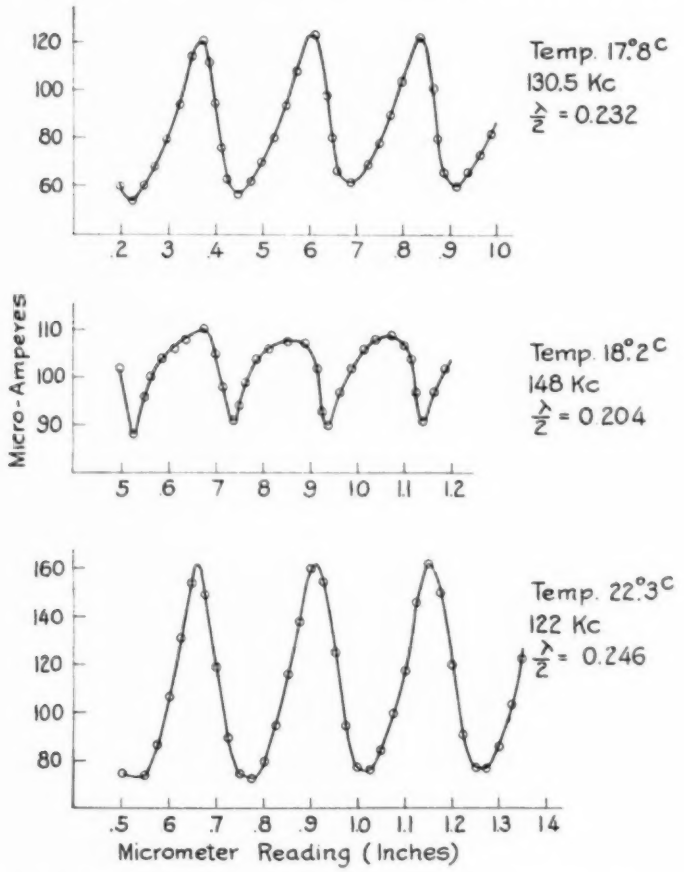

Fig. 5. Curves showing magnitude of series current variations obtained with interferometer and differences in general shape at various frequencies.

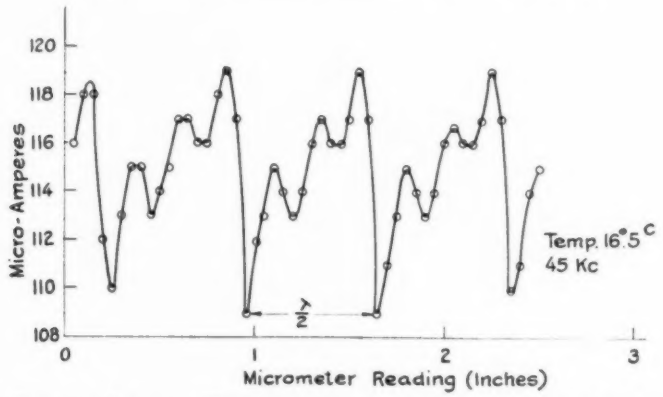

Fig. 6. "Fine Structure" curve. The standing wave system involves both a fundamental frequency and a third harmonic.

tion. The positions of the nodal and antinodal planes were accurately located in the liquid alone. Then with temperature and frequency unchanged a plane parallel slab of the solid was immersed in the sound beam and the relative displacements of the nodal and antinodal planes were ascertained. That is, the difference in acoustical path in the container when the liquid alone was present and when the solid was inserted in the beam was deduced from the micrometer readings, thus:

Let $d =$ actual thickness of slab traversed by the beam

$$\mu = \frac{V_s}{V_l} = \frac{\text{Velocity of sound in solid}}{\text{Velocity of sound in liquid}}.$$

Then the displacement of the nodal planes can be shown to be:

$$\Delta s = d(\mu - 1)/\mu$$

whence $\mu = d/(d - \Delta s)$.

This simple method works quite well when the product $V\rho$ for the solid is not greatly different from that product in the liquid, where V is the velocity of sound in the substance and ρ its density. This is the case in natural woods and wood compositions, in many varieties of bakelite and in rubber compounds. Table I illustrates the method for an amber bakelite of French manufacture.

TABLE I. *Illustration of measurement of velocity of sound in an amber bakelite of French manufacture.* Temperature 21°C. When micrometer reads zero reflector face is about 3 inches from source.

Micrometer Readings at Nodal Planes		Shift due to bakelite	Calculations
Oil alone	Amber bakelite in oil		
0.019	0.180	0.161	Measured thickness of slab = 0.412 in.
0.318	0.479	0.161	Average shift = 0.161 in.
0.620	0.780	0.160	$\mu = 0.412/0.251 = 1.64$
0.922	1.083	0.161	Known velocity in oil $= 1.50 \times 10^5$ cm/sec
1.223	1.384	0.161	$\therefore V_s = 1.50 \times 10^5 \times 1.64 = 2.46 \times 10^5$ cm/sec
1.526	1.687	0.161	
1.825	1.988	0.163	

However, if the two respective products mentioned above are very dissimilar, then it is necessary to choose such a thickness of material as will yield optimum transmission at a particular frequency. Generally, it is more convenient to use a slab of fixed thickness and then to find that frequency for which transmission of sound through the material is a maximum. This condition is realized when the slab thickness is an integral number of half wave-lengths. The theory of this method was suggested by Lord Rayleigh.[13] Boyle and Rawlinson[14] amplified Rayleigh's analytical treatment and applied it directly to supersonics. Later Boyle and Froman[15] verified their

[13] Rayleigh, Theory of Sound, Vol. II, p. 86.

[14] Boyle and Rawlinson, Roy. Soc. Canada, Trans. **22**, 55 (1928).

[15] Boyle and Froman, Canada Jour of Research **1**, 405 (1929).

theoretical conclusions by experiments in which they showed that at normal incidence transmission is a maximum when the thickness of the plate is an integral number of half wave-lengths. On the other hand, if the thickness is an integral odd number of quarter wave-lengths reflection is a maximum.

Fig. 7 is a sample curve showing the sharpness of selective transmission for a given thickness of commercial aluminum. As in the previous arrangement, the metal slab was immersed in oil at normal incidence. Series current through the interferometer source was observed at nodal and antinodal posi-

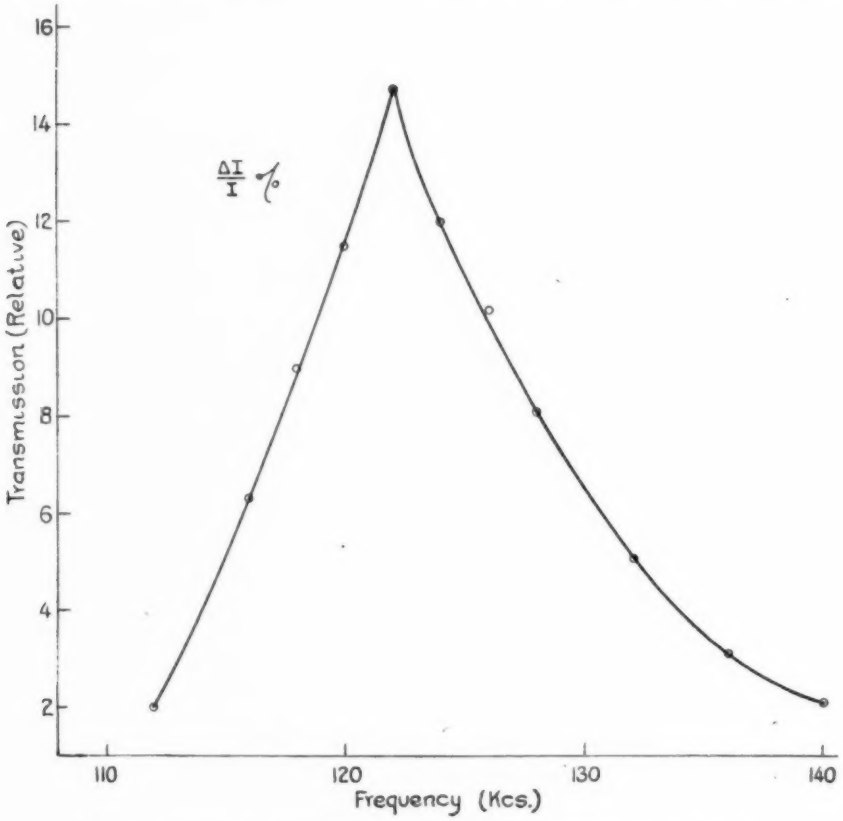

Fig. 7. Change in relative transmission with frequency for a slab of aluminum 0.825" thick.

tions of the reflector for the range of frequencies noted. The difference between maximum and minimum currents divided by their sum is the ratio $\Delta I/I$ used as ordinates in the curve. This ratio indicates the relative transmission of any substance assuming that no selective absorption or scattering is present. The frequency for which the specimen is an integral number of half wave-lengths is thus readily determined. In general, by varying the thickness of the material studied; or, by changing the frequency of the source sufficiently, the exact number of half wave-lengths included in a given sample can be ascertained. Quite often, the approximate number of half waves

in the substance may be calculated from a preliminary knowledge of some of its physical properties. The determination of the supersonic velocity in the solid from the measured wave-length in it and the frequency of the source is then easily verified by the nodal displacement method described above.

Example: Thickness of aluminum slab = 0.825 inches = $\lambda/2$. Best transmission frequency = 122 kc.

$$\therefore V = 122 \times 10^3 \times 0.825 \times 2 \times 2.54 = 5.11 \times 10^5 \text{ cm/sec.}$$

Displacement method in oil: Av. shift at 126 kc = 0.583 inches.

$$\mu = 0.825/0.242 = 3.31$$

$$\therefore V = 1.5 \times 10^5 \times 3.31 = 5.12 \times 10^5 \text{ cm/sec.}$$

Temperature 21°C.

One of the photographs shows slabs of brass, aluminum, and bakelite used in these measurements as well as a holder for the slab which permits other than perpendicular incidence to be used.

Small quantities of liquids.—When only small quantities of liquids are available, (say, less than 100 cc) the methods so far described are not readily applicable. In the first place the measurement of wave-length in the specimen must of necessity be made very close to the sound generator. And as was pointed out earlier, the phase relations close to the source are such as would tend to diminish the sharpness of nodal plane locations. Also the number of wave-lengths that are measurable in the liquid is small; hence the accuracy is reduced. Furthermore, it is often undesirable to have the liquid come in contact with the reflector and container, especially if these are not gold or platinum plated. Such difficulties were obviated in the present experiments by putting the small quantities of liquid to be tested in a parallel walled cell, which was immersed in a liquid medium of known acoustic properties. For example, the procedure for a specimen of turpentine was as follows: a bakelite cell was immersed in the oil previously studied. The cell was filled with the same oil. Micrometer readings for a series of nodal planes in the oil were recorded. Now with the turpentine in the cell, all other conditions remaining the same, the displacement of the nodal planes was measured. The supersonic velocity in the liquid was calculated by the same formula as in the experiment with the bakelite slab, thus:

Shift due to 1 inch layer of turpentine = −0.115 in. $\mu = 1/1.115 = 0.897$.

$$\therefore V = 1.5 \times 10^5 \times 0.897 = 1.34 \times 10^5 \text{ cm/sec.}$$ Temperature 21°C

In Fig. 8, curve I was taken when transformer oil only separated the reflector from the source; curve II was taken after the parallel walled cell filled with the same oil had been interposed in the acoustic path; and curve III when turpentine had been substituted for the oil.

Gases.—For measuring supersonic velocities in gases the Pierce interferometer is perhaps the simplest method yet devised. Fig. 9 shows a curve obtained in air with a Rochelle-salt crystal instead of quartz in the Pierce circuit. At lower frequencies in air, magnetostrictive rods served admirably well

as sources of a stationary wave system. The driving circuit for the rods was similar to that described by Pierce.[16] On the other hand, for the measurement of sound absorption in gases, the Pierce arrangement may lead to erroneous results. For it should be noted, that both the frequency and amplitude of the exciting e.m.f. are influenced by the resonant reaction of the gas column upon the crystal. The change in frequency is so small that only in cases of extreme accuracy need it be taken into account. However, it is the periodic fluctuation

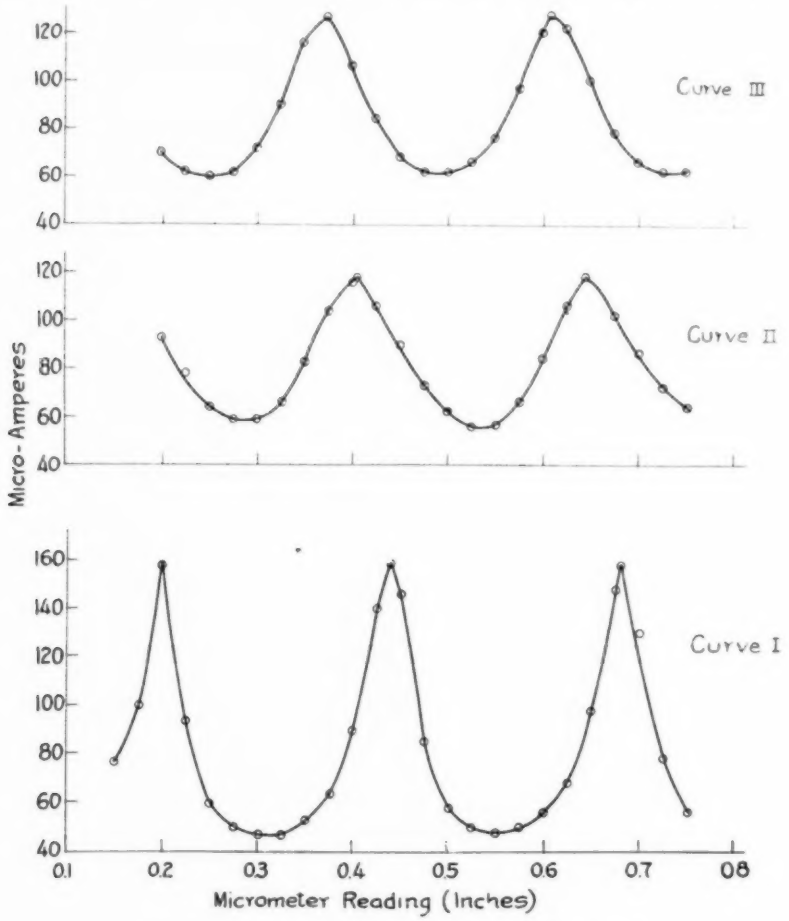

Fig. 8. Shift in position of nodal planes illustrated.

in amplitude of the e.m.f. across the crystal that makes possible the location of the nodal and antinodal planes in the gas. That is, the vacuum tube acts as a rectifier and the changes in the rectified plate current, as the length of the gas column is altered, are a measure of variations in the e.m.f. across the crystal.

The experiments of Pielemeier, Reid, and others show that as the length of the acoustic path in the gas is increased, the changes in plate current di-

[16] G. W. Pierce, Am. Acad. Proc. 63, 1 (1928).

minish. This diminution is due largely to absorption. Nevertheless, absorption coefficients calculated from this rate of diminution are inconclusive unless we possess an exact knowledge of the operating—not the static— characteristics of the tube and in addition how the emitted sound wave amplitude varies with that of the driving e.m.f., as well as what part the received sound wave amplitude plays in determining the net e.m.f. across the crystal. Observations made at 130 kc show that the rate of diminution of plate current variations, with increasing path length, may be altered at will by a factor of 80 percent merely by changing circuit constants.

In order to eliminate some of these difficulties Hubbard[17] proposes to use two quartz crystals tuned approximately to the same frequency. One crystal is used in a master oscillator circuit which supplies an e.m.f. of constant frequency and amplitude, to the second crystal serving as a driven source of

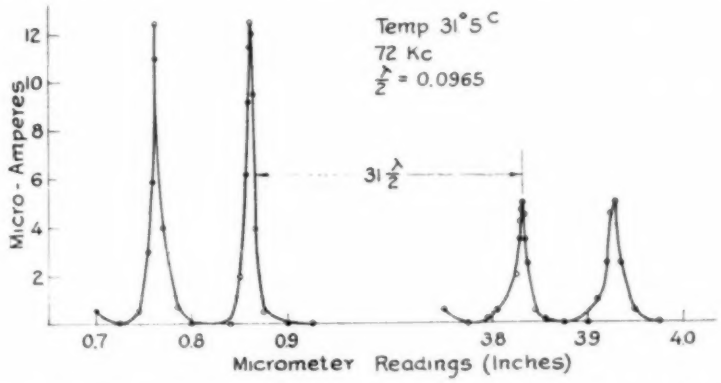

Fig. 9. Air interferometer curve. The change in magnitude of the peaks with increasing path length is shown in pronounced fashion.

sound. This method should prove valuable if and when constant mechanical amplitude can be maintained in the second crystal during a complete cycle of changes introduced by the motion of the reflector in the gas. Inherently, a quartz crystal displays a rather narrow resonance curve, and the task of holding to a fixed point on this curve as the reflector is displaced is troublesome even though the temperature remains constant.

To attain the same end, we have developed a circuit which promises to be useful in absorption measurements. The schematic diagram is shown in Fig. 10. Three electrodes are used on the crystal plate, similar to an arrangement of Cady.[18] The essential feature of this method is that it permits the amplitude of the exciting e.m.f. to be maintained constant, irrespective of the reaction of the gas column, by varying the resistance marked *P*. Moreover, since regeneration is employed, the difficulty in the two crystal system arising from the necessity of exact tuning is eliminated.

Another method for the determination of absorption coefficient of super-

[17] J. C. Hubbard, Phys. Rev. **36,** 1668 (1930).
[18] W. G. Cady, U. S. Patent No. 1472583, Oct. 30, 1923.

sonic waves in gases which appears to be free from many of the difficulties mentioned above is an adaptation of the hot wire microphone of Tucker and Paris.[19] Richardson[20] has shown the possibility of using a single wire for the measurement of sound decay in tubes at low frequencies. The scheme proposed here is to mount a very fine platinum wire cross on a ring which is inside the gas container (c) and is subject to small displacements parallel to the sound beam and may be moved independently from the reflector. Further investigation of this sort may be reported later.

From the foregoing discussion it is readily seen that the general use of the interferometer is considerably enhanced by having similar sound generators available in pairs For example if the second source is placed in the position

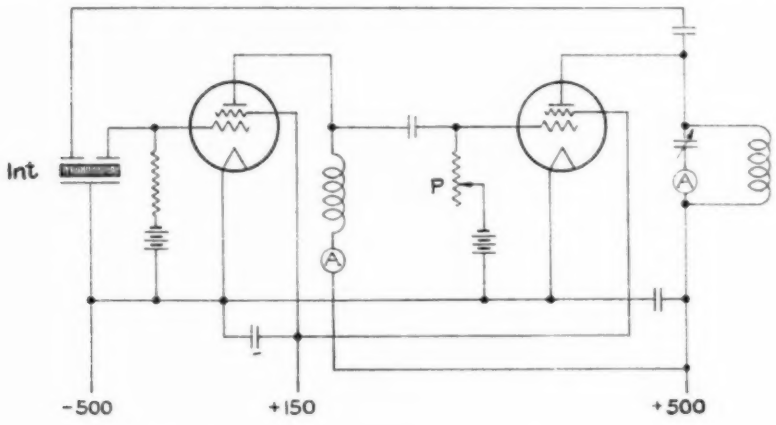

Fig. 10. Improved circuit for gas interferometer.

normally occupied by the reflector and these two identical generators are excited by the same electrical driving circuit, the amplitude of the interfering sound waves may be made to be nearly equal and the precision of velocity measurements be extended. Since this method was tried, Boyle and Froman[21] have described a similar scheme for producing stationary waves. In one set of our experiments two sources were so disposed that either alone acted as the sound generator while the other served as a reflector. Also, the movable was made to receive supersonic waves while the fixed acted as a transmitter, after the manner of Hehlgans.[22] In absorption measurements two identical generators are most valuable.

The authors are indebted to Mr. Emil Kaiser for his constructive interest in the design of the apparatus and to Mr. John Boyd for his careful and precise workmanship of the various parts.

[19] Tucker and Paris, Roy. Soc. Phil. Trans. **221,** 389 (1921).
[20] E. G. Richardson, Roy. Soc. Proc. **A112,** 522 (1926).
[21] Boyle and Froman, Nature **126,** 602 (1930).
[22] Hehlgans, Ann. d. Physik **86,** 587 (1928).

LETTERS TO THE EDITOR

Prompt publication of brief reports of important discoveries in physics may be secured by addressing them to this department. Closing dates for this department are, for the first issue of the month, the twenty-eighth of the preceding month; for the second issue, the thirteenth of the month. The Board of Editors does not hold itself responsible for the opinions expressed by the correspondents.

Relations between Hall Effect and Resistance

Measurements of the Hall effect have been made on sputtered gold films, while the films were heated in air from room temperature to 110°C. These show a relation between the Hall e.m.f. and resistance like that obtained for tellurium films (Phys. Rev. **30,** 673 (1927)). During the first heating after the film was sputtered, the Hall e.m.f. and resistance alike underwent a rapid decrease, in one case to values of both Hall e.m.f. and resistance only one-tenth that of the initial values. This relation is then a property of metals and not a peculiarity of tellurium. Wait and Mackeown have previously shown the Hall e.m.f. to be independent of resistance during aging of the film, and the tellurium films showed two types of aging; (1) a decrease in resistance independent of the Hall effect, and (2) a decrease in Hall e.m.f. in proportion to resistance, similar to the proportionality to resistance, (3) when the latter decreased with increase in temperature. This proportionality also held (4) when the resistance increased with increase in temperature. Processes (3) and (4) are reproducible.

Wait explained process (1) by showing that the measured e.m.f. should be the sum of the e.m.f.'s across the granules. This measured e.m.f. should be constant, while the decrease in resistance was due to the elimination of the interstices between the granules.

If we assume that the decrease in resistance on heating, in the case of metals and films which have a negative temperature coefficient of resistance, is due not to the increase in the number of so-called "free" electrons, but to the increase in the ease with which the electron passes from one atom to another, the proportionality between Hall e.m.f. and resistance in processes (2), (3), and (4) is readily accounted for. In the initial non-reproducible decrease of resistance and Hall e.m.f. there is undoubtedly a coalescence of particles, decreasing the difficulty with which the electron can pass from atom to atom. The thermal agitation should occasionally bring an electron of one atom near to the orbit of another atom so that the electron in passing from atom to atom climbs over a smaller potential hill. Again, greater thermal agitation may cause greater obstruction to the drift of the election from atom to atom in the current stream, giving the usual positive temperature coefficient of resistance. Since e.m.f. is work per electron, the Hall e.m.f., on this basis, should be proportional to the resistance in each of the three stages; (2) the initial decrease of Hall e.m.f. and resistance; (3) when the temperature coefficients of resistance and of Hall e m.f. are negative; and (4) when the coefficients are positive.

With the increase in ease with which an electron passes from atom to atom there is probably also an increase in the number of electrons separating from atomic centers and taking part in conduction, giving the same result as above described in processes (3) and (4) but not accounting for process (2), if the number of "free" electrons depends only on temperature.

F. W. WARBURTON
J. W. TODD
Department of Physics,
University of Oklahoma,
February 25, 1931.

Note on the Structure of Groups in Crystals

In the February 15th number of the Physical Review, (**37,** 447, 1931) is published a letter to the Editor from Mr. M. L. Huggins, which was based upon a short abstract of a paper given by me at the Chicago Meeting of American Physical Society last year. I find

it rather unfortunate that Mr. Huggins has based his letter on this abstract, as I am now preparing for publication a full account of the results I have obtained during my investigations of the last 3 years on groups $(XO_3)^{-m}$ in crystals. It seems necessary to me to give a few comments on Mr. Huggins' letter.

In the letter is stated that I, in agreement with earlier work on the crystal structure of $NaClO_3$ and $NaBrO_3$ (Kolkmeijer, Bijvoet, and Karssen,[1] Dickinson and Goodhue[2]) describe the XO_3-group in these crystals as tetrahedral groups with one corner missing. This passage obviously must give the reader the false impression that these earlier investigators already had determined the structure of these interesting groups. This is not the case as every one familiar with the above papers can ascertain. I have shown that the structure proposed by the Dutch investigators for $NaClO_3$ and $NaBrO_3$, as well as that proposed by Vegard,[3] is incorrect.[4] The structure given by Dickinson and Goodhue is inaccurate, and their results therefore do not allow conclusions to be drawn with regard to a possible non-planar XO_3-group. Dickinson and Goodhue were as a matter of fact themselves aware of the inaccuracy, and only remark about the XO_3-group that the halogen lies nearly in the plane of the oxygens, indicating that they are considering the XO_3-group to be a coplanar group. There is thus a rather wide step from this conception of the XO_3-group to mine. The first description of "tetrahedral" groups XO_3 in crystals was given by me in 1928,[4] and has been dealt with also in other of my papers on these groups.[5]

It surprises me somewhat to learn that Mr. Huggins finds it necessary to point out the elementary fact that the two displaced electrons in the XO_3-group can be correlated to a Lewis electron pair. I thought the interpretation of e.g. the ClO_3-ion according to the Lewis hypothesis was familiar to everyone. So far the application of the principles of shared electron pairs on the atomic arrangement in inorganic crystals has proved unsuccessful, while considerations of the crystal structure from point of view of ions, ionic dimensions, ionic polarizability, and crystal energy in the hands of such men as W. L. Bragg, K. Fajans, V. M. Goldschmidt, F. Hund, L. Pauling, A. E. van Arkel, J. A. Wasastjerna, and others have given very valuable and important results.

Until one is able to treat the quantization of the electrons in polyatomic groups completely on the basis of wave mechanics, we must be satisfied with rough approximations. It is obvious that one cannot consider such groups to be purely ionic in character. The point of view I have taken with regard to the groups XO_3 is the familiar one of considering the constituents primarily as ions, and then take into consideration the deformation taking place in the electron clouds. The final continuous distribution of electron density may then be regarded as an approximation to the statistical continuity of density one will get from a quantum mechanical treatment. Judging from the results already obtained by this point of view I see at present no advantage in introducing the conception of shared electron pairs in crystals of this kind.

The most important factor which is independent of the point of view one takes is, of course, the total number of valence electrons in the group. In my paper on the groups XO_3 soon to be submitted I have devoted a chapter to the relation between the number of valence electrons and the symmetry of molecules or groups XY_2 and XY_3. If we limit ourselves to considering groups containing atoms of relatively low atomic number I have showed that the following rule holds for all observations hitherto obtained:

A group or molecule $\begin{cases}(XY_2)^{-m}\\(XY_3)^{-m}\end{cases}$ has a $\begin{cases}\text{co-}\\\text{co-}\end{cases}$ $\begin{matrix}\text{linear}\\\text{planar}\end{matrix}$ structure if the condition $\begin{matrix}\Sigma v=2\times p\\\Sigma v=3\times p\end{matrix}$ is satisfied. Here Σv denotes the total number of valence electrons in the group or molecule, while p is the number of valence electrons in the inert gas following atom Y in the periodic system if the number of valence electrons on the other hand has to be expressed by an equation of the form $\begin{matrix}\Sigma v=2\times p+\Delta\\\Sigma v=3\times p+\Delta\end{matrix}$ the group or

[1] Kolkmeijer, Bijvoet, Karssen, Proc. Roy. Acad. Amsterdam **23,** 644 (1920).

[2] Dickinson and Goodhue, J. Am. Chem. Soc. **43,** 2045 (1921).

[3] L. Vegard, Zeits. f. Physik **12,** 289 (1922); Norske Vid.-Akad. Skr. Oslo Nr. 16, 1922.

[4] W. H. Zachariasen, Norske Vid.-Akad. Skr. No. 4, p. 143, 1928; Zeits. f. Krist. **71,** 517 (1929).

[5] W. H. Zachariasen, Zeits. f. Krist. **71,** 501 (1929); Paper in print in Phys. Rev.

molecule has an angular or pyramidal structure. The deviation from co-linearity or co-planarity probably increases with increasing Δ. A few examples of the kind of structures we may expect according to this rule may be given.

Co-linear: CO_2, ON_2, CS_2, $(NN_2)^-$, $(HF_2)^-$
Angular (polar): OH_2, SO_2, OO_2? (ozone), SH_2, NO_2, $(NO_2)^-$
Co-planar: $(BO_3)^{-3}$, $(CO_3)^{-2}$, $(NO_3)^-$, SO_3, BH_3, BF_3
Pyramidal (polar): $(PO_3)^{-3}$, $(SO_3)^{-2}$, $(ClO_3)^-$, $(AsO_3)^{-3}$, $(SeO_3)^{-2}$, $(BrO_3)^-$, $(OH_3)^+$, NH_3, PH_3, AsH_3, PF_3, PCl_3 and so on.

In no case is there observed a contradiction to the rule, so it may be used with some confidence for predictions. For a more complete information about my work on the groups I can refer to my paper which is to be published shortly.

W. H. ZACHARIASEN

Ryerson Physical Laboratory,
University of Chicago,
February 28, 1931.

Interpretation of the Spectra of Rare Earth Crystals

From the work of J. Becquerel, Brunetti, Ephraim, Freed and Spedding, and others, it is known that the absorption spectra of rare earth crystals consist of narrow bands which become resolved into sharp lines as the temperature of the crystals is lowered. The lines tend to gather into multiplets, and arise from energy levels which resemble in their behavior the energy levels of atoms subjected to electric and magnetic fields much more than they resemble the levels of molecules. For example, the positions of the lines are but very little influenced by the negative ions present, and such influence amounts only to the expected slight shifting caused by the different electric fields set up by the various ions in the lattice. Furthermore, the lines do not fade out as the temperature is lowered, but are still strong at the temperature of liquid helium. Again, the lines are polarized, as would be the case if the levels were split apart by electric fields.

In a paper which is to be published soon in this journal, Dr. Freed and I have presented a partial energy-level diagram for Gd^{+++} self-consistent within the accuracy we were able to attain (1 cm^{-1} for position, 4 cm^{-1} for resolution), derived from eight sets of data. The data were:[1,2,3] Absorption spectra of $GdCl_3 \cdot 6H_2O$ at ordinary temperatures, and at that of liquid nitrogen and of liquid hydrogen. Gd^{+++} even at room temperatures gives sharp spectra, but as the temperature is lowered the lines shift somewhat owing to changes in the effective electric fields caused by the ingathering of the crystal lattice;[4,5] Absorption spectra of $GdBr_3 \cdot 6H_2O$ at room and liquid nitrogen temperatures;[6,7] Transverse Zeeman effect on the a and b axis of monoclinic

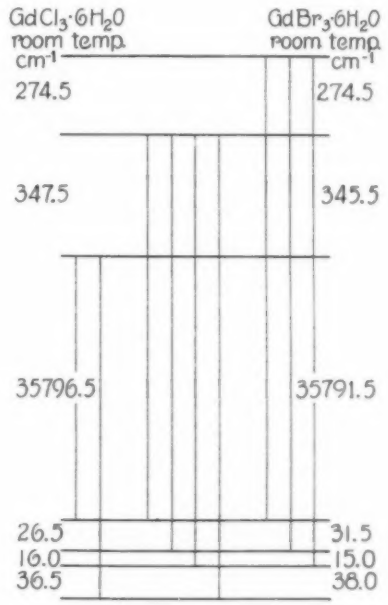

Fig. 1.

[1] F. Hund, Linien Spektren, Julius Springer, Berlin.

[2] Woltjer and Kammerlingh Onnes, Leiden Comm. No. 167 C.

[3] Giauque, J. Am. Chem. Soc. **49,** 1870 (1929).

[4] (a) H. A. Kramers, Proc. Amst. Acad. **32,** 1176 (1929); **33,** 9 (1930). (b) H. A. Kramers et J. Becquerel, Proc. Amst. Acad. **32,** 1190 (1929). (c) J. Becquerel, W. J. de Haas, et H. A. Kramers, Proc. Amst. Acad. **32,** 1206 (1929). (d) H. A. Kramers, Proc. Amst. Acad. **32,** 1196 (1929) and private conversation.

[5] Freed and Spedding (a) Nature **123,** 525 (1929); (b) Phys. Rev. **34,** 945 (1929); (c) J. Am. Chem. Soc. **52,** 3747 (1930); (d) Phys. Rev. **35,** 1408 (1930).

$GdCl_3 \cdot 6H_2O$;[6] Longitudinal Zeeman effect on the c axis of $GdCl_3 \cdot 6H_2O$. The diagram, shown in Fig. 1, is not consistent with other methods of reasoning. For instance, in his brilliant work on complex spectra, by making use of Russell-Saunders coupling and the Pauli exclusion principle, Hund calculates the basic levels of the rare earth ions. He then calculates the magnetic susceptibilities of the gaseous ions and his values agree remarkably well with those obtained experimentally from the solids themselves. For Gd^{+++} he obtains an ^8S term, which is single, as are all S terms. Wolljer and Kamerlingh Onnes[2] have measured the magnetic susceptibility of $Gd_2(SO_4)_3 \cdot 8H_2O$ from 1.3°K to room temperature, and Giauque[3] shows that their results are in perfect accord with the assumption of an ^8S basic level.

Kramers and J. Becquerel,[4] from their work on the paramagnetic rotation of polarized light in xenotime, conclude that the rotation is due to the presence of Gd^{+++} ions in the mineral, and that the Gd^{+++} is in the ^8S state, which is split into several components in the crystal field. Even in the anhydrous crystals with which they were dealing the splitting is not expected to amount to more than a few cm^{-1}. Certainly in the hydrated salts which were used by Giauque and by Freed and me the effect must be much less, less even than our resolving power.

The diagram as it is presented requires either metastable levels of high energy or wide splitting in the lower level, both forbidden by the arguments set down above. However, if the electron distributions in the rare earth elements are examined, it becomes apparent how these conflicting notions may be brought into agreement. According to the Bohr-Stoner scheme, the distribution of electrons in Gd^{+++} ion is as follows:

$1s$	$2s$	$2p$	$3s$	$3p$	$3d$	$4s$	$4p$	$4d$	$4f$	$5s$	$5p$
2	2	6	2	6	10	2	6	10	7	2	6

In previous papers Dr. Freed and I point out that the optically and magnetically active $4f$ electrons give rise in solids to atomic rather than molecular spectra since the complete $5s$ and $5p$ shells partially shield the $4f$ electrons and tend to prevent close coupling between them and neighboring ions and water molecules. There are two ways in which one of the $4f$ electrons may be excited. Firstly, it may remain under this screening influence of the $5s$ and $5p$ shells. To do this, however, n and l of the electron can not change since the exclusion principle forbids any other values. Therefore the only possible excitation comes about through one of the spins reversing itself, thus giving rise to sextet terms. A jump of this sort rarely occurs in atomic spectra and, moreover, it is to be expected that the energy involved would be large. Secondly, the electron may jump outside the strong protection of the $5s$ and $5p$ shells and occupy the $5d$, $5f$, and $5g$ or higher shells, but most probably the $5d$ shell. In this event, Russell-Saunders coupling would presumably be effective for each part of the atom, but owing to the same screening activity on the part of the $5s$ and $5p$ levels it would be much weaker between the halves and would result in $j-j$ coupling. In this instance a $^7F_0$ term would be formed inside and would join with the $^2D_{3/2}$ term outside to give the combined term, $[^7F_0{}^2D_{3/2}]3/2$. Of course, other types of coupling are possible, especially if the splitting of the terms caused by the electric fields of the crystals is large as compared with the $j-j$ coupling. At least there would be a strongly coupled part inside joined by a relatively weak bond to the excited electron outside.

If this is true it would be expected that the intervals, $^7F_0-{}^7F_1$, $^7F_1-{}^7F_2$, and so on would occur in the spectra. Although as a first approximation they would be equal for terms of the type, $[^7F_2{}^2D_{3/2}]7/2[^7F_2{}^2D_{3/2}]9/2$, there would nevertheless be some differences, greater or less depending on the difference in energy of the terms coupling with them. Also, splitting of the levels, $[^7F_2{}^2D_{3/2}]7/2[^7F_2{}^2D_{3/2}]5/2$, owing to the electric fields in the crystal, should be nearly alike, but under high dispersion differences should become apparent. This is precisely what is found to be the case. I am just now repeating the work cited above, using a spectrograph with a dispersion of 2A per mm and have found small differences, amounting to about 1 cm^{-1}, between splitting arising from different groups.

Evidences of coupling of the sort suggested should also be found in the gaseous spectra of the rare earths, so that very different terms from those predicted on the basis of Russell-Saunders coupling would be obtained. The spectra would be closely analogous to x-ray spectra with the exception that the energy values of the optical levels are of such an order of magnitude that their interaction with the x-ray levels can no longer be ignored.

It may be well to mention a few of the more striking facts noted when the spectra are photographed with an instrument of high dispersion. Ordinarily, perhaps half the lines are doublets of about 1 cm^{-1} separation, but if the crystals are under strain many more lines resolve and the separation becomes greater. This splitting may be attributed to the action of the electric fields in the crystal on the basic level. Professor Kramers[4d] has suggested that the ^8S level should dissolve into four slightly separated levels. These, with the rules of selection which are applicable, should give separations of the sort observed. Just as was anticipated, the spectrum of a triclinic crystal photographed by Mr. G. C. Nutting and me shows the dissolution into pairs to be much more pronounced, with several of the lines which apparently were single in the monoclinic $GdCl_3 \cdot 6H_2O$ resolved clearly into doublets. In a magnetic field the double lines split into several components, usually five or more, and in most instances it seems that still more components would appear under higher dispersion. As a usual thing the lines tend to separate into two groups of components which, under low dispersion, show as doublets of the sort reported by J. Becquerel, and Freed and Spedding.

FRANK H. SPEDDING
National Research Fellow
University of California,
Berkeley, California,
February 20, 1931.

High Velocity Vapor Jets at Cathodes of Vacuum Arcs

From measurements of the force of recoil on the cathode of an arc drawn in a high vacuum, and from measurements of the amount of cathode material which was lost, Tanberg[1] has calculated the mean velocity of the material leaving the cathode to be the extraordinarily high one of over 10^6 cm per sec. K. T. Compton[2] has proposed a theory of the development of high molecular velocities, but explains that, ". . . this criticism does not alter Mr. Tanberg's basic conclusion regarding a high speed neutral vapor stream. It merely suggests an electrical mechanism for the acquiring of these speeds instead of assuming a terrifically high temperature at the cathode."

Close scrutiny of Dr. Compton's suggestion that high velocity neutral molecules leave the cathode as a result of the existence of an accommodation coefficient for the positive ions neutralized at the cathode, indicates, however, that the velocity of these molecules cannot be nearly as great as the velocity obtained by Tanberg. The maximum velocity of the neutralized ions cannot be expected to be much greater than that corresponding to the cathode drop, whereas Tanberg observed velocities of an order corresponding to 70 volts. Hence, if the reaction of the neutralized positive ions is to account for the force upon the cathode observed by Tanberg, the stream of neutralized positive ions leaving the cathode with part of their original energy must be of much greater density than the high velocity stream calculated by Tanberg. In fact, Compton, by assuming that all the positive ions participate in the reaction, calculates that the average energy of the neutralized ions need be less than 0.4 volt to give the force measured by Tanberg.

The high speed stream of Tanberg must still be assumed to leave the cathode *region*, even though the mechanism proposed by Compton may possibly account for the way in which force is communicated to the cathode itself. Because of the high vacuum, the only material leaving the cathode region is substantially only the material lost from the cathode, which Tanberg weighed. The force on the cathode must equal the momentum of the material leaving the cathode *region*, regardless of whether this material acquires its velocity at the cathode surface or elsewhere in the region.

The argument for the necessary existence of Tanberg's high speed stream seems to be valid unless there is a high density of gas in the vessel in which the experiment is carried out. In such a case, the lower speed neutralized positive ions of Dr. Compton could communicate their momentum to many gas molecules, without any of them acquiring a high velocity. But a high gas pressure in the tube during the period of arcing does not seem likely. To obtain a high density of copper vapor throughout the vessel would require almost complete reflection of copper atoms at the walls of the vessel, a condition which does not seem very probable for heavy metal atoms. If such complete reflection did occur, one would expect to have a uniform deposit of copper on all parts

[1] Tanberg, Phys. Rev. **35**, 1080 (1930).
[2] K. T. Compton, Phys. Rev. **36**, 706 (1930).

of the containing vessel. Actually, however, experiment shows that the deposit is most dense directly opposite the cathode spot, with practically no deposit behind the cathode, the distribution of density following a cosine law roughly. So, little reflection must occur, condensation must take place on first impact, and vapor must flow from the cathode region at a rate just equal to the rate of vaporization measured by Tanberg. Since the momentum measured by Tanberg is carried by the mass he used, the velocity he calculated must be correct.

In the same way, the calculated high velocity of vapor striking a vane 2 cm from the cathode can be in serious error only if considerable reflection from the vane occurred,—a condition which does not seem to be true. Thus, if the force on the cathode is due to the reaction of neutralized ions, as proposed by Compton, some mechanism must exist whereby the many neutralized ions of low velocity transfer their momentum to the few atoms leaving the cathode region, with consequent high velocity.

The cathode spot itself, on the metal, need not be, and probably is not, at a high temperature. The experiment merely shows that a very high velocity vapor stream issues from the cathode region. A similarly high reaction upon the cathode of the mercury arc has been observed recently by Kobel.[3]

Whether or not to ascribe a high temperature to such a high velocity vapor stream is merely a matter of use of words. Perhaps, for the sake of emphasizing the unusual magnitude of the velocity, one may speak of the temperature of the vapor jet through the relation $3kT/2 = mv^2/2$.

Experiments to measure the magnitude of the vapor jet velocity by an independent means are in progress in this laboratory.

JOSEPH SLEPIAN
R. C. MASON

Research Laboratory,
Westinghouse Elec. and Mfg. Co.,
February 25, 1931.

[3] Kobel, Phys. Rev. **36**, 1636 (1930).

Knowledge of Past and Future in Quantum Mechanics

It is well known that the principles of quantum mechanics limit the possibilities of exact prediction as to the future path of a particle. It has sometimes been supposed, nevertheless, that the quantum mechanics would permit an exact description of the past path of a particle.

The purpose of the present note is to discuss a simple ideal experiment which shows that the possibility of describing the past path of one particle would lead to predictions as to the future behaviour of a second particle of a kind not allowed in the quantum mechanics. It will hence be concluded that the principles of quantum mechanics actually involve an uncertainty in the description of past events which is analogous to the uncertainty in the prediction of future events. And it will be shown for the case in hand, that this uncertainty in the description of the past arises from a limitation of the knowledge that can be obtained by measurement of momentum.

Consider a small box B, as shown in the figure, containing a number of identical particles in thermal agitation, and provided with two small openings which are closed by the shutter S. The shutter is arranged to open automatically for a short time and then close again, and the number of particles in the box is so chosen that cases arise in which one particle leaves the box and travels over the direct path SO to an observer at O, and a second

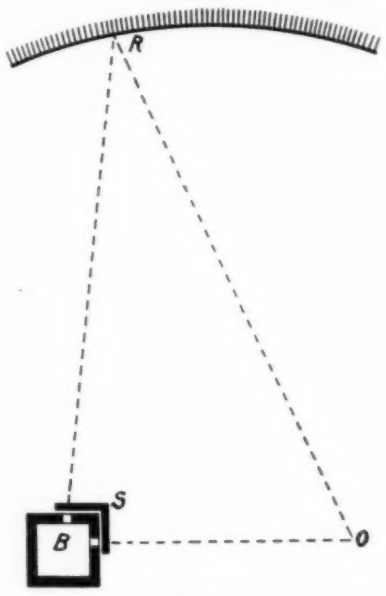

Fig. 1.

particle travels over the longer path *SRO* through elastic reflection at the ellipsoidal reflector *R*.

The box is accurately weighed before and after the shutter has opened in order to determine the total energy of the particles which have left, and the observer at *O* is provided with means for observing the arrival of particles, a clock for measuring their time of arrival, and some apparatus for measuring momentum. Furthermore the distances *SO* and *SRO* are accurately measured beforehand, —the distance *SO* being sufficient so that the rate of the clock at *O* is not disturbed by the gravitational effects involved in weighing the box, and the distance *SRO* being very long in order to permit an accurate reweighing of the box before the arrival of the second particle.

Let us now suppose that the observer at *O* measures the momentum of the first particle as it approaches along the path *SO*, and then measures its time of arrival. Of course the latter observation, made for example with the help of gamma-ray illumination, will change the momentum in an unknown manner. Nevertheless, knowing the momentum of the particle in the past, and hence also its past velocity and energy, it would seem possible to calculate the time when the shutter must have been open from the known time of arrival of the first particle, and to calculate the energy and velocity of the second particle from the known loss in the energy content of the box when the shutter opened. It would then seem possible to predict beforehand both the energy and the time of arrival of the second particle, a paradoxical result since energy and time are quantities which do not commute in quantum mechanics.

The explanation of the apparent paradox must lie in the circumstance that the past motion of the first particle cannot be accurately determined as was assumed. Indeed, we are forced to conclude that there can be no method for measuring the momentum of a particle without changing its value. For example, an analysis of the method of observing the Doppler effect in the reflected infrared light from an approaching particle shows that, although it permits a determination of the momentum of the particle both before and after collision with the light quantum used, it leaves an uncertainty as to the time at which the collision with the quantum takes place. Thus in our example, although the velocity of the first particle could be determined both before and after interaction with the infrared light, it would not be possible to determine the exact position along the path *SO* at which the change in velocity occurred as would be necessary to obtain the exact time at which the shutter was open.

It is hence to be concluded that the principles of the quantum mechanics must involve an uncertainty in the description of past events which is analogous to the uncertainty in the prediction of future events. It is also to be noted that although it is possible to measure the momentum of a particle and follow this with a measurement of position, this will not give sufficient information for a complete reconstruction of its past path, since it has been shown that there can be no method for measuring the momentum of a particle without changing its value. Finally, it is of special interest to emphasize the remarkable conclusion that the principles of quantum mechanics would actually impose limitations on the localization in time of a macroscopic phenomenon such as the opening and closing of a shutter.

ALBERT EINSTEIN
RICHARD C. TOLMAN
BORIS PODOLSKY
California Institute of Technology,
February 26, 1931.

Deviations from Kerr's Law at High Field Strengths in Polar Liquids

When an electric field is established in some substances they become doubly refracting with their "optic axes" in a direction parallel to the lines of force. This phenomenon was discovered by Kerr[1] and is known as the Kerr electro-optical effect. Kerr and others[2] have shown that if n_1 and n_2 are the refractive indices for the components of the light vibration parallel and perpendicular, respectively, to the lines of force, then their phase difference after passing through the electric field is

$$D=\frac{2\pi l(_1n-n_2)}{\lambda}=2\pi BlE^2$$

where λ is the wave-length of the light, l is the length of the light path through the electric field whose magnitude is E. B is Kerr's constant, but has been found to vary with different substances, wave-lengths and tempera-

[1] Kerr, Phil. Mag. (4) 50, 337, 446, (1875).

[2] See G. Szivessy, Handbuch der Physik, 724–808, 21, 1929.

tures. In the present work a method has been devised for testing the possible dependence of B upon the magnitude of E. The well-known theories[3,4] show to a sufficient degree of approximation that

$$B \propto \frac{(n_0^2-1)(n_0^2+2)(K+2)^2}{n_0 T}\left((1+\phi\frac{\mu^2}{T}\right)$$

where n_0 is the index of refraction, K is the dielectric constant, T the absolute temperature and μ the electric moment of the molecule. It has been shown that in polar substances the dielectric constant varies with the strength of the applied electric field, and has been explained as due to an electrical saturation.[5] Therefore in polar liquids B might be expected to decrease with increasing E.

In the present experimental arrangement light from an incandescent filament, made parallel by a lens, plane-polarized by a nicol prism, passed through a Kerr cell 5 cm in length and 3 mm spacing between the plates, then through a second Kerr cell 25 cm in length with a 3 mm spacing between the plates and finally through a second nicol prism crossed with respect to the first. The plane of polarization of the light made an angle of 45° with the lines of force in the first Kerr cell while the plane of the plates of the second cell was 90° from that of the first. A high voltage d.c. potential was applied directly across the first Kerr cell and a variable running tap-water resistance. The second Kerr cell was attached in parallel with just enough of the resistance so that the double refraction in the first Kerr cell was exactly compensated by that in the longer second Kerr cell. The electric field in the first cell was therefore more than twice that in the second. The potential across the first cell and the resistance was then, for example, changed from 30,000 volts per cm to 60,000 volts per cm, so that any change in B with increasing E would appear as a lack of compensation of the light. In the case of CS_2 which is non-polar, practically no light was observed to pass the second nicol prism, that is, the double refraction in the first cell continued to be compensated by that in the second within the limits of precision. However, in the case of carefully distilled chloroform, which is polar, it was found necessary to lower the potential across the second Kerr cell (many times the least amount detectable) in order to make the two cells compensate each other or, again, to reduce the intensity of the light passing the second nicol to zero. This shows that for chloroform B decreases with increasing electrical field. Since the amount of light passing an arrangement of the kind here described is $I = I_0 \sin^2 D/2$ the method is very sensitive to small variations in Kerr's law and gives a simple and precise way of studying electrical saturation effects. The method is being improved and refined in order to make a study of both liquids and gases. A detailed description of the method and a discussion of the results will appear later.

J. W. Beams

University of Virginia,
March 3, 1931.

[3] See Debye, Marx Handbuch der Radiologie, **5**, 754–776, (1924).

[4] Raman and Krishman, Phil. Mag. **3**, 724–735, (1927).

[5] See Debye, Polar Molecules, Chem. Catalog Co., 109, (1929).

BOOK REVIEWS

Gruppentheorie und Quantenmechanik. HERMANN WEYL. Second Edition. Pp. 358. S. Hirzel, Leipzig, 1931. Price, bound, RM 26.

The quantum theory has made it desirable for physicists to become acquainted with mathematical subjects of which heretofore they were allowed to remain blissfully ignorant. This mathematical apparatus is related on the one hand to partial differential equations (Schroedinger's wave-mechanics) and on the other to the theory of Hermitean quadratic forms and unitary transformations (statistical interpretation). In the third place the quantum theory makes use of the noncombining properties of term systems in the solution of special problems as well as in the familiar justification of the exclusion principle. An attempt has also been made by Dirac to introduce a symbolism having no direct relation to our number system (q numbers) which yields the numerical results necessary for physical applications only in the final stage of the symbolic operations.

For the physicist interested in the most direct experimental implications of the quantum theory the interrelations between these fields of pure mathematics are of little interest. The main parts of the subject may be presented in a small amount of printed space as has been done by Heisenberg in The Physical Principles of the Quantum Theory. Elementary developments of the noncombining properties of angular momenta and the related intensity relations are well known and the symmetry properties of electronic proper functions are easily handled in most practical cases by Slater's method. From a certain point of view a deeper study of the mathematical landscape seems, therefore, superfluous.

The transformation theory of classical dynamics is perhaps also superfluous in the same sense and the theory of Maxwell-Faraday stresses could be subjected to the same criticism. The engineer has little occasion to refer to either and for the same psychological reason many physicists approach the study of the more fundamental mathematical aspects of quantum theory with a certain amount of disdain. This fact does not affect however either the beauty or the usefulness of these subjects and in fact an elegant application of Weyl's presentation of the group of rotations has been made by Kramers in a recent paper on intensity formulas.

In Weyl's book the quantum mechanics is presented from the point of view of a mathematician and so far as the reviewer is able to judge in the best taste and with the most powerful machinery. The interrelations between the different aspects of the same mathematical problem are kept in mind throughout. As indicated by the title the guiding principle is that the matrices representing physical quantities define transformations which are representations of certain abstract groups. Operations with abstract groups correspond to the q number calculus. The contents of the first edition have been amplified by the addition of a discussion of the Heisenberg-Pauli wave field theory. The fifth chapter dealing with the group of permutations has been rewritten in a much more elementary form. The connection of the symmetric group with the group of homogeneous linear transformations has been kept in the foreground. Dirac's treatment of permutations as dynamical variables falls in naturally with the methods used here. This is a convenient place for reference to formulas and derivations for group characters of the symmetric group.

Throughout the book many pertinent mathematical subjects have been treated in an elegant and efficient manner. As an example section 3 of Chapter II devoted to spherical harmonics gives in three pages all the necessary material. The treatment of Dirac's relativistic equations is also very good and thorough. The reading of the book is greatly facilitated by a list of symbols used which has been added in the new edition. Contents: I. Unitary geometry II. Physical principles and simple problems of quantum theory. III. Groups and their representations. IV. Applications of groups to angular momenta, Dirac's relativistic equations, the wave field theory, V. The symmetric group.

G. BREIT

Henley's 20th Century Book of Recipes, Formulas and Processes. Edited by HISCOX. Pp. 809, Norman W. Henley Publishing Co., New York, 1930. Price $4.00.

This book, as the title indicates, gives many recipes and formulas which may be of value to the laboratory technician or the home shop-worker. The material, taken from various lines of industry and craftsmanship, is alphabetically arranged throughout the book, with a supplementary index at the end which is a help where there is more than one popular nomenclature for the subject matter under inquiry. The printing is good and the type of a size easy to follow.

I believe the book is better suited for the amateur home worker than it is for the professional laboratory man who has at least a meager idea of what the industrial and scientific library holds in the way of literature along the various lines. Material from the trades is necessarily brief giving more of an outline than a workable procedure for the novice. For the research worker who is at a standstill for want of information on technical manipulation, the book may yield an inspiration for a new attempt. The latitude of the material might be a boon under such circumstances.

WM. B. HALIDAY

Atlas of Physical and Inorganic Chemistry. A. VON ANTROPOFF AND M. VON STACKELBERG. 29 charts and descriptive volume 64 pp. Verlag Chemie, G.m.b.H. Berlin 1929. Price RM 42.00.

The atlas consists of 29 charts (11 x 14.25 inches) printed on stiff card board, accompanied by a descriptive volume of the same size. The plates show the material in the form of histograms or columnar diagram. The following physical and chemical quantities are represented: (1) The periodic table. (2) The electron shells of the atoms. (3) Atomic diameters. (4) Ionic diameters. (5) Ionization potentials. (6) The crystal structure of the elements. (7) Melting and boiling points of the elements. (8) Mechanical properties of the elements in the solid state. (9) Atomic frequencies of the elements. (10) The atomic force constant. (11) Specific and atomic electrical conductivities. (12) Valencies of the elements. (13) Normal electrode potentials. (14) Heats of combustion. (15) Melting and boiling points of the chlorides and the electrical conductivities in the fused state. (16) Hydrides. (17) Carbides. (18) Nitrides. (19) Solubilities of hydroxides, carbonates, sulphates, chlorides, sulfides and a few other salts. (20) Isotopes. (21) The geochemical distribution of the elements. (22) The occurrence of the elements in the earth's crust and in the whole earth.

The printed volume which supplements the charts gives in every case a short discussion and the necessary definitions of the topics illustrated in the diagrams. It seems to the reviewer that the atlas is, on the one hand, too large for convenient desk use and on the other hand too small for the use with large classes. It should find its principal use with small seminar groups where a few individuals need the material as a basis for discussion.

GEORGE GLOCKLER

Les Quanta. G. DÉJARDIN. Pp. 224. Armand Colin, Paris, 1930. Price 10f.50 unbound.

Within its appointed scope as an elementary exposition of the conceptions and fundamental experiments underlying the quantum theory, this book seems for the most part quite successful. Short chapters on radiation theory and specific heats present the basic ideas of the Planck radiation formula and the Einstein-Debye theory of specific heats of solids. Chapters on the photoelectric effect and x-rays give the salient features of the Auger effect, the angular distribution of photo-electrons, the absorption of x-rays, and the Compton effect. Considerable space is devoted to a discussion of classical mechanics, Bohr's atomic theory and correspondence principle, Sommerfeld's fine structure formula and similar topics from pre-quantum mechanics atomic physics. After a short chapter on thermionics, photochemistry and Raman effect the book closes with a few pages on wave mechanics. The explanations seem uniformly clear and the material well chosen. The reviewer, however, doubts the efficacy or the need of retaining the older theoretical explanations even in elementary treatments such as this one, for in many respects the conceptions associated with the newer theory are distinctly simpler than their progenitors, and besides, once learned they will not need to be unlearned for at least some time to come.

E. L. HILL

What Is a Syncro-Clock?

MORE than ten years ago, before the synchronous motor-driven clock was popularized for domestic use, the General Radio Company began development of such an instrument for use in the laboratory. It was our initial idea that the Syncro-Clock would be driven by a vacuum-tube oscillator having a fairly stable frequency characteristic and that the clock would therefore furnish a means of determining the average frequency of the oscillator during a given time interval. This development has been steadily carried forward, many models built, and now we are able to make commercially available a Syncro-Clock having a number of useful and interesting features:

1. The Syncro-Clock offers one of the most precise methods possible of measuring the frequency of an oscillator. Readings are secured in terms of our Mean Solar Day and are integrated throughout the period of measurement.

2. When operated by a source of exactly 1000 cps. the Syncro-Clock keeps true time, the only error being that of the standard.

3. Shafts rotating with a constant angular velocity are available for turning stroboscope discs, for operating seconds and tenths-of-seconds contactors, and for driving small generators to produce other frequencies the stability of which are definitely determined by the frequency of the driving source.

The General Radio Company makes use of this device in its standard-frequency assembly, our name for a system which determines frequency directly in terms of the Mean Solar Day. Using a Syncro-Clock we compare the time kept by our piezo-electric oscillator — Syncro-Clock system with the time intervals determined daily by the U. S. Naval Observatory and transmitted to us via Arlington Time Signals.

Syncro-Clocks have many applications to time and frequency-measuring problems. If this brief description interests you, we should be glad to send you further details.

Ask for Catalog F-Y

GENERAL RADIO COMPANY

OFFICES ' LABORATORIES ' FACTORY

CAMBRIDGE A, MASSACHUSETTS

PACIFIC COAST WAREHOUSE: 274 BRANNAN STREET, SAN FRANCISCO, CALIFORNIA

INFORMATION FOR CONTRIBUTORS TO THE PHYSICAL REVIEW

Purpose of the Review is to publish articles that add to our knowledge of experimental or theoretical physics.

Articles which have not previously been published may be submitted by any physicist whether American or not. Each manuscript will be acknowledged by the Managing Editor as soon as received. An article to be considered must be in English and in a form ready for publication; it must be provided with a preliminary abstract prepared in accordance with the directions given on a following page. Carelessly written articles and figures not carefully drawn will be returned for revision. All manuscripts should be typed double space and symbols written in with great care so as to be quite clear to the printer.

Suggestions as to Contents. On account of the high cost of printing, brevity is of great practical importance. Historical summaries of previous results and also discussions which consider various possible explanations without leading to definite conclusions should be made very brief, except in special cases. The greater part of the paper should be devoted to the actual new results and to a concise presentation of the conclusions to which they lead. Attention should be directed to the more accurate and more conclusive experiments, omitting any which add nothing. The amount of detail included should be governed somewhat by the importance of the results and their interest to physicists.

Suggestions as to form. Clearness is of great importance. Pains should be taken to insure that the order and form of presentation are such as to enable the reader to grasp the new information as easily and quickly as possible. In general the order should be: Statement of the problem and of the purpose, scope and general method of the investigation, followed by a description of the apparatus, experiments and results in such order as to bring out clearly the evidence for the main conclusions, the paper ending with perhaps a brief discussion of the significance and bearing of the results on other problems. Avoid the historical or laboratory note-book style; use rather the text-book or lecture style. Footnotes should be numbered consecutively and each reference should contain author's name.

Abbreviations. Omit periods after such symbols for units as the following: cm, mm, kv, lb, A, °C; also after I, II, . . . and percent, and after headings in columns in Tables. Write a.c., e.m.f., abscissas, disk, in vacuum, wave-length, x-rays, percent. Refer to figures as Fig. 1, Figs. 3 and 4; and to equations as: Eq. (5); Eqs. (7) and (8). Number equations on the right.

Mathematics. Indicate divisions by a slant line where possible. Avoid unusual symbols, symbols with rules over them, cumbersome fractions.

Figures or illustrations. Use only jet black ink, on white or on blue-lined cloth or paper. Tracing cloth is especially suitable. Curves plotted or traced on such cloth or paper may have co-ordinates ruled in black at desired intervals, say every centimeter or inch, as blue lines are not reproduced photographically. *Colors other than blue and black should be avoided.* Indicate observed points on all plots. Arrange material in each figure compactly. It is well when possible, to make the longer dimension horizontal, as larger reproduction can then be permitted; if vertical figures are necessary space may be saved by making two of the same height, and putting them side by side. *All lettering should be at least $\frac{3}{16}$" high* for an 8"×10" figure, so as to be legible after reduction. Lettering left in pencil will be inked in by a draftsman in this office. In general each figure and table should have a caption, describing it briefly. Reduce the number of tables and figures to the necessary minimum.

Proofs. Galley proof of each article is sent directly from the publishers to the author and should be corrected with great care so as to eliminate all errors, as page proof cannot always be submitted. Only necessary changes should be made; extensive additions will mean the delay of a month in publication. All corrected proof should be sent promptly with the Manuscript to THE PHYSICAL REVIEW, University of Minnesota, Minneapolis.

Permission to republish any article is given, if proper acknowledgment is made.

Reprints ordered on the proper form with the return of the galley proof, will be furnished by the printer according to the prices given on the form.

Back Numbers Urgently Wanted

of the

PHYSICAL REVIEW

We will pay $2.00 each for copies of the January, February, April and May issues of Volume 7, 1916; the January and February issues of Volume 9, 1917; January issue of Volume 11, 1918; also $1.00 for copies of the January, 1927, issue.

Send to the Physical Review, University of Minnesota, Minneapolis, Minnesota.

FREE FALL APPARATUS

Fitch Design

Average errors within .5%

Free fall over distances regulated by observer.

Time recorded without other aids than stop watch determinations.

The drum upon which record is made is uniformly rotated by No. 850 Mechanical Timer and this is timed by a stop watch.

Double magnetic control for recording beginning and ending of drop of falling body.

Designed according to the original suggestions of Prof. A. L. Fitch of the University of Maine.

Conveniently arranged for wall mounting.

Independent of frequency of laboratory current.

Does not require any accessory apparatus. (Our No. 850 Mechanical Timer is included in the price given below and may also be used for timing other devices.)

No. 850B Free Fall Apparatus, complete as illustrated..... *$95.00*

Send for new bulletin describing more completely this method and this new instrument.

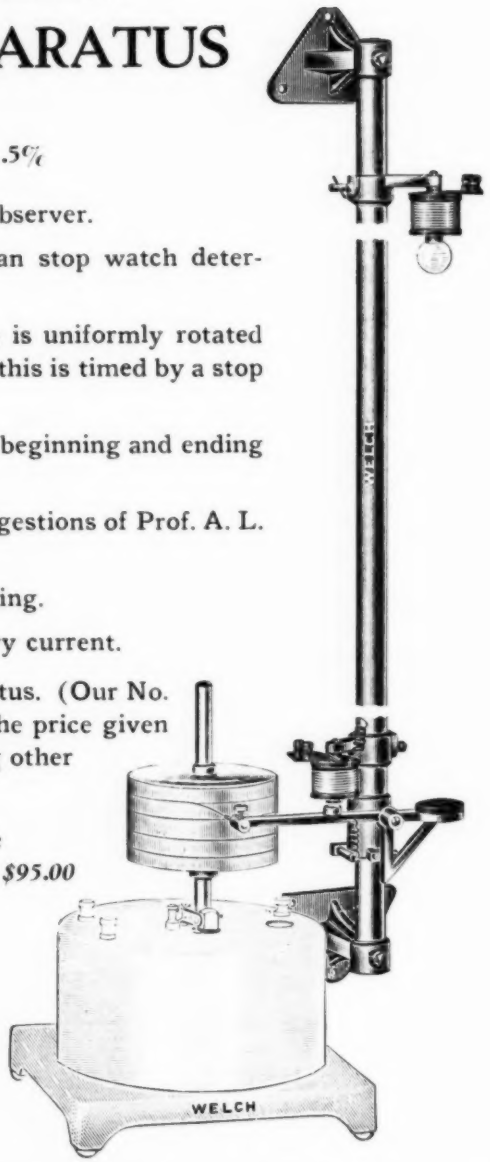

W. M. Welch Manufacturing Company

Manufacturers, Importers and Exporters of Scientific Apparatus, Furniture, and School Supplies

General Offices: 1515 Sedgwick St., CHICAGO, ILL., U. S. A.

Scientific Apparatus Factory and Warehouse:
1516 Orleans St., Chicago, Ill.

Laboratory Furniture Factory:
600 S. Sixteenth St.,
Manitowoc, Wisconsin

Branch Offices:

342 Madison Av.
NEW YORK CITY, N.Y.

1916 West End Av.
NASHVILLE, TENN.

34th & Broadway
KANSAS CITY, MO.

2220 Guadalupe St.
AUSTIN, TEXAS

Pacific Coast Distributors:

Braun-Knecht-Heimann Co., Ltd.
576-584 Mission Street,
San Francisco, California.

Braun Corporation, Ltd.
365 New High Street,
Los Angeles, California.

Reviews of Modern Physics

The April, 1931 issue (Volume 3, number 2) will contain

Electrical Discharges in Gases. Part II.
By Irving Langmuir and K. T. Compton

Some Physical Characteristics of Speech and Music
By Harvey Fletcher

The Infrared Spectra of Polyatomic Molecules. Part I
By David M. Dennison

Yearly subscription price
to members of the American Chemical Society and to members of the American Physical Society..... $3.00
to all others..... 4.00
Single copies..... 1.25

REVIEWS OF MODERN PHYSICS
University of Minnesota, Minneapolis, Minnesota

A New Math. Tool

EDGAR DEHN
ALGEBRAIC CHARTS

for solving quadratic, cubic and biquadratic equations. Price in special folder $1.00, library edition $1.50 bound.

Patents Pending

Size 6 by 9½ inches, 14 sheets

NOMOGRAPHIC PRESS
509 Fifth Ave., New York

Handy Reference Cards

of the most probable values of the GENERAL PHYSICAL CONSTANTS as estimated by Raymond T. Birge in the July issue of

THE PHYSICAL REVIEW SUPPLEMENT

Tables of the values of the general physical constants taken from Birge's article are printed on two stiff cards, 8½ x 11", bound together with linen tape.

Price 50 cents

Reviews of Modern Physics
University of Minnesota
Minneapolis, Minnesota

A better rotator offering physics teachers a new field of quantitative and qualitative experiment—

SPECIAL FEATURES

A range of speed from nearly zero r.p.m. up to the maximum speed of the motor.

Reversal of direction of rotation without stopping and starting the motor.

Perfect control of speed by amounts which vary from an imperceptible change to a rapid acceleration in either direction.

Instant adjustment of the direction of the rotating spindle through 360°, permitting the use of objects suspended below.

Constancy of speed, permitting quantitative experiments to be made.

Ease of measurement of speed of rotation of spindle, by spring-attached gear-driven speed counter, which may be engaged or disengaged instantly.

No. F1020 for 110 volts AC $60.00

CENTRAL SCIENTIFIC COMPANY
LABORATORY APPARATUS AND SUPPLIES
CENCO Chemicals
NEW YORK - BOSTON - CHICAGO - TORONTO - LOS ANGELES

The Cenco Friction Drive Rotator with variable speed control and electric motor drive

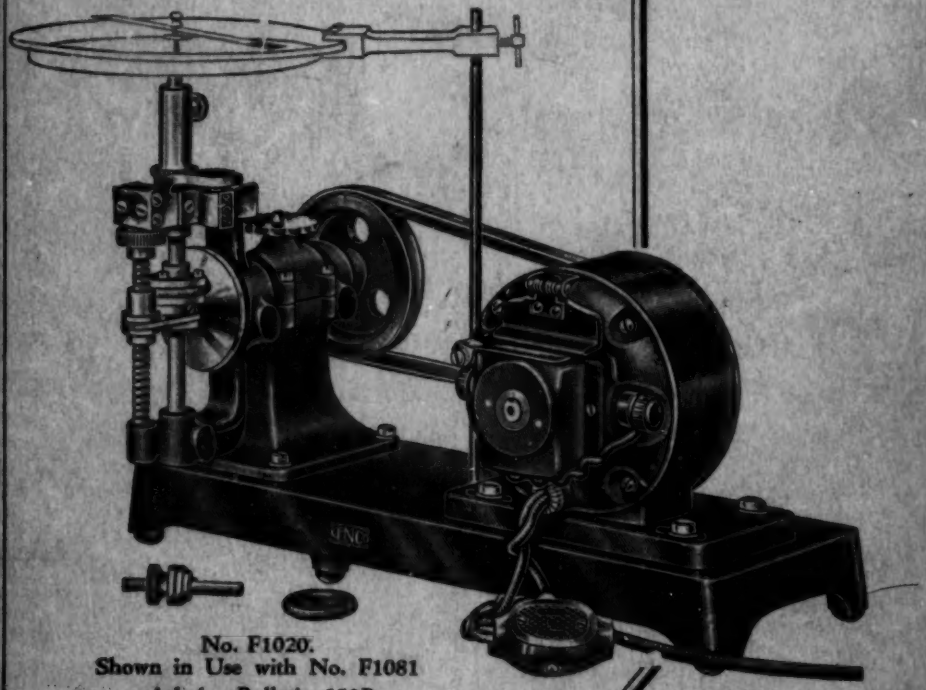

No. F1020.
Shown in Use with No. F1081
Ask for Bulletin 150P

GEORGE BANTA PUBLISHING COMPANY, MENASHA, WISCONSIN